Design of Novel Drug Delivery Polymeric Complexes via Innovative Crosslinking Reactions

Wilbert O.L. Sibanda

A thesis submitted to the Faculty of Health Sciences, University of the Witwatersrand, in fulfilment of the requirements for the Degree of Master of Science in Medicine (Pharmacy), Johannesburg

Supervisor: Professor Viness Pillay, Department of Pharmacy and Pharmacology, University of the Witwatersrand, Johannesburg, South Africa

Co-Supervisor: Professor Michael P. Danckwerts, Department of Pharmacy and Pharmacology, University of the Witwatersrand, Johannesburg, South Africa

Declaration

I, Wilbert Sibanda declare that this thesis is my own work. It is being submitted for the degree of Master of Science in Medicine (Pharmacy) in the Faculty of Health Sciences at the University of the Witwatersrand, Johannesburg. It has not been submitted before for any degree or examination at this or any other University.

This 1st day of April 2004

Summary

This thesis presents a multifaceted approach which comprehensively describes the design of novel drug delivery polymeric complexes through the application of innovative crosslinking reactions. These reactions have been built on the statistical and mathematical principles governing the technique of Design of Experiments. At the outset, pertinent aspects covering the importance of rate-controlled drug delivery in achieving superior therapeutics is presented. In addition, the fundamental mechanisms which regulate the complex behaviour of polymeric materials are outlined, placing emphasis on the mathematical models which demonstrate the critical need to be able to synchronize the processes of matrix hydration, relaxation, disentanglement, erosion and dissolution. Initially, the Plackett-Burman Design was evaluated to develop a crosslinked polymeric oilisphere device for the in vitro site-specific delivery of Mentha piperita oil. This design proved to be highly successful in rapidly identifying the appropriate release rate-modifying variables through the application of stepwise regression optimization and Artificial Neural Networks. Having assessed the utility of Design of Experiments and receiving positive feedback on its predictive power over the physicochemical and physicomechanical properties of the crosslinked matrices, the study progressed into the design and development of a novel zinc-alginate-pectinate complex based on a statistical combination of independent variables derived from a high resolution quadratic Box-Behnken Design. All studies from this point onwards employed either ibuprofen or theophylline as model drugs. Based on the response outcomes for matrix resilience, rupture energy, yield value, viscoelasticity, drug encapsulation efficiency and dissolution, it became evident that a greater degree of crosslinking was achieved in the case of the zinc-pectinate complex. This study did not aim to undertake numerical optimization on the experimental output, but rather to select a candidate formulation based on specific constraints, for further manipulation. In order to manipulate the stress-strain properties and drug releasing potential of the candidate zinc-pectinate system, a novel crosslinked ethylenic homopolymer was synthesized. This synthesis was also based on a Box-Behnken Design, which allowed for stringent mathematical optimization of the new polymeric material. This material, synthesized through a unique combination of organic and inorganic crosslinkers, is the first to be reported in this study. Incorporation and evaluation of the crosslinked ethylenic homopolymer within the candidate zinc-pectinate matrix was based on a Face-Centred Central Composite Design, which ultimately led to the development of a range of optimized dissolution profiles capable of drug delivery in a zero-order manner over several hours to days, either with or without a lag-phase.

Acknowledgements

1. Ms. M.J. Maboka: For the persistent encouragement
2. Ms. J. Sibanda: For the smile that gave me courage and determination
3. Mr. O.L. Sibanda: For being the pillar of my strength
4. Mr. G. Sibanda and the rest of the family: For their unfailing encouragement and interest
5. Mr. M. Snyman: For assistance with typing of this thesis
6. Professor M.P. Danckwerts: For constant guidance and support
7. Professor V. Pillay: For imparting vast knowledge which I have acquired
8. Dr. A.M. Viljoen: For providing assistance whenever required
9. Ms. S. van Vuuren: For professionalism in handling my research grants
10. Last but not least: I would like to thank God for His love

Publications

Experimental Design for the Formulation and Optimization of Crosslinked Oilispheres Developed for *In Vitro* Site-Specific Release of *Mentha piperita* Oil, Wilbert Sibanda, Viness Pillay, Michael P. Danckwerts, Alvaro M. Viljoen, Sandy van Vuuren and Riaz A. Khan – AAPS PharmSciTech, 5(1), 1-14, 2004.

Presentations

1. Physicochemical Manipulation of Ethylenic Homopolymeric Matrices for the Design of Variable Drug-Releasing Gelispheres, American Association of Pharmaceutical Scientists Annual Meeting, Salt Lake City, USA, 2003.
2. Statistical Optimization by a Central Composite Design on Repeating Vinyl Alcohol Units: Custom-Made Rate-Controlled Multiparticulate Units for Drug Delivery, American Association of Pharmaceutical Scientists Annual Meeting, Salt Lake City, USA, 2003.

3. Application of a Face-Centred Central Composite Design for the Optimization of Polymer Matrices, Academy of Pharmaceutical Sciences 24th Annual Congress, Durban, South Africa, 2003.
4. Induction of Salting-Out of Ethylenic Homopolymers: A New Drug Delivery Approach, Academy of Pharmaceutical Sciences 24th Annual Congress, Durban, South Africa, 2003.
5. Experimental Design and Modelling of Bioactively-Charged Gelispheres, 37th South African Pharmacology Congress, University of Stellenbosch, Bellville, South Africa, 2003.
6. Preliminary Evaluation of the Crosslinking Potential of Vinyl Polymers, 37th South African Pharmacology Congress, University of Stellenbosch, Bellville, South Africa, 2003.
7. Novel Oral Crosslinked Oilisphere Delivery System for the Encapsulation of Peppermint Oil, American Association of Pharmaceutical Scientists Annual Meeting, Toronto, Canada, 2002.
8. Plackett-Burman Approach for the Novel Design of Crosslinked Oilisphere Matrices for Targeted Delivery of *Mentha piperita* Oil, 3rd International Conference on Pharmaceutical and Pharmacological Sciences, Boksburg, South Africa, 2002.
9. Box-Behnken Design for Zinc-Alginate-Pectinate Complexes, 3rd International Conference on Pharmaceutical and Pharmacological Sciences, Boksburg, South Africa, 2002.

Table of Contents

Chapter Three

Design of Experiments: A Statistical and Mathematical Approach to Optimization of Function Variables

Chapter Four

Testing the Utility of a Two-Level Screening Design for the Formulation and Optimization of a Novel Crosslinked Delivery System for *Mentha piperita* Oil

Chapter Six

Synthesis and Sensitivity of a Novel Crosslinked Ethylenic Homopolymer Derived from Native Polyvinyl Alcohol

List of Figures

List of Tables

Chapter One

Rate-Controlled Drug Delivery: Importance and Key Principles

1.1 Introduction

The control of the intensity and the duration of drug action have been of interest to pharmaceutical scientists for many years. However, only recently has this technology been exploited commercially to a large extent. This new generation technology has led to more complex mechanisms used for rate-modulation of bioactives.

The advantages resulting from modulation of drug action include, the maintenance of therapeutic effect over an extended period of time, especially if a continuous action at a therapeutic level is essential (Praveen, 1990; Danckwerts, 1996; Pillay and Fassihi, 2002a).

Another important advantage is the convenience offered to the patient by this type of design due to the decrease in dosing frequency (increased patient compliance). Optimization of drug action, including drug safety, may also be handled by controlling the rate of drug delivery to the physiological absorption surfaces.

In practice, controlled drug release products are frequently necessary for chronic drug administration such as in the case of calcium channel blockers (nifedipine and diltiazem) and beta adrenergic blockers (propranolol and metoprolol) for the management of angina and hypertension. This does not preclude the application of other pharmacological drug classes in the design and development of advanced drug delivery systems.

The ideal attributes of a rate-modulated drug delivery system include:

(i) Flexible programming: Ability to accommodate the pharmacokinetics of various

drugs,

(ii) Precise programming: Capability of precise control for a constant delivery rate,

(iii) Relatively insensitive to the physiological variables such as gastric motility and rate of emptying, gastrointestinal pH, fluid volume, and content, absence/presence and concentration of enzymes, absence/presence of food, physical position and activity of subject, individual variability and pre-existing/new disease states,

(iv) Predictable rate of delivery based on physicochemical principles,

(v) Capable of a high level of drug dispersion,

(vi) Maintenance or enhancement of drug stability,

(vii) Controlling mechanism does not significantly affect the mass of the dosage form, and

(viii) Applicable to a wide range and variety of drugs, chemicals, proteins, macromolecules, vaccines, hormones and other bioactives.

There are numerous factors that affect the *in vivo* performance of controlled release formulations and these include:

(i) Physiological Factors:

(a) Prolonged drug absorption,

(b) Size of absorption window, and

(c) Gastrointestinal blood flow and degree of perfusion.

(ii) Biopharmaceutic and Pharmacokinetics Factors:

(a) Effect of gastrointestinal pH on drug release rate,

(b) First pass metabolism,

(c) Variability in urinary pH and effect on drug elimination, and

(d) Enzyme induction/inhibition upon multiple dosing.

(iii) Pharmacologic Factors:

(a) Change in drug effect upon multiple dosing,

(b) Sensitization/tolerance, and

(c) Change in metabolic profiles, if active metabolites are present.

1.2 Clinical Aspects of Novel Drug Delivery Systems

The clinical rationale for the development of novel drug delivery systems is to achieve safer, more efficacious therapy, and to promote patient compliance by decreasing the cost and increasing the ease of use. The sophistication in pharmaceutical research required to achieve these objectives is multidisciplinary and requires an understanding of the pathophysiology of disease, knowledge of the pharmacokinetics, pharmacodynamics and physicochemical properties of the drug (Turner, 1990).

With continued advances in understanding the molecular basis of diseases, it may be possible to identify the precise biochemical defect present in each patient. With this knowledge and the development of novel drug delivery systems, it may be possible to target specific therapeutic agents in order to provide safer and more efficacious therapeutics. Progress is continually being made along these lines in several clinical disciplines such as gene therapy and encapsulation of DNA and plasmid vectors (Perez et al., 2003).

1.3 Technology Applied in this Study

Hydrophilic swellable polymers used in the development of drug delivery devices in their native state, usually demonstrate rapid gelation, first-order dissolution, and non-synchronized erosion/relaxation in relation to the timescale required for modulated drug delivery (Pillay and Danckwerts, 2002). In their study, these researchers have shown that these limitations can be significantly solved through the process of chemical crosslinking and salting-out which essentially changes the extent of polymer entanglement and hence

the rate of disentanglement.

Recent work has shown that through the use of specific formulation excipients, the inherent properties of certain polymeric materials may be altered *in situ* for the provision of specific release profiles (Pillay and Fassihi, 1999a; 2000a; 2000b). The effects resulting from salting-out and complexation of polymers induced through chemical crosslinking may include phase transitions within the gel microstructure, alteration of water mobility rates and changes in the degree of polymeric dehydration (Pillay and Danckwerts, 2002).

The increase in the glass transition temperature (T_g), and the mobility of polymeric chains is significantly reduced and thus, in conjunction with crosslinking and salting-out phenomena, overall solubility of the polymeric system may be reduced. Crosslinks tend to create three-dimensional voids or pockets within the polymeric matrix and hence, diffusion of the imbibed medium becomes more restrained, thereby controlling matrix relaxation and erosion. These effects may potentially influence the nature of an already complex hydrated polymeric system, and subsequently the regulation of drug transport (Pillay and Danckwerts, 2002).

1.4 Motivation for the Present Study

We have recently identified in our laboratory at the University of the Witwatersrand, Department of Pharmacy and Pharmacology, that the salting-out/crosslinking of polymers such as polyvinyl alcohol (PVA), alginate and pectin, induced in a very novel and *specific* manner, may be particularly advantageous for the achievement of rate-adjusted drug delivery through the development of modified intelligently-reacting polymers (Pillay, 2002).

It is the objective of this research to investigate the *specificity* and applicability of this crosslinking process which to date has not been elucidated in biomedical research as a

potential approach for drug delivery. For example, this crosslinking process provides modified matrices which are brittle in the unhydrated state, plastic to pseudoplastic in the hydrated state and low to highly soluble but gellable with superswellable properties. This approach of polymeric crosslinking allows for the formation of discrete spherical, elliptical and disk-shaped entities termed "gelispheres" or "oilispheres" depending on the encapsulated bioactive agent and rate-modulating mechanism.

Various formulation strategies will be adopted to develop novel drug delivery systems with the aim of achieving steady-state release.

1.5 Overall Aim and Objectives of this Study

1. Application of Experimental Design to develop statistically and mathematically robust combinations of experimental formulations,
2. Synthesis of crosslinked polymers using the above designs by ionotropic gelation,
3. Physicochemical and physicomechanical analysis of crosslinked matrices employing several approaches:
   - (i) *In vitro* dissolution studies,
   - (ii) Polymer gravimetric transitions,
   - (iii) Bioactive encapsulation efficiency,
   - (iv) Textural profiling analysis,
   - (v) *In situ* viscoelastic transitions of sequentially crosslinking polymer solutions,
   - (vi) Particle size analysis of crosslinked entities,
   - (vii) Mathematical and kinetic modelling of experimental data,
   - (viii) Predictive power of Artificial Neural Networks,
   - (ix) Differential Scanning Calorimetry (DSC),
   - (x) Fourier Transform Infra-Red Spectroscopy (FTIR), and
   - (xi) X-ray Diffraction (XRD).

Chapter Two

Fundamentals of Drug Delivery Systems Design

2.1 Introduction

Hydrogels are typically polymeric materials that absorb a significant amount of water (>20% of their dry weight) while maintaining a distinct three-dimensional structure (Cascone et al., 1995). This definition encompasses both dry polymers that swell when placed in water and pre-swollen elastic materials.

In recent years, there has been an explosion in the interest of polymer-based delivery devices. Such devices can enhance drug stability by protecting labile drugs from denaturants in the body, control the release rate of therapeutic agents and help achieve site-specific delivery, as in the case of colonic drug-targeting.

These polymeric materials possess four key properties: differential rates of gelation, permeability, swelling, and biocompatibility (Cascone et al., 1995). Their ability to retain high water content provides excellent biocompatibility since impurities can be easily extracted. Their soft, rubbery nature reduces mechanical irritation. In addition, their hydrophilic character minimizes interfacial tension. Very often the permeability of hydrogels to water, drugs, and other solutes are adjusted over a broad range by changing the gel precursor, crosslinker, or conditions of synthesis in order to modulate drug transport within the gel and hence drug delivery.

The reproducible and controllable swelling kinetics of hydrogels are a result of their time-dependent permeability dynamics which allow therapeutic agents to be delivered in a prescribed manner.

2.2 Thermodynamic Phenomena of Hydrogels

2.2.1 Equilibrium Swelling

While permeability characteristics and biocompatibility are desirable properties of hydrogels, they usually demonstrate low mechanical strength.

The amount of water absorbed is a function of the hydrophilicity of the polymer, the network structure and the number of ionized groups on the polymer. The basic swelling theory assumes that swelling of the hydrogel is a result of several independent free-energy changes which occur when the gel is mixed with a solvent as seen in Equation 2.1.

$$\lambda G_{tot} = \lambda G_{mix} + \lambda G_{elas} + \lambda G_{ions} + \lambda G_{elec} \qquad \textit{(Equation 2.1)}$$

where λG_{tot} = total free energy change, λG_{mix} = mixing of polymer chains with solvent molecules, λG_{elas} = elastic response to changes in the configuration of the polymeric network, λG_{ions} = mixing of ions from solution and from the polymer with the solvent, and λG_{elec} = changes in electrostatic interactions of ionized groups upon swelling (Lai et al., 2000).

It is conceptually more convenient to convert the free-energy terms to osmotic swelling pressures, using thermodynamic relations. The Flory-Huggins Theory can also be used to calculate the enthalpy and entropy changes associated with laying out a polymer chain on a lattice by applying the Flory-Huggins interaction parameter, which indicates the degree of interactions between solvent and the polymer molecules. Interaction parameters are generally between 0 and 1 when polymer-solvent interactions dominate, and dissolution is favoured.

2.2.2 Permeability

While equilibrium swelling may be a key characteristic of the hydrogel, its permeability

makes it highly attractive for drug delivery. Hydrogels can be rendered impermeable, semipermeable or highly permeable to virtually any class of solute and hence applicable to a wide variety of drug delivery problems e.g. drug solubility limitations.

Two basic mechanisms, namely the "pore" and "partition" theories are assumed to explain solute diffusion through hydrogels. In the "pore" mechanism, the solute moves only through water-filled regions of the gel, whereas in the "partition" mechanism, solute transport is assumed to involve thermodynamically-controlled dissolution into the polymer.

One of the early models used to interpret diffusion through polymer networks was that proposed by Yasuda and Rosengren (1971). These researchers introduced a free-volume theory which assumes that the solute moves only within water-filled regions of the gel. The diffusion coefficient is proportional to $[\exp(-V_s/V_f)]$, where V_s is the characteristic volume of the solute and V_f is the free volume inside the gel. The free volume V_f is assumed to be linearly related to the weight fraction of water inside the gel. Combining these relationships results in the following:

$$Log\ (D_g) = Log\ (D_o) - k/(q-1) \qquad \textit{(Equation 2.2)}$$

where D_g = diffusion coefficient of the solute in hydrogel, D_o = diffusion coefficient of the solute in solvent, k = constant solute volume and the free volume of water, and q = degree of swelling.

2.2.3 Swelling Kinetics

The third major property of hydrogels is their controllable swelling kinetics. Since the solute permeability is directly related to the degree of swelling, control of swelling leads to control of the solute permeability, and hence drug release.

The relative importance of relaxation and diffusion, can in principle be estimated from the

Deborah Number, D_e (Reiner, 1969), where:

D_e = *Time of Relaxation/Time of Observation* *(Equation 2.3)*

Thus when $D_e<<1$, relaxation is faster than diffusion and Fickian diffusion is observed. This occurs well above the glass transition temperature (T_g), where gels are rubbery and the diffusion coefficient is generally a strong function of concentration. Fickian diffusion in a constant manner is observed for $D_e>>1$. This corresponds to diffusion which occurs in a glassy polymer well below T_g, where polymer relaxation is slow and its structure is unchanged by the diffusion process (hence the gel does not swell in this region). When $D_e=1$, relaxation and diffusion interact, leading to transport not explained by Fickian diffusion (non-Fickian or anomalous transport).

2.3 Microsphere Technology in Rate-Modulated Drug Delivery

Particles applied in drug delivery in the range from 100nm-1μm are termed microspheres. Those smaller than this are termed nanoparticles (Juliano, 1980; Chawla et al., 2000).

Drugs with a range of water solubilities can be incorporated into microspheres by including them in polymer solutions using various techniques outlined below. Substantial interest in the application of polymer-based microspheres as drug carriers results from their ability to regulate drug release rates and more importantly their ability to produce desirable biopharmaceutical characteristics (Widder et al., 1982, Soppimath et al., 2001).

2.3.1 Advantages of Microspheres

(i) Predictable Gastrointestinal Transit Times:

After ingestion of an oral non-disintegrating dosage form, it resides in the stomach for an unpredictable time. To understand the implications of this initial state of the gastrointestinal transit, it is important to mention the role of the stomach in terms of its

anatomical structure and motor functioning either during the interdigestive or digestive phases, a phenomenon referred to as the Migrating Myoelectric Complex (MMC) (Mojaverian, 1991; Davis et al., 1986).

During the interdigestive phase, the empty stomach displays a cyclic motion that can be divided into four phases as follows:

(a) Phase 1: An inactive quiesant phase with little or no contractions which lasts up to 60 minutes,

(b) Phase 2: Consists of irregular and intermittent sweeping contractions,

(c) Phase 3: Comprised of acute eruptions of peristaltic waves in the proximal and distal gastric areas, lasting between 5 and 15 minutes. This phase empties the stomach contents and indigestible debris. This explains why it is almost impossible to prolong the residence of multiple-unit systems (e.g. microspheres) in the stomach (Harris and Robinson, 1990), and

(d) Phase 4: The transient period of decreasing activity until the next cycle.

Single-units are retained in the stomach until Phase 3 of the MMC returns. Thus after a meal, the pylorus appears to act as a sieve allowing small particles to filter through but retaining larger particles (Muller and Blum, 1981).

(ii) Independence from Cardiac and Pyloric Contraction/Relaxation Activities:

Highly soluble drugs administered within pellets, disperse in the gastric fluids and are emptied with food. Due to their small sizes, multiple-units easily pass through the cardiac and pyloric sphincters regardless of whether they are contracted or relaxed.

(iii) Induce Less Localized Gastrointestinal Disturbances:

There is a reduction in local side-effects such as nausea, vomiting, abdominal pain, and gastric irritation due to the dispersive nature of multiple units.

(iv) Achievement of Site-Specific Drug Delivery:

The biopharmaceutical, pharmacokinetic, and pharmacodynamic characteristics of a drug molecule often combine to largely reduce the drug molecule's intrinsic activity. A simple equation illustrating this, is presented by Sahoo and co-workers (2002).

Observed Activity = Intrinsic Activity x Drug at Receptor *(Equation 2.4)*

Any process or phenomenon that reduces the amount (and frequency) of drug arriving at its pharmacological receptor will result in that molecule producing a lower observed therapeutic effect.

There are two potential directions that can be taken to improve (or optimize) the action of a drug. The first is the design of new biologically-active molecules which are both potent and selective for particular receptors such as the renowned "Ehrlich's Magic Bullet" approach (Harris and Robinson, 1990).

The second option is the one employed in the present study, which involves the "Magic Missile" approach. This purports the use of carrier systems ("Missile Delivery") that will target active molecules to specific sites in the body. Upon reaching the site, drug is released either passively or via a specific site-recognition event (Sahoo et al., 2002).

Thus targeted delivery is highly dependent on the physicochemical and biophysical interactions between multiple-units and the physiological system (Burczak et al., 1994).

The ideal characteristics of a targeted drug delivery system include:

(i) Restricted drug distribution to the target,

(ii) Prolonged control,

(iii) Ready access to tissue parenchyma,

(iv) Controllable and predictable rate of drug release,

(v) High loading capacity for drugs and drug types,

(vi) Ideal therapeutic amounts of drug release,

(vii) Minimal drug leakage during transit to the target,

(viii) Drug protection,

(ix) Biocompatible surface properties,

(x) Biodegradable targeted delay systems, and

(xi) Ease of synthesis or formulation.

2.4 Techniques for the Preparation of Microspheres

2.4.1 Coacervation Phase Separation

Coacervation encapsulation (or microencapsulation) is a three-part process comprised of the formation of a droplet, coacervative wall and capsule.

Coacervation involves the separation of a liquid phase (coating material) from a polymeric phase and then wrapping this phase as a uniform layer around suspended core particles. Coacervation may be brought about when the surface energy between the core and coatings material are adjusted by varying some critical parameters of the system such as temperature, pH or composition. The coating material is then solidified by means of heat, crosslinking, or solvent removal techniques (Orienti et al., 2001; Meese et al., 2002).
The microcapsules are usually collected by filtration or centrifugation, washed with an appropriate solvent, and subsequently dried by standard techniques to yield free-flowing discrete particles.

Coacervation may also be subdivided into aqueous phase separation and non-aqueous phase separation techniques. This technique, also referred to as "oil-in-water" microencapsulation, has been used to encapsulate citrus oil, vegetable oil and vitamin A (Paradossi et al., 2002).

Non aqueous (organic) phase separation also referred to as "water-in-oil" encapsulation, comprises a hydrophobic coating and a water-soluble or water-insoluble core. This process has been investigated for the encapsulation of solid food additives such as ferrous sulphate (Bolassa and Fanger, 1971).

The major disadvantage of coacervation is that even though it is efficient, it is also very expensive and difficult to scale-up.

2.4.2 Extrusion-Spheronization

This technique involves the formation of pellets coated with a candidate drug that can be filled into a capsule. Spheronization is a rapid method to produce spherical pellets of uniform size and shape as well as smooth surfaces. Spheronization enables the spraying of an even film coating. This technique is often used in the pharmaceutical industry for drug encapsulation and subsequent tableting of drug products.

The required conditions for this process are good deformation and binding properties of the material, and the ability to plastically deform. The technology of low pressure extrusion and spheronization is a fast procedure for continuous pelletization. The disadvantage of this technique is that it is a tedious process and requires specialized equipment.

One of the major techniques employed for the synthesis of hydrogels involves the formation of crosslinked linear or branched polymers using crosslinking reagents such as divalent/trivalent ions or ultraviolet light (Figure 2.1).

2.4.3 Crosslinking Technology

Crosslinks can be formed with many di-functional compounds capable of condensing with the pendant hydroxy groups contained within hydrophilic polymers. The reaction is

normally carried out in solution, although suspension polymerization may also be used to form crosslinked matrices. The solvent is typically water, although other solvents such as alcohols can be used (Thanoo et al., 1992).

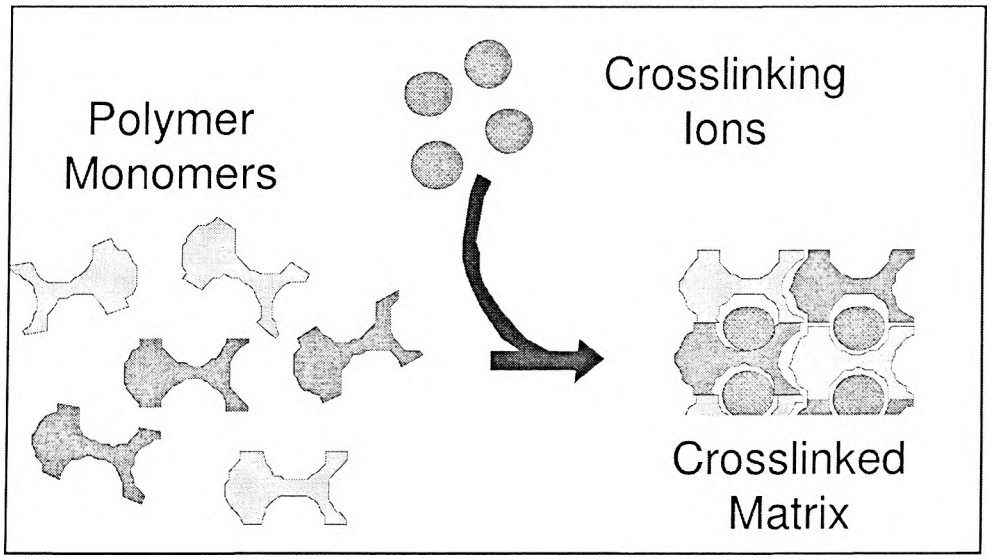

Figure 2.1 Schematic illustrating a typical crosslinking process (source: http://www.labsearch.org).

The extent to which the resulting gel is crosslinked is typically defined in terms of the nominal crosslink ratio, X (Ravve, 2000). This parameter is defined as the ratio of the moles of the crosslinking agent used to the moles of polymer repeating units present. A nominal number-average molecular weight between crosslinks, M_c, can be related to X as follows for di-functional crosslinkers:

$$M_c = M_r/2X \qquad \textit{(Equation 2.5)}$$

where M_r is the molecular weight of the repeating unit.

When polymerization proceeds in a three-dimensional manner, some period after it has progressed to a certain threshold, gelation occurs. This well-defined transition during

polymerization is known as the gel point and at this point the reaction mixture changes from a viscous liquid to an elastic gel (Ravve, 2000).

The present study extensively explores this method for the formation of "intelligent" polymeric materials.

2.5 Hydrational Dynamics within Polymers

Drugs administered should ideally be delivered at a predetermined rate into the systemic circulation. If the delivery rate is lower than this ideal rate, the drug-plasma level may be below the minimum effective concentration (MEC). On the other hand, if the delivery rate is above this ideal rate, there is a risk of central and local effects. This may even lead to toxic effects due to the drug-plasma level spiking above the maximum safe concentration (MSC) (Figure 2.2a,b).

Essentially, drugs should be delivered at a constant rate for the attainment of zero-order kinetics. Over the years, several mechanisms have been studied to obtain zero-order kinetics, including osmosis, erosion, diffusion, swelling and/or a combination of these processes (Davis et al., 1986; Colombo et al., 1987).

In addition, various physical designs have been developed, namely bilayer and triple layer technology (Colombo et al., 1987). In the case of swelling-controlled systems polymeric matrices are loaded with drug uniformly dispersed within the matrix.

In the case of partially or completely crosslinked systems, strong secondary bonds with such aqueous media. Water in effect acts as a plasticizer and lowers the T_g of the glassy polymer below room temperature and hence converts it into its rubbery state.

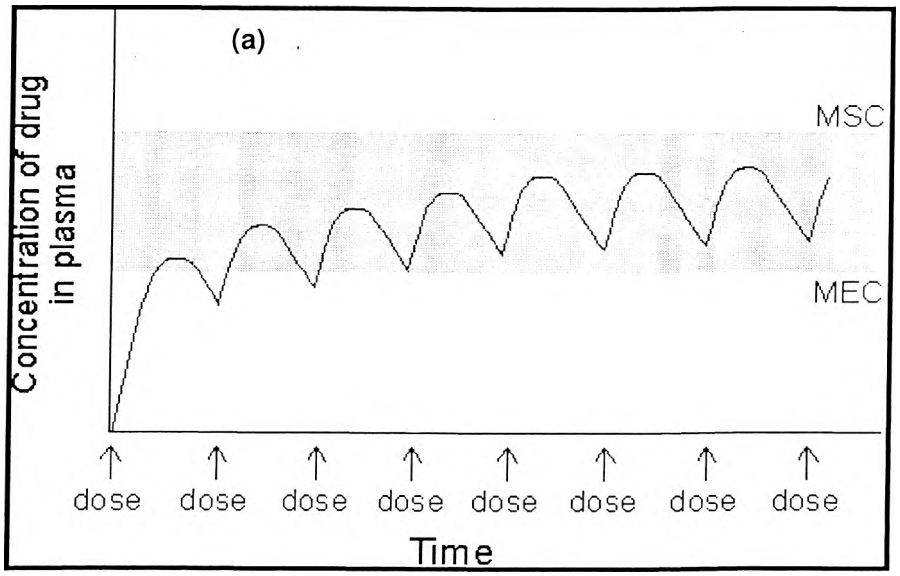

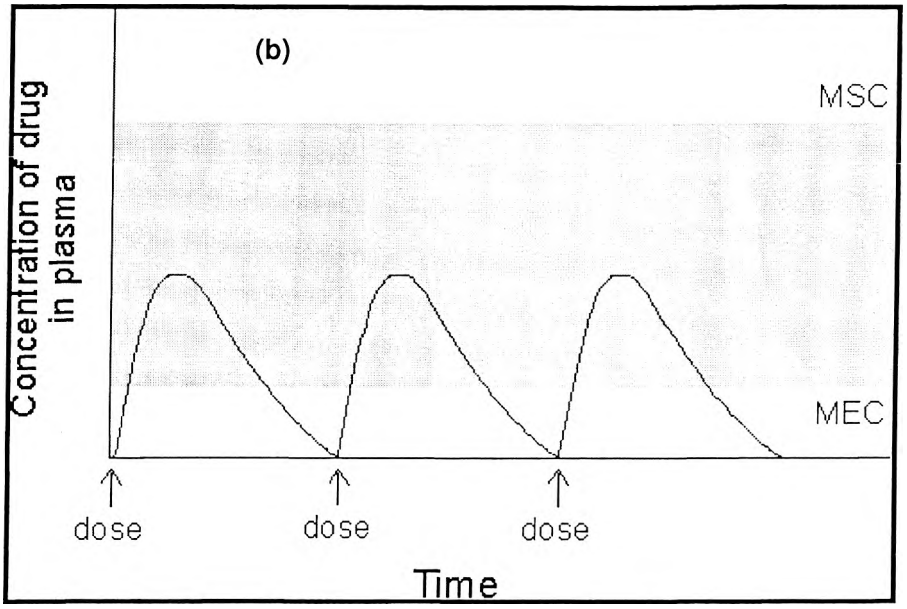

Figure 2.2 Drug plasma concentration-time curve after the administration of (a) Eight, and (b) Three equal oral doses (MSC = Maximum Safe Concentration; MEC = Minimum Effective Concentration) (source: http://www.as.dmu.ac.uk/pharmscape/tour_6.htm).

As the water diffuses into the polymeric matrix a boundary is formed, namely the swelling front. This front separates the glassy phase from the rubbery phase. Within the rubbery phase, the matrix contains both dissolved and undissolved drug. The boundary between these entities is referred to as the diffusion front. In addition, there is an erosion front at the peripheral surface as the polymer subsequently erodes.

2.5.1 The Homogeneous Swelling Model

This model proposed by Siepmann and co-workers (1999) employs diffusion to simulate water penetration into the matrix. Based on the concentration profile at an instantaneous time, an estimate of the volume of water within the matrix can be calculated. The total volume is assumed to be the sum of the initial polymer volume and the calculated volume of water. In this model, the entire polymer swells even if water has only penetrated a short distance into the matrix.

2.5.2 The Sequential Layer or Non-Homogeneous Swelling Model

In a more recent model by Siepmann and Peppas (2001), a variation of the above homogeneous model is proposed. The assumption is that the polymer matrix is composed of a series of sequential layers which swell one after the other, as in the case of the homogeneous model. Both of these models assume the existence of a concentration-dependent diffusion gradient for water.

However, an ideal model should account for the occurrence of simultaneous swelling, diffusion and erosion which provides a way to simulate non-instantaneous drug dissolution by modelling a dissolution zone between the swelling and diffusion fronts, and not having to make assumptions about homogeneous or heterogeneous swelling (Yang and Fassihi, 1997).

2.5.3 The Power Law Model

This equation describes the diffusion of drug through polymeric materials (Ritger and Peppas, 1987):

$M_t/M_\infty = k_1 t^n$ *(Equation 2.6)*

where M_t and M_∞ are the amounts of drug released at time t and the total amount of drug within the polymer, k_1 is a release constant and n is a release exponent indicative of the profile shape.

2.5.4 The Peppas-Sahlin Model

This model (Peppas and Sahlin, 1989) accounts for polymer matrices that undergo both diffusion and relaxation during drug release. The release kinetics of the drug is explained by the following mathematical expression:

$M_t/M_\infty = k_1 t^n + k_2 t^{2n}$ *(Equation 2.7)*

where in this case k_2 is a relaxation constant.

2.5.5 The Hopfenberg Model

This model (Hopfenberg, 1976) was developed for polymeric matrices exhibiting surface erosion. Essentially polymers erode by two distinct mechanisms, bulk erosion and surface erosion. In surface erosion, the rate at which the polymer transforms into a water-soluble material is more rapid than the rate at which water penetrates into the polymer. This means that the device thins out but still maintains its structural integrity (Katzhendler et al., 1997). In this model drug release from erodible slabs, cylinders, and spheres are described as follows:

$M_t/M_\infty = 1 - (1 - K_1 t)^n$ *(Equation 2.8)*

where in this case K_1 is an overall erosion rate constant.

2.6 Criteria for Determination of Model Suitability

In practical data analysis, it is always unclear which as to which model provides the best fit. The general tendency is to use familiar functions, but their accuracy and applicability may be questionable.

In this work, the fit of data to the above models were determined by the Akaike information Criterion (AIC), Schwartz Criteria (SC), and Condition Number (CN). Pillay and Fassihi (1999a) have detailed the importance of these three critical parameters in the selection of appropriate model fitting.

Chapter Three

Design of Experiments: A Statistical and Mathematical Approach to Optimization of Function Variables

3.1 Introduction

Experimental design is one of the first and most important stages of any scientific study. It helps in constructing a precise mathematical description of the process in the region of experimentation through conducting a statistical analysis and finally selecting the shortest path to process optimization (Hendrix, 1979; Semval, 1997; Schwartz et al., 2002).

This is the stage where questions like what factors influence product yield, what parameters determine product purity, what variables or conditions are responsible for the outcome of a given test and what is their precision, are asked.

Pharmaceutical formulation and process problems are normally characterized by multiple objectives. In designing a pharmaceutical product, for example, the scientist must often meet pre-set control limits, which define or influence such a dosage form, for example unit cost, physical stability, chemical stability, or bioavailability of the active ingredient.

The parameters describing these dosage form characteristics represent response or dependent variables, and any limits or conditions placed on these response variables represent the objectives. The magnitude of the observed value for each response variable generally depends upon levels of one or more of the controllable (independent) variables.

3.2 Selection of the Design

Selection of an appropriate experimental design depends on the objectives of the

experiment and the number of factors to be investigated.

Since laboratory experimentation is often very expensive and time consuming, planning of an optimum number of experiments is crucial. The statistical design of experiments is a procedure for conducting the minimum number of trial experiments for obtaining the optimal conditions of the variables or factors for a response. The levels of a factor range from low to high.

Some known techniques of statistical experimental design are Factorial Analyses, Plackett-Burman Matrices and Response Surface Methods, but the most commonly employed approach is the Factorial Analysis at two levels (2^N). The two-level Factorial Design allows for an evaluation of N variables and their interactions, by changing them at two levels (low and high). The statistical analysis of the results allows for the determination of their significance and the determination of an experimental equation which associates the variables with the results. However, with an increase in the number of experiments, the increased output of useful information may be doubtful. This is due to the fact that the third and higher order interactions are generally statistically and physically insignificant, hence the choice of Fractional-Factorials instead of Full-Factorials are often selected (Gohel and Amin, 1999).

3.3 Experimental Design Objectives

3.3.1 Comparative Objective

If one or several factors are under investigation, but the primary goal of the experiment is to make a conclusion about one *a-priori* factor (in the presence of, and/or existence of other factors), the question of interest is whether or not that factor is "significant". This therefore, is a comparative problem requiring a comparative design solution, which ideally is a linear model (e.g. Factorial Design).

3.3.2 Screening Objective

The primary purpose of the experiment is to select or screen out the few important main effects from many less important ones. The Screening Designs are also termed main effect designs (e.g. Plackett-Burman) and are described by linear models.

3.3.3 Response Surface Objective

This high resolution design is employed to estimate interactions and quadratic effects, and therefore provides an idea of the (local) shape of the response surface under investigation. Hence such designs termed Response Surface Methods. These methods are used to:

(i) Find improved or optimal process settings,

(ii) Troubleshoot process problems and weak points, and

(iii) Make a product or process more robust against external and non-controllable influences (robust meaning relatively insensitive to these variables).

3.3.4 Optimal Fitting of a Regression Model Objective

This is for modelling a response as a mathematical function (either known or empirical) of a few continuous factors. This provides "good" model parameter estimates (i.e. unbiased and minimum variance).

3.4 Design Selection

Table 3.1 Criteria for Selection of an Experimental Design

Number of Factors	Comparative	Screening/Factorial	Response Surface
1	1-Factor completely randomized design	None	None
2-4	Randomized block design	Full Factorial	(a) Central Composite (b) Box-Behnken
>5	Randomized block design	(a) Plackett-Burman	None

3.4.1 Types of Factorial Designs

3.4.1.1 Full-Factorial Design

This design tries every possible combination of all the parameters under investigation. The disadvantage of this method is that the number of experiments may be too large and hence too costly. There are three ways to solve the above problem namely, reduce the number of levels of each parameter, reduce the number of parameters, or use a Fractional-Factorial.

3.4.1.2 Fractional-Factorial Design

This is a Factorial experiment in which only an adequately chosen fraction of the treatment combinations required for the complete factorial experiment is selected. This technique is often used for product and process design as well as process troubleshooting. Based on the result of fractional experiments, input factors can be identified and then investigated more thoroughly in subsequent high resolution designs.

3.4.2 Types of Response Surface Methods

Response Surface Methods are based on the fundamental assumption that the influence of the random input variables on the random output parameters can be approximated by a mathematical function. Hence, Response Surface Methods locate the sample points in the space of random input variables such that an appropriate approximation function can be found most efficiently; typically, this is a quadratic polynomial. Therefore, a Response Surface analysis consists of two steps:

(i) Performing the simulation loops to calculate the values of the random output parameters that correspond to the sample points in the space of random input variables, and

(ii) Performing a regression analysis to derive the terms and the coefficients of the approximation function.

The fundamental idea of Response Surface Methods is that once the coefficients of a suitable approximation function are found, one can directly use the approximation function instead of looping through the finite model elements.

3.4.2.1 Central Composite Design

These types of experimental designs are variants of the Response Models of the second order. The design consists of three types of points namely, axial points (2^N axial points are created by a screening analysis), cube points (2^N cube points are derived from a Full-Factorial Design), and centre points (points in the centre are created by a nominal design). There are three types of Central Composite Designs (Figure 3.1) namely, Central Composite Circumscribed (CCC), Central Composite Inscribed (CCI) and Central Composite Face-Centred (CCF). The CCD is used to determine the coefficients of a second-order Response Surface Model. The advantage is that a small number of experiments are required. The CCI and CCC are also rotable designs and are preferred when model evaluations are expensive.

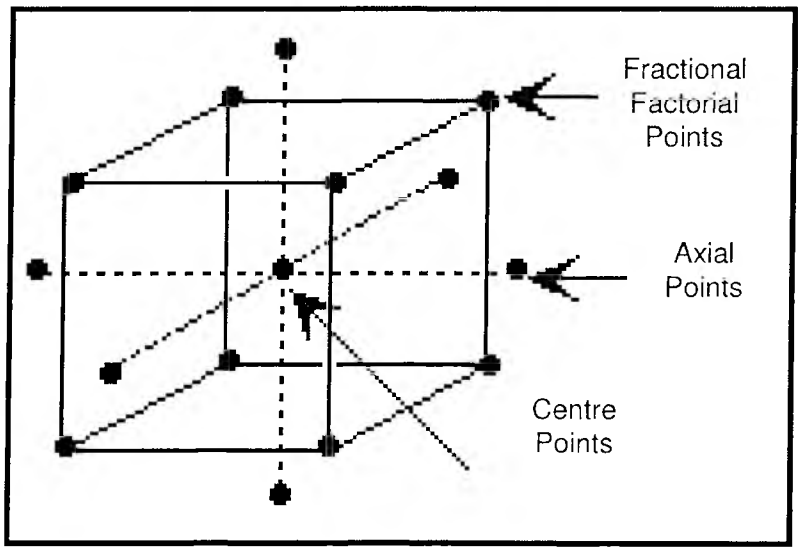

Figure 3.1 Statistical points of a Central Composite Design (source: http://www.jmp.com/product/design_of_experiments/optimum.shtml).

3.4.2.2 Box-Behnken Design

This design does not have simple matrix generators; instead it is constructed by combining two-level Factorials with incomplete block designs. It also has complex confounding of interactions. The design is economical and therefore particularly useful when it is expensive to perform necessary experimental runs.

3.4.2.3 Advantages of Response Surface Methods

(i) They often require fewer simulation loops than a Monte Carlo Simulation method,

(ii) They can evaluate low probability levels,

(iii) The goodness-of-fit parameters provide a good approximation function as to how accurate the approximation function describes the "true" response parameter values. The goodness-of-fit can provide a warning of when the approximation function is insufficient, and

(iv) The individual simulation loops are inherently independent. This makes the Response Surface Method an ideal candidate for parallel processing.

3.4.2.4 Disadvantages of Response Surface Methods

(i) The number of required simulation loops depends on the number of random input variables, implying that if there is a large number of random input variables then a probabilistic analysis would be impractical, and

(ii) These methods are not suitable for cases where a random output parameter is a non-smooth function of the random input variables.

3.4.3 Types of Screening Designs

The screening analysis creates 2^N sample points. These points are defined by the rule that one of the parameters has a minimum or maximum value, while all other parameters have nominal values.

3.4.3.1 Plackett-Burman Design

An example of a screening technique is the Plackett-Burman Design shown below:

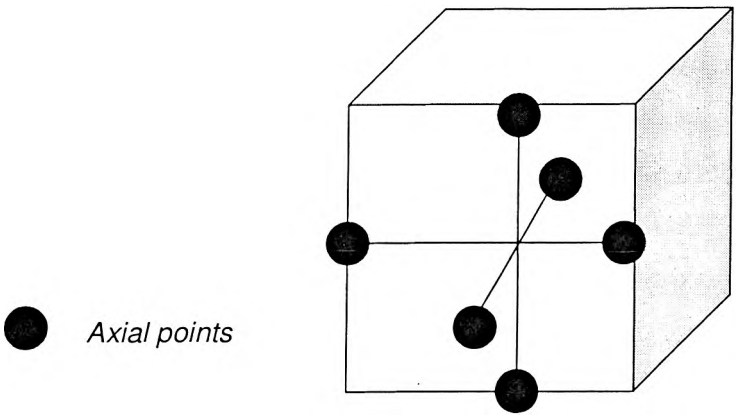

Figure 3.2 Statistical points of a Plackett-Burman Design.

When one requires to screen a large number of factors to identify those that may be important (i.e. those that are related to the dependent variables of interest), one should employ a design that allows one to test the largest number of main factor effects with the least number of observations. Such designs confound all interactions with new main effects. Hence such designs are sometimes called saturated designs, since all information in those designs is used to estimate the parameters, leaving no degrees of freedom to estimate the error term for the analysis of variance (ANOVA). Therefore, this approach provides efficient estimations, ignores interactions and is used in a matrix form.

Chapter Four

Testing the Utility of a Two-Level Screening Design for the Formulation and Optimization of a Novel Crosslinked Delivery System for *Mentha piperita* Oil

4.1 Introduction

Irritable bowel syndrome (IBS), a functional disorder of the intestines, is characterized by severe abdominal cramps and constipation with alternating periods of diarrhoea. Population-based studies in the United States estimate the prevalence of IBS at 10-20% and the incidence at 1-2% per year. An estimated 20-50% of gastroenterology referrals relate to this symptom-complex (Madden and Hunter, 2002).

The primary cause of IBS appears to be related to altered intestinal motility patterns. Patients experience rigid contractions and pain in the bowel, which are responsible for the sensation of bloating, discomfort, and urgency, a symptom-complex also enforced by the hypothesized "brain-gut-axis" theory (Allescher, 2003; Dunn et al., 2003). In general, smooth muscle relaxants are beneficial in the treatment of abdominal pain associated with IBS. Over the years many drug classes have been used for the alleviation of IBS symptoms, including antidiarrhoeals, antiflatulants, anticholinergics, opiates, low-dose antidepressants and most recently serotonin antagonists. The use of latter drug class had generated significant controversy based on reports which have shown an increased incidence in abdominal surgeries in patients with pre-exiting IBS (FDA, 2002).

In recent years there has been a shift towards the use of natural products for IBS therapy, a frequent trend observed in the treatment of many other disease conditions. *Mentha piperita* oil, an essential oil, also commonly known as peppermint oil, is obtained from the leaf of the peppermint oil plant which geographically is found in a myriad of species [e.g. *Mentha x piperita* (Lamiaceae)]. The distinct pungent mint odour of *Mentha piperita* is

emitted from the leaf's secretory glands, as shown in the scanning electron micrograph (Figure 4.1). Multi-centre clinical trials have demonstrated significant alleviation of the symptoms manifested in IBS through use of *Mentha piperita* oil. Specifically the ability of the oil to alleviate IBS-induced abdominal pain and distension is related to its blockade of calcium influx, thereby inhibiting abnormal smooth muscle contraction of the colon (Hills and Aaronson, 1991; Beesley et al., 1996).

Furthermore, it is known that overgrowth of enteric bacteria exacerbates the IBS symptom-complex by fermentation of ingesta, which leads to elevated production of gas (King et al., 1998; Zar et al., 2002). This gas becomes locked in the colon and hence extends to increased abdominal pain and cramps. The main component of *Mentha piperita* oil, menthol, has been shown to have profound antimicrobial effects (Pattnaik et al., 1997). This pharmacologic action may consequently be manipulated to suppress the overgrowth of gas-forming enteric microbes.

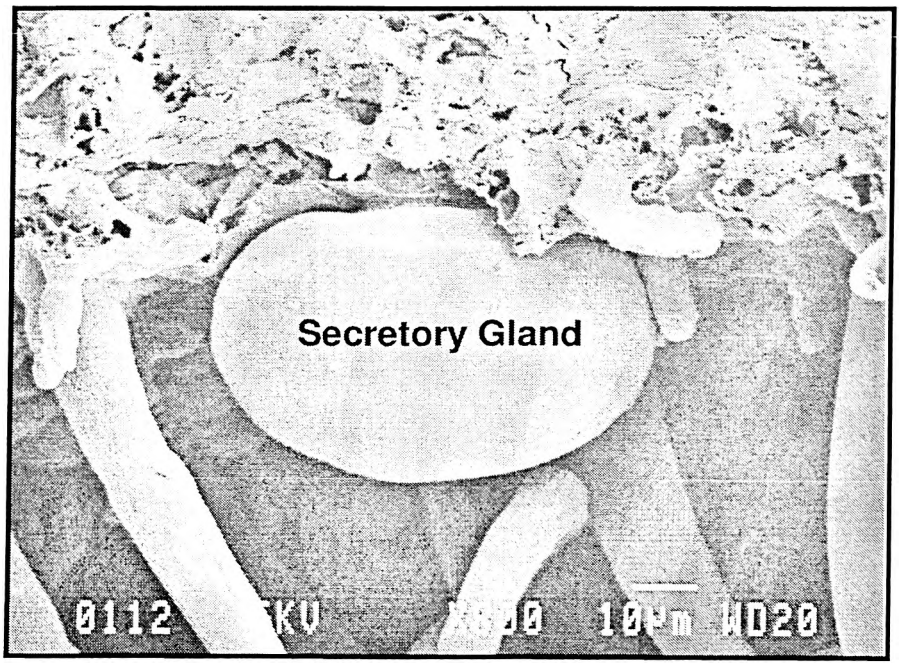

Figure 4.1 Scanning electron micrograph of the secretory gland embedded in the leaf of the *Mentha piperita* oil plant.

In the present study, the design and development of a novel crosslinked calcium-aluminium-alginate-pectinate oilisphere complex was undertaken to achieve site-specific delivery of *Mentha piperita* oil conducive to microenvironmental conditions simulating the proximal and distal intestine, including the colon. Enteric delivery of this oil is essential for three reasons since: (i) contact with the gastric mucosa results in muscle relaxation and hence severe oesophageal reflux; (ii) it is hydrolyzed at gastric pH; and (iii) treatment should be localized to the afflicted region of the gut, namely the intestine and colon. Currently, enteric coating of monolithic dosage forms is the most widely used approach to achieve intestinal delivery of *Mentha piperita* oil (Liu et al., 1997; Kline et al., 2001; Micklefield et al., 2003; Weydert et al., 2003). One of the key problems with monolithic drug delivery systems is their unpredictable and erratic gastrointestinal transit times, which is compounded by variable gastric emptying rates. In IBS patients this rate is furthermore largely influenced by the hypothesized "brain-gut axis" relationship (Rosemore and Lacy, 2002; Wood, 2002; Nakai and Kumakura, 2003). Decreased amplitude and cycle length of migrating motor complexes and increased frequency of clustered contractions are observed in IBS patients. Traditionally, this erratic rate of gastric emptying has more negatively impacted the responses elicited by enteric-coated systems such as tablets and softgels. Erratic emptying behaviour of monolithic dosage forms, which do not disintegrate in the stomach, can lead to variable absorption and pharmacologic response.

This study attempts to circumvent the above dilemma through the application of novel multiple-unit technology that would deliver an appropriate dose of *Mentha piperita* oil in a predictable time to the intestine. In general, it is well-recognized that multiple-unit systems have the following advantages: (i) demonstration of predictable gastrointestinal transit times since each unit is independent from the contraction/relaxation activities of the cardiac and pyloric sphincters of the stomach, (ii) less localized gastrointestinal disturbances due to their dispersive capability, and (iii) provide predictable site-specific

drug targeting based on the application of pH-dependent polymers in their formulation.

In the present study, we postulate that in IBS patients, where treatment of a massive membranous surface is required, the rate and site at which the drug is delivered will have a significant impact on the success of the therapy. The dispersive capability of swellable multiple-unit matrices such as the proposed oilisphere system in this work, will allow for more extensive interaction between the intestinal membrane and oil, instead of the localized effect achieved with traditional monolithic preparations.

Hence, to achieve the objective of this study, a Plackett-Burman design was adopted. The application of this optimization technique would provide an efficient and economical method to acquire the necessary information to understand the relationship between the controllable (independent) and performance (dependent) variables. The independent variables that were evaluated included different levels of alginate and/or pectin exposed to varying reaction times in an aqueous calcium chloride, aluminium chloride and/or aluminium sulphate crosslinking solution. The responses measured from these reactions included matrix resilience, hardness, total fracture energy, erosion and the pH-dependent *in vitro* release characteristics. Final formulation selection was achieved using a constrained optimization technique. In addition, Artificial Neural Networks (ANN) was employed as an alternative technique to predict the physicochemical and physicomechanical properties of the oilispheres using the response data derived from the Plackett-Burman design (Sibanda et al., 2004).

4.2 Materials and Methods

A low-viscosity sodium alginate (1%w/v aqueous solution at 21°C 35cP) was obtained from TIC Gums (Maryland, USA). Low methoxyl citrus pectin (degree of esterification 34-38%) was donated by Herbstreith and Fox (Neuenburg/Wurttemberg, Germany). Anhydrous calcium chloride, aluminium chloride and aluminium sulphate were purchased

from Sigma (Missouri, USA). *Mentha piperita* oil (peppermint oil) was obtained from Aromatherapy Oils (Johannesburg, South Africa). Spectrophotometric grade 1-octanol was purchased from Fluka Chemicals (Buchs, Switzerland).

4.2.1 Formulation of Crosslinked Oilispheres

Oilispheres loaded with *Mentha piperita* oil were formulated in accordance with a Plackett-Burman design having polymer/crosslinking agent concentrations/crosslinking reaction times and combinations as depicted in Tables 4.1 and 4.2. The reader is referred to the section on "*Developing the Experimental Design*" for a more comprehensive explanation of Tables 4.1 and 4.2.

Table 4.1 Normalized Factor Levels of the Independent Variables for the Plackett-Burman Design

Variable	Factor level		Units
	-1	1	
Sodium Alginate	0	1.5	%w/v
Pectin	0	1.5	%w/v
Calcium Chloride	0	4	%w/v
Aluminium Chloride	0	4	%w/v
Aluminium Sulphate	0	4	%w/v
Crosslinking Reaction Time	0.5	6	hours

A quantity of sodium alginate and/or pectin (see Tables 4.1 and 4.2) was dissolved in deionised water and made up to volume (100mL). To this solution, 50mL of *Mentha piperita* oil was added. Thereafter this multi-component solution was gently homogenized for 2 minutes to produce a polymer-oil emulsion (Vortex-Mixer model 947, England). The crosslinking solution was prepared by dissolving an appropriate quantity of calcium chloride, aluminium chloride and/or aluminium sulphate (see Tables 4.1 and 4.2) in deionised water and made up to 1000mL.

Table 4.2 The Plackett-Burman Matrix

Oilisphere Formulation	Run Order	Sodium Alginate (%w/v)	Pectin (%w/v)	Calcium Chloride (%w/v)	Aluminium Chloride (%w/v)	Aluminium Sulphate (%w/v)	Crosslinking Reaction Time (hours)
F1	7	0	1.5	4	4	0	6
F2	11	1.5	0	4	0	0	0.5
F3	6	1.5	0	0	0	4	6
F4	12	0	1.5	0	0	0	6
F5	14	1.5	1.5	0	4	0	0.5
F6	2	1.5	1.5	0	4	4	0.5
F7	5	0	0	0	0	0	0.5
F8	9	1.5	0	4	4	0	6
F9	3	0	0	4	4	4	0.5
F10	13	0.75	0.75	2	2	2	3.25
F11	4	0.75	0.75	2	2	2	3.25
F12	8	0	0	0	4	4	6
F13	10	1.5	1.5	4	0	4	6
F14	1	0	1.5	4	0	4	0.5

Oilispheres were formed by carefully titrating the above polymer-oil emulsion at 2mL/minute into the crosslinking solution by means of a 6-channel peristaltic pump (Desaga, Heidelberg) fitted with Pharmed® tubing (Cole-Parmer, USA) having a flat-tip 19-guage opening. On completion of the titration process, the formed oilispheres were agitated in the crosslinking solution for an additional 30 minutes. Thereafter, the oilisphere matrices were allowed to cure under dark conditions (±21°C) for a predetermined period of time (see Tables 4.1 and 4.2). Following this curing phase, the crosslinking solution was decanted and the oilispheres were washed with 3x500mL volumes of deionised water. The oilispheres were then air dried at ±21°C for 48 hours under an extractor.

4.2.2 Physicomechanical Analysis of Crosslinked Oilispheres by Textural Profiling

To determine the resilience behaviour, fracture energy, and matrix hardness of the oilispheres, a TA.XT.*plus* Texture Analyzer (Stable Micro Systems, England) fitted with a 36mm cylindrical steel probe and 5kg load cell was used. In order to determine the effect of hydration of the oilispheres on resilience behaviour, a modified USP 25 rotating paddle

method was used to hydrate the oilispheres (Pillay and Fassihi, 1998). The oilispheres were placed in dissolution vessels containing 900mL phosphate buffer at pH 6.8 maintained at 37°C. At appropriate time intervals (up to 5 hours) the oilispheres were removed from the medium and analyzed in accordance with the textural parameters listed in Table 4.3. At each sampling point a quantity of 10 oilispheres were analyzed. The fully integrated data acquisition, analysis and display software i.e. Texture Exponent Version 3.2 (Stable Micro Systems, England) was employed. Data acquisition was performed at 200 points per second.

Table 4.3 Textural Parameters Employed for Total Fracture Energy, Matrix Hardness and Resilience Testing

1 Parameters	Total Fracture Energy and Matrix Hardness Settings	Resilience Settings
Pre-test speed	1 mm/s	1 mm/s
Test speed	0.2 mm/s	0.2 mm/s
Post test speed	0.2 mm/s	0.2 mm/s
Compression force/distance	60N	50% strain
Trigger type	Auto	Auto
Trigger force	0.5 g	0.5 g
Load cell	5kg	5kg

Figure 4.2 depicts typical force-distance profiles used to determine the responses mentioned in Table 4.3. Figure 4.2a depicts the calculation of matrix resilience, which is provided by the ratio of the AUC between anchors 2 and 3, and 1 and 2. An anchor may be defined as a perpendicular drop to divide area boundaries.

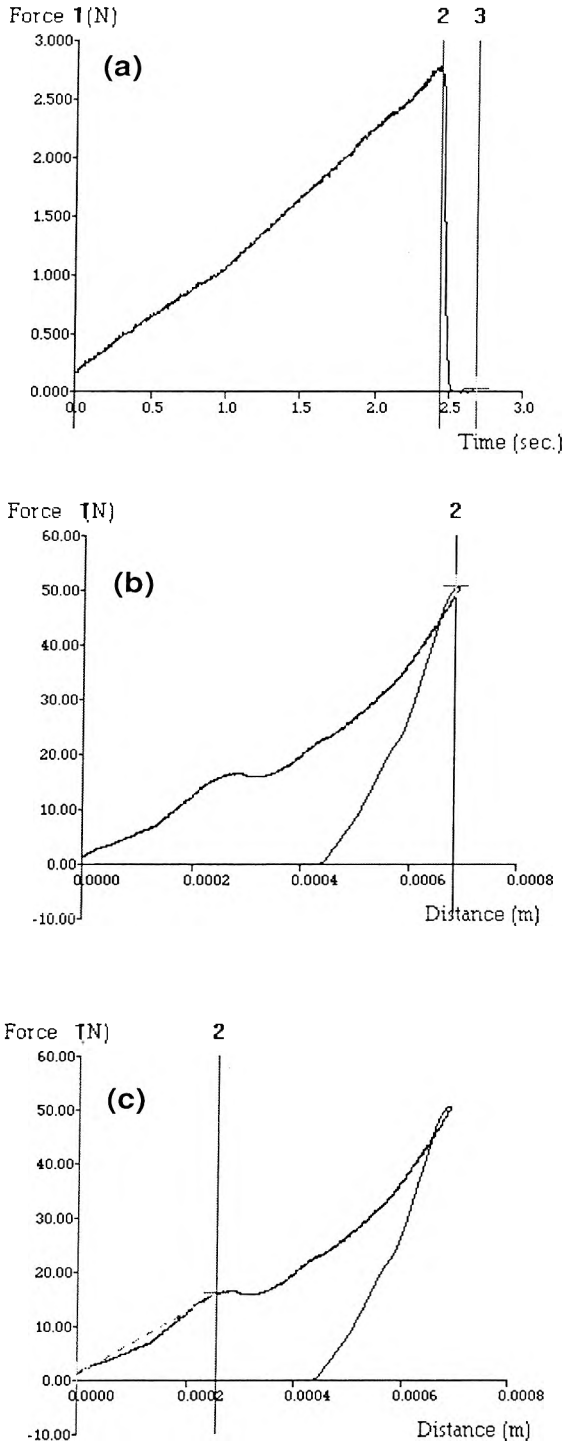

Figure 4.2 Typical textural analysis force-time and force-distance profiles of crosslinked oilispheres for the determination of: (a) Matrix resilience, (b) Total fracture energy, and (c) Matrix hardness. (In all cases it was observed that SDs<0.03 were obtained, N=10).

Figure 4.2b indicates the calculation of total fracture energy, which is provided by the total AUC for a force-distance profile resembling the various phases of matrix fracture (i.e. AUC between anchors 1 and 2). The first break in the upward gradient is indicative of a primary facture or rupture phase which results in a force reduction. However, on further application of force, the residual unfractured material undergoes complete rupture, and hence the force peaks at 60N. Figure 4.2c depicts the calculation of matrix hardness which is indicated by the steepness of the upward gradient up to the primary fracture phase, namely between anchors 1 and 2. In general, a steeper gradient indicates a harder matrix.

4.2.3 Developing the Experimental Design

A Plackett-Burman design was developed in this study to screen, evaluate and eventually optimize a preliminary formulation from several crosslinked polymeric matrices comprised either singly, or in combination, of sodium alginate and/or pectin. The normalized factor levels for the independent variables (concentrations of polymer/s, crosslinking agents and duration of crosslinking reaction time) are shown in Table 4.1. Unhydrated matrix resilience (%), hydrated matrix resilience (%) in buffer media pH 3 and 6.8, matrix hardness (N/m), total fracture energy (Joules) and normalized matrix erosion in buffer media pH 3 and 6.8 were selected as the dependent variables (responses) in order to evaluate the physicochemical properties of the crosslinked matrices. The screening matrix was compiled using Microsoft Excel 2002 Macros (Office XP, 2002) namely Essential Regression and Experimental Design software Version 2.2 (Pennsylvania, USA). The generated matrix required 14 experimental runs including 2 centre points (also referred to by oilisphere formulation number, *F#*), which are depicted in Table 4.2. The formulations were produced and tested in a random sequence. The regression model (Equation 4.1) encompassing 7 linear terms was as follows:

$$Response = b_0 + b_1*[SA] + b_2*[P] + b_3*[CC] + b_4*[AC] + b_5*[AS] + b_6*C \quad \textit{(Equation 4.1)}$$

where the terms in parenthesis represent the concentrations of polymers and crosslinking agents, $b_0....b_6$ are the regression coefficients of the system, SA = sodium alginate, P = pectin, CC =calcium chloride, AC = aluminium chloride, AS = aluminium sulphate, and CRT = crosslinking reaction time.

4.2.4 Oilisphere Size Analysis

The various oilisphere formulations were subjected to particle size analysis by employing a nest of sieves ranging from 5000-150μm agitated on a sieve shaker set at medium amplitude for 5 minutes (Octagon 200 Test Sieve Shaker, Endecotts Ltd., England). The various size fractions were stored separately in glass vials until further use.

4.2.5 Calibration Curve of Mentha piperita Oil in 1-Octanol

Mentha piperita oil was dissolved in 1-octanol to produce a series of standard solutions: 0.05, 0.1 and 0.15mg/mL. Their absorbance values were determined at the wavelength maximum of 230nm. Using this information a calibration curve was constructed (Figure 4.3). Note that the buffer, polymers and excipients did not show any absorbance readings or interference at 230nm.

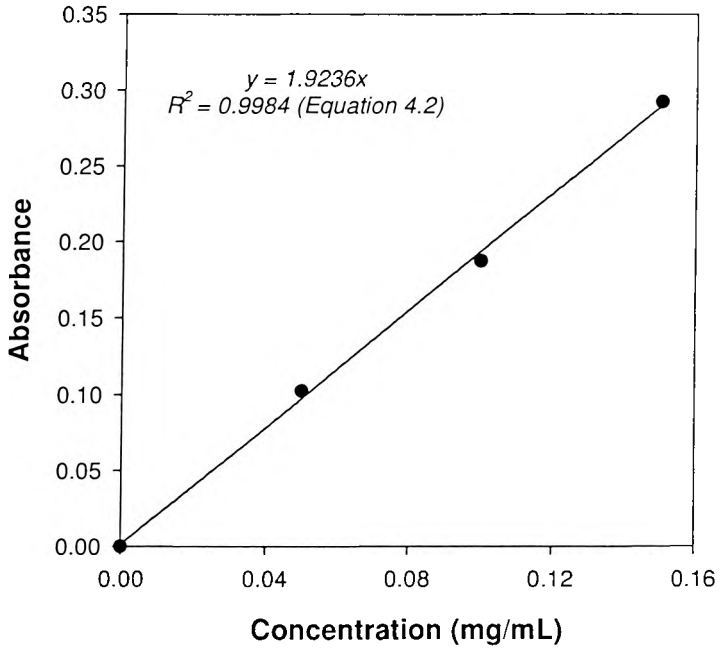

Figure 4.3 Calibration curve of *Mentha piperita* oil in 1-octanol. (In all cases it was observed that SDs<0.01 were obtained, N=3).

4.2.6 Determination of Mentha piperita Oil Encapsulation

50mg of oilispheres from each formulation was triturated in a mortar and pestle to release the oil. To this pulverized mass, 100mL 1-octanol was added to separate the oil and thereafter transferred to a 500mL beaker. 100mL deionised water was added to the 1-octanol phase to dissolve any remaining polymeric fragments in order to ensure complete release of the oil. The 1-octanol-water combination was gently magnetically stirred for 1 hour to facilitate the complete diffusion (partitioning) of oil into the 1-octanol phase. This two-phase system was allowed to stand for a further hour. 5mL samples were withdrawn from the 1-octanol layer and analyzed by ultraviolet spectroscopy at 230nm for oil content (Beckman DU 650 ultraviolet spectrophotometer). All determinations were performed in triplicate.

The encapsulation efficiency was determined by using the following equation:

Oil Encapsulation Efficiency = (AQ/TQ) x 100 *(Equation 4.3)*

where AQ is the actual quantity of oil encapsulated within the oilisphere and TQ is the theoretical quantity of oil expected within the oilispheres. Note that drug content determination is inherent in calculating the *AQ* of encapsulated oil.

Among many of the other components, menthol (bioactive agent) was the subject of analysis in *Mentha piperita* oil. A calibration curve of menthol obtained by gas chromatography was validated against ultraviolet spectroscopy and reflected no significant differences ($p<0.05$). Ultraviolet spectroscopy was selected due to ease of manipulation.

4.2.7 In Vitro Release Studies

In vitro release studies (Caleva Dissolution Apparatus, model 7ST) were performed on optimized formulations using a modified USP 25 rotating paddle method in a two-phase media system maintained at 37°C (Pillay and Fassihi, 1998). The lower phase consisted of 350mL USP-recommended buffers of either pH 1.5, 4 or 6.8, while the upper phase consisted of 200mL 1-octanol. The buffers were also chosen to complement the Biopharmaceutics Classification System. The 1-octanol layer served as a sink for *Mentha piperita* oil as its diffusion occurred from the lower to upper phase. Dissolution studies were conducted on a quantity of oilispheres equivalent to 50mg of *Mentha piperita* oil. The oilisphere samples were introduced into the buffer phase below a ring-mesh device (Pillay and Fassihi, 1998) prior to the addition of 1-octanol (Figure 4.4).

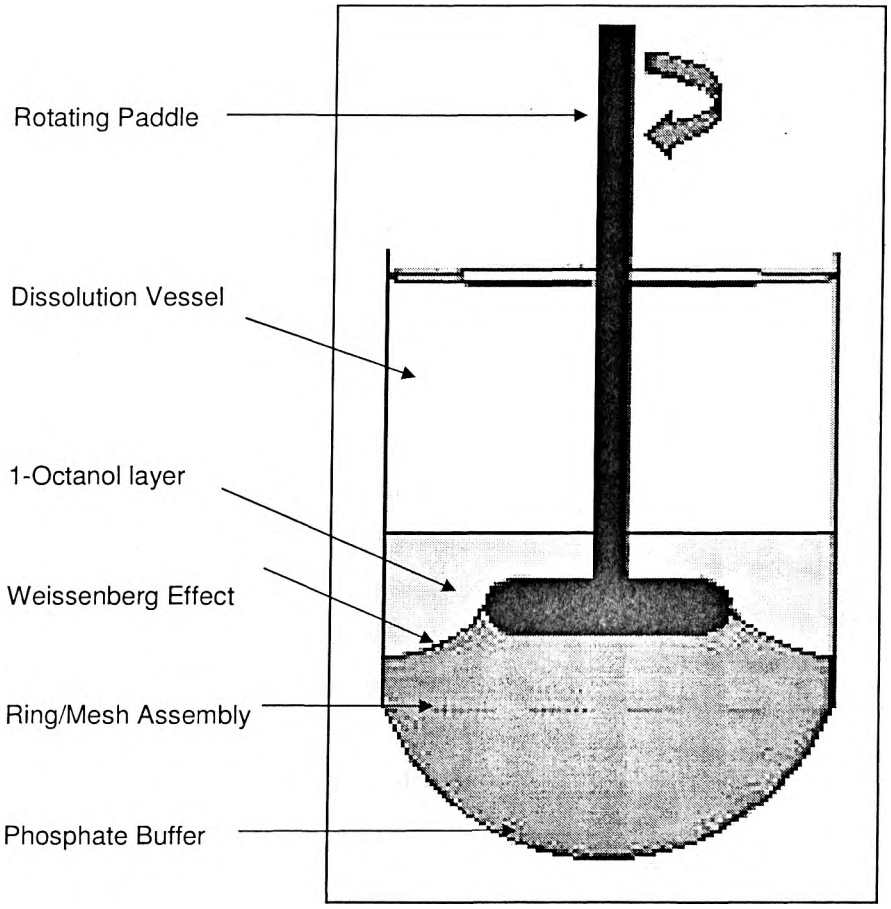

Figure 4.4 Schematic of the two-phase release medium within a dissolution vessel.

The rotating paddles were operated at 50rpm. 5mL samples of 1-octanol were withdrawn at appropriate time intervals over a period of 12 hours and analyzed by ultraviolet spectroscopy at 230nm. An equivalent volume of oil-free 1-octanol was replaced into each vessel sampled. In cases where dilution of samples was required, an appropriate correction factor was employed.

4.2.8 Determination of Matrix Gravimetric Changes

50mg of oilispheres were accurately weighed to four decimals and placed into dissolution vessels containing 500mL buffer of pH 3 and 6.8 maintained at 37°C. The oilispheres were agitated at 50rpm using the above-described modified USP 25 rotating paddle apparatus. The entire quantity of oilispheres remaining in the buffer medium was

removed at appropriate time intervals (up to 8 hours). The oilispheres were placed on pre-weighed petri-dishes and dried to constant weight at 21°C under an extractor. The mass of the dried residue was determined and expressed as the normalized matrix weight change computed from their initial mass deviation. All determinations were performed in triplicate.

4.2.9 Microwell Plate Coating of Oilispheres

A novel fusion coating procedure was developed to attach oil-free crosslinked and uncrosslinked peripheral layers around the oilispheres. Individual oilispheres were introduced into microwells having a 200µL capacity. In the first case, a 2%w/v binary coating solution of a 1:1 combination of alginate and pectin was prepared (viscosity of 920cP at 21°C), of which 50µL was added to each microwell containing an oilisphere. The microwell plate was thereafter agitated on a vortex (Genie Vortex-2, Scientific Industries, USA) for 30 seconds in order to ensure that the oilispheres were completely coated with the binary mixture. This procedure provided an uncrosslinked peripheral layer around the oilispheres. In the second case of attaching crosslinked layers around the oilispheres, the same procedure was applied, except for the addition of 50µL of the crosslinking agent comprised of an aqueous solution of 4%w/v each of aluminium sulphate, aluminium chloride and calcium chloride. After addition of the crosslinking agent the microwell plate was agitated on the vortex for 30 seconds to allow for fusion to occur. The oilispheres (uncrosslinked and crosslinked layers) were then dried at ±21°C for 48 hours under an extractor.

4.2.10 Microbiological Assay of Mentha piperita Oil

Minimum inhibitory concentrations (MIC) were determined for *Mentha piperita* oil against common gas-forming enteric flora: *Proteus vulgaris, Serratia odorifera, Enterobacter, Salmonella typhi, Salmonella enteriditis, Citrobacter, Enterococcus faecalis, Klebsiella*

pneumonia, Candida albicans, Staphylococcus aureus, Escherichia coli and Yersinia enterolitica.

4.2.11 Data Analysis

The Plackett-Burman screening design was built and analysed using the Microsoft Excel 2002 Add-in, Essential Regression and Experimental Design software Version 2.2 (Pennsylvania, USA). Textural analysis of data was performed on Texture Exponent Version 3.2 (Stable Micro Systems, England). Statistical significance was analyzed by a paired two-tailed student t-test at a 95% confidence interval ($p<0.05$) (Microsoft Excel 2002). All least squares analyses performed to determine the mechanisms of *Mentha piperita* oil release was analyzed on WinNonlin Professional Edition Version 3.3 (Pharsight, USA) using the Gaussian-Newton (Levenberg-Hartely approach). Prediction of data by Artificial Neural Networks (ANN) was conducted on NeuroSolutions Version 4.22 (NeuroDimension Inc., USA).

4.3 Results and Discussion

4.3.1 Sieve Analysis

Typically unimodal and bimodal size distributions were observed, showing the 2mm oilispheres as having the highest frequency (Figure 4.5). This size fraction was chosen for all investigations in this study. Bimodal distribution was attributed to deaggregation of the homogenized droplets into smaller and larger populations during the crosslinking process as a result of a high interfacial tension that would be expected between the surface of the aqueous crosslinking solution and the oily residue around the periphery of the droplets.

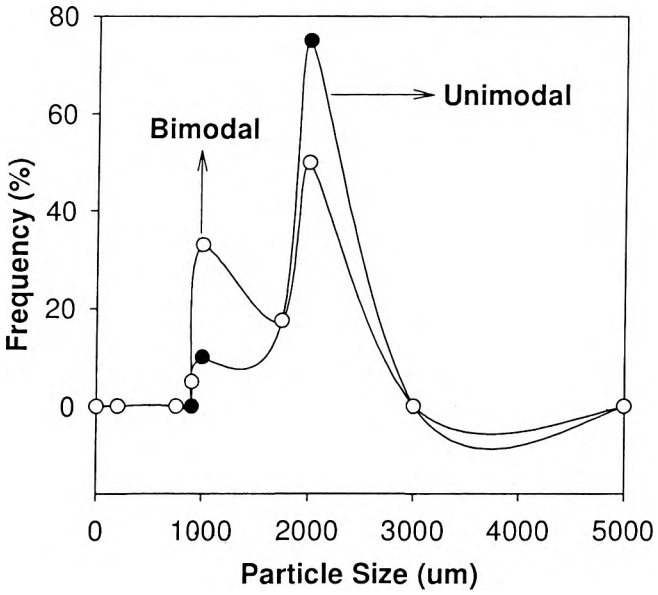

Figure 4.5 Size distributions of the crosslinked oilisphere matrices indicating unimodal and bimodal profiles. (In all cases it was observed that SDs<0.06 were obtained, N=3).

This oily residue may have prevented rapid interaction between the polymer and crosslinking solution, hence leading to heterogeneous separation of a single droplet.

4.3.2 Drug Encapsulation

Encapsulation of *Mentha piperita* oil within the crosslinked matrices ranged between 6-35mg per 100mg oilispheres (Figure 4.6). This was attributed to the differences in the degree of crosslinking and hence the variation in the encapsulation efficiency. Oilispheres with a low crosslink density demonstrated low oil encapsulation. A relationship between specific textural analysis parameters and the degree of crosslinking have already been established (Pillay and Danckwerts, 2002).

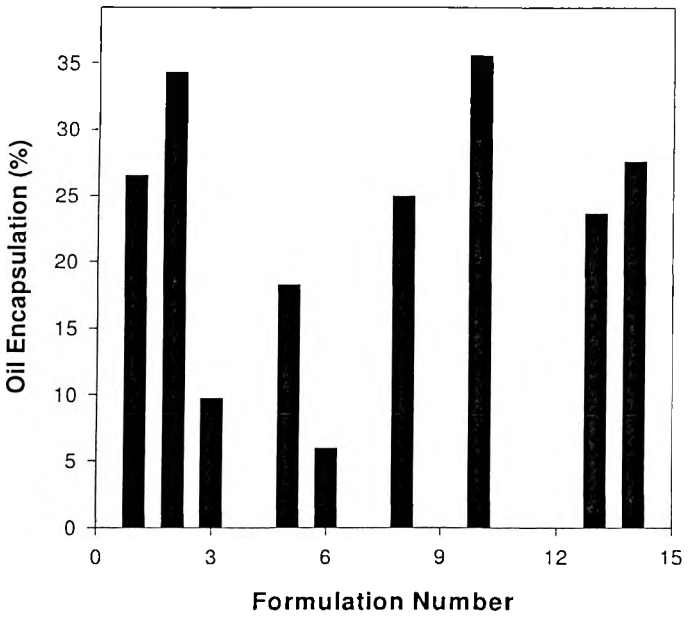

Figure 4.6 Encapsulation efficiency of *Mentha piperita* oil within the crosslinked matrices. (In all cases it was observed that SDs<0.1 were obtained, N=3).

4.3.3 Gravimetric Transitions of the Crosslinked Matrix

It should be noted that matrix erosion can have an impact on the release of drugs and other bioactive substances from their delivery systems. In this study, essentially two types of weight change behaviour were noted upon hydration of the oilispheres in either phosphate buffer pH 3 or 6.8 (Figure 4.7a,b).

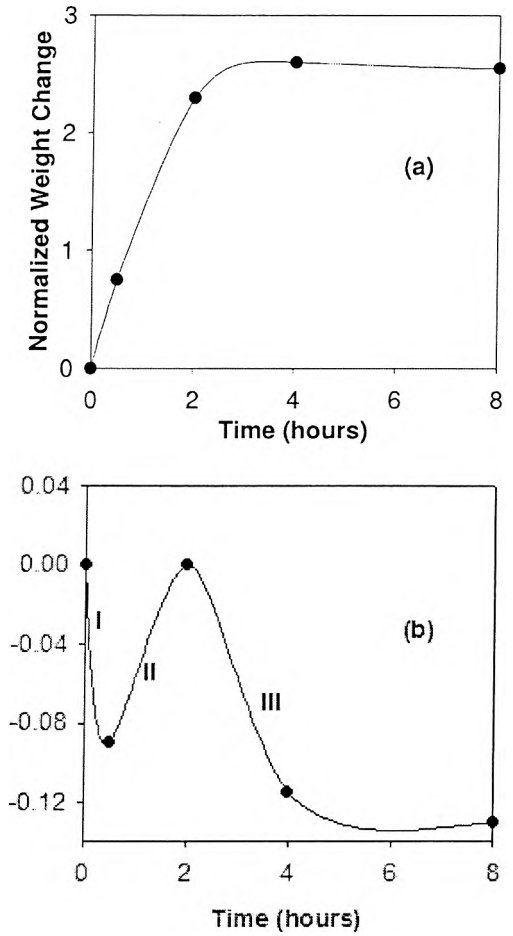

Figure 4.7 Erosional behaviour of the crosslinked oilispheres depicting (a) ion sequestration, and (b) 3 phases of ion loss, sequestration and matrix erosion. (In all cases it was observed that SDs<0.1 were obtained, N=3).

In the first instance there was an increase in the oilisphere weight during the first 2 hours of hydration. This was attributed to the sequestration of phosphate ions from the release medium, which was thereafter followed by a plateau (Figure 4.7a). The ionic threshold concentration for sequestration has previously been mathematically described by Pillay and Fassihi (1999a). Curve-fitting of these data (Figure 4.7a) indicated that such behaviour followed an exponential rise to a maximum (R^2>0.99), as described by the following equation:

$$M_t = M_0(1 - e^{-k_{seq}t}) \qquad \textit{(Equation 4.4)}$$

where M_t = mass of matrix at time t, M_0 = original mass of matrix, and k_{seq} = exponential rate constant of ion sequestration.

In the second instance (Figure 4.7b), three phases were observed. Initially there was a rapid decline in the matrix weight (Phase I), followed by ion sequestration (Phase II) and then rapid erosion to a plateau (Phase III), indicating complete matrix dissolution. Curve-fitting of this data indicated that these phases could be described by the following equations, each producing an R^2>0.99:

- Phase I: Simple exponential loss of soluble ions from the surface of the oilisphere:

$$M_t = M_0 e^{-k_{sol}t} \qquad \textit{(Equation 4.5)}$$

where k_{sol} = first-order solubility constant rate of the ions.

- Phase II: As the oilisphere starts to swell, it exponentially sequesters these ions back into the matrix:

$$M_t = M_0 e^{k_{seq}t} \qquad \textit{(Equation 4.6)}$$

where k_{seq} = exponential rate constant of ion sequestration.

- Phase III: Higuchi-type erosion of the matrix represented by the cube root of time equation:

$$M_t = k_{ero}\sqrt[3]{t} \qquad \textit{(Equation 4.7)}$$

where k_{ero} = matrix erosion rate constant.

4.3.4 Physicomechanical Behaviour of Crosslinked Polymeric Oilispheres

Textural profiling revealed a decrease in the fracture energy, and increase in matrix hardness and resilience, in relation to the statistical combinations and concentrations of the crosslinkers. In general, aluminium chloride and sulphate provided a matrix reinforcing function while calcium chloride principally crosslinked the polymeric system, as determined from preformulation work. Through these preliminary studies the specific crosslinkers were selected as the ionotropic agents in this study.

The crosslinked oilispheres were spherically shaped with a uniform diameter of approximately 2mm. In addition, their surfaces appeared homogeneous and dense. Macros run on Texture Exponent Version 3.2 were able to calculate various parameters namely matrix resilience (unhydrated and hydrated), matrix hardness and total fracture energy. The experimental values for these parameters may be found in Table 4.4, and this clearly outlines that all oilisphere formulations had very low fracture energy values i.e. the matrix was very fragile and hence ruptured upon application of a force of 60N.

4.3.5 Stepwise Regression Analysis

Using Essential Regression and Experimental Design Software, repeated forward and backward stepwise regression was employed to generate the equations for each response parameter which was fitted to a linear polynomial model (Equation 4.1). The predicted and experimental values for each response parameter shown in Table 4.4 is correlated by the Cook's Distance (CD) which essentially measures the overall influence of each observation on the regression coefficients, including the intercept. The CD values presented in Table 4.4 are rounded-off to two decimal places for convenience. The complete values up to six decimal places were used for correlation purposes. Figure 4.8 and 4.9 depict a close correlation between the experimental and predicted data obtained for each of the response parameters in relation to the formulation outlined in the Plackett-Burman design ($p<0.05$). Based on the extreme intra-response variability (Table 4.4) it is

evident that crosslinking significantly changes the matrix structural-dynamics.

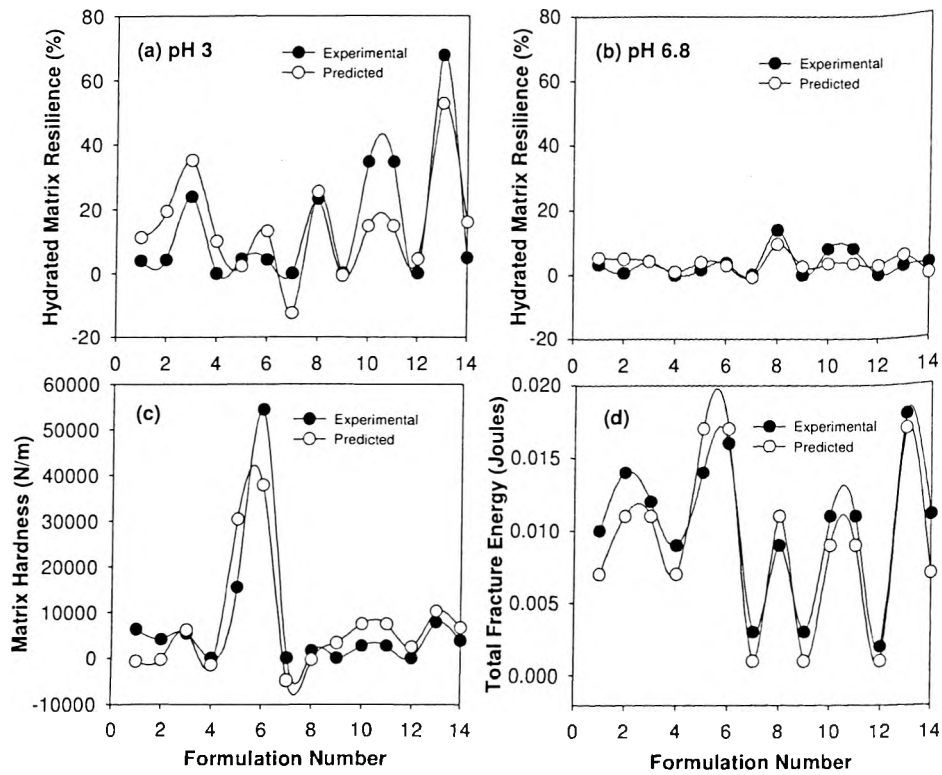

Figure 4.8 Correlation between experimental data and values predicted by the response models for: (a) hydrated matrix resilience in buffer medium pH 3, (b) hydrated matrix resilience in buffer medium pH 6.8, (c) matrix hardness, and (d) total fracture energy. Note that the unhydrated matrix resilience (not shown) was overall ≈20% higher than that of the hydrated matrices. (In all cases for the experimental studies it was observed that SDs<0.02 were obtained, N=10).

Table 4.4 Correlation between Predicted and Experimental Responses Generated from the Plackett-Burman Design

Oilisphere Formulation	Unhydrated Matrix Resilience			Hydrated Matrix Resilience pH 3			Hydrated Matrix Resilience pH 6.8			Matrix Hardness			Total Fracture Energy			Normalized[4] Matrix Erosion pH 3			Normalized Matrix Erosion pH 6.8		
	Exp[1] (%)	Pred[2] (%)	CD[3]	Exp (%)	Pred (%)	CD	Exp (%)	Pred (%)	CD	Exp (N/m)	Pred (N/m)	CD	Exp (J)	Pred (J)	CD	Exp	Pred	CD	Exp	Pred	CD
F1	8.48	27.92	0.32	3.98	11.18	0.08	3.22	5.28	0.10	6341.82	-674.55	0.22	0.010	0.007	0.04	0.301	0.141	0.03	0.561	-1.131	0.03
F2	3.08	38.11	0.46	4.27	19.35	0.36	0.63	4.96	0.46	4142.10	-329.75	0.09	0.014	0.011	0.02	0.003	-0.008	0.06	-0.186	-0.208	0.01
F3	7.97	38.11	0.32	23.93	35.10	0.20	4.25	4.21	2.87	5433.84	6142.50	0.02	0.012	0.011	0.12	2.341	2.031	0.02	4.264	1.932	0.02
F4	0	27.92	0.13	0	10.08	0.16	0	0.97	0.08	0	-1504.70	0.01	0.009	0.007	0.02	0	0.308	0.03	0	0.384	0.03
F5	102.01	77.68	0.14	4.47	2.279	0.00	1.56	3.91	0.02	15571.76	30530.60	1.03	0.014	0.017	0.00	1.724	1.508	0.04	-0.035	-0.768	0.01
F6	71.02	77.68	0.32	4.23	13.07	0.12	3.75	2.92	0.13	54411.6	37846.40	0.10	0.016	0.017	0.00	0.012	0.099	0.02	-0.726	-0.299	0.04
F7	0	-11.65	0.25	0	-	0.25	0	-0.73	0.01	0	-4859.60	0.01	0.003	0.001	0.02	0	0.007	0.05	0	0.357	0.02
F8	47.64	38.11	0.03	23.23	12.41	0.03	13.93	9.51	0.01	1582.42	-343.20	0.04	0.009	0.011	0.22	-	-0.252	0.01	-0.841	-0.051	0.03
F9	0	-11.65	0.06	0	25.41	0.06	0	2.58	0.48	0	3286.40	0.04	0.003	0.001	0.02	0.531	-0.001	0.01	0	-0.690	0.03
F10	53.72	33.02	0.04	34.64	-	0.01	8.04	3.49	0.16	2641.74	7461	0.05	0.011	0.009	0.00	0	-0.022	0.02	-0.916	-0.002	0.02
F11	53.72	33.02	0.02	34.64	0.522	0.01	8.04	3.49	0.01	2641.74	7461	0.02	0.011	0.009	0.00	-	-0.412	0.02	-0.916	-0.002	0.08
F12	0	-11.65	0.01	0	14.71	0.03	0	2.83	0.01	0	2442.80	0.02	0.002	0.001	0.03	0.330	0.001	0.05	0	0.981	0.02
F13	94.95	77.68	0.49	67.76	14.71	0.37	2.51	5.67	0.19	7864.98	10341	0.03	0.018	0.017	0.09	-	0.481	0.02	-0.665	0.288	0.04
F14	19.65	27.92	0.01	4.77	4.439	0.20	2.89	-0.26	0.24	3822.48	6654.70	0.07	0.011	0.007	0.03	0.330	-0.478	0.01	-0.563	-0.818	0.03

[1] *Experimental value for response*
[2] *Predicted value for response*
[3] *Cook's Distance*
[4] *Values are normalized such that the reference point is zero*

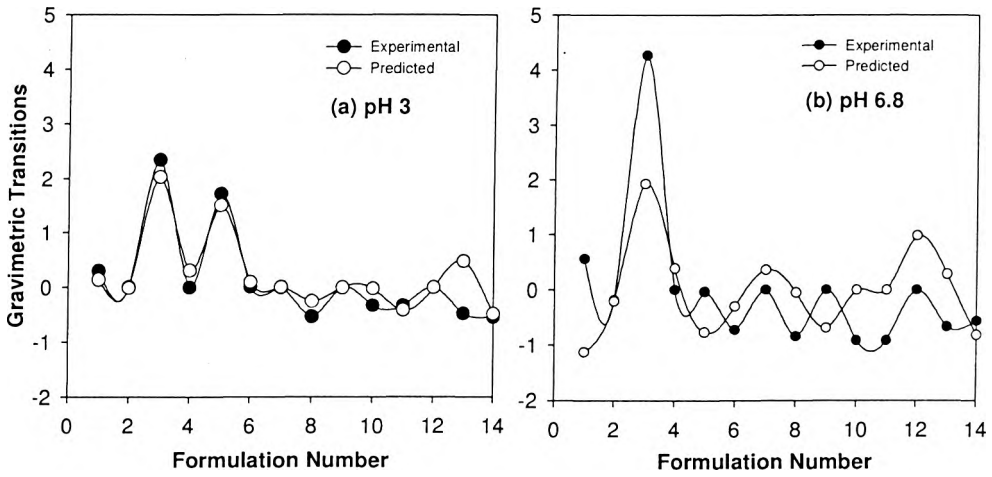

Figure 4.9 Correlation between experimental data and values predicted by the response model for gravimetric transitions in buffer media of pH 3 and pH 6.8. (In all cases for the experimental studies SDs<0.05 were obtained, N=10).

4.3.6 Constrained Optimization

A constrained optimization technique was employed to generate the optimum setting for the oilisphere formulation using maximization of the fracture energy as the major optimization objective. Among different techniques that were available for solving constrained optimization problems, the most popular appeared to be the Lagrangian and Simplex methods. In this study, optimization was undertaken using the Lagrangian method introduced by Fonner and co-workers (1970), which could be achieved by employing the Microsoft Excel 2002 Solver function (Lin et al., 2001; Pillay and Danckwerts, 2002).

Maximization of the total fracture energy was selected as the most favourable parameter (response) for formulation optimization over two other popular parameters, namely unhydrated matrix resilience and matrix hardness. Tables 4.5 and 4.6 provide a detailed analysis of the mathematical fit of data for each response function and their levels of significance. This analysis is required for the selection of the objective function to be

applied in the constrained optimization.

Regression on the unhydrated matrix resilience and matrix hardness resulted in suitable R^2 values, while significantly high CV values were obtained. On the other hand, the total fracture energy provided a compatible set of statistical values i.e. high R^2 and low CV.

The selection criteria applied to these objectives critically depend on the chemical properties of the crosslinked matrix, as outlined in a recent paper by Pillay and Danckwerts (2002) which showed that the degree of crosslinking is a critical parameter that regulates various properties of the oilispheres such as the dynamics of matrix erosion, swelling and drug release. In the present study, experimental results indicate that optimum crosslinking is associated with maximum fracture energy (Tables 4.4, 4.5 and 4.6).

The following constraint boundaries (%w/v or hours) for the independent variables were imposed in a similar manner as outlined in the work of Pillay and Danckwerts (2002) in terms of polymer manipulation, total fracture energy data, and generation of ideal drug release rates:

(i) $1 \leq$ [sodium alginate] ≤ 2

(ii) $1 \leq$ [pectin] ≤ 2

(iii) $1 \leq$ [calcium chloride] ≤ 6

(iv) $1 \leq$ [aluminium chloride] ≤ 6

(v) $1 \leq$ [aluminium sulphate] ≤ 6

(vi) $0.5 \leq$ crosslinking reaction time (hours) ≤ 6

Table 4.5 Complete Fit of Functions for Response Parameters and their Respective Regression Diagnostics

Responses Measured	Plackett-Burman Equations	R^2	Durbin-Watson d Index (%)	CV (%)
Unhydrated Matrix Resilience (%)	$b_0+b_1*[SA]+b_2*[P]+b_3*[CC]+b_4*[AC]+b_5*[AS]+b_6*CRT$ *(Equation 4.8)*	0.74	1.45	77.26
Hydrated Matrix Resilience: pH 3 (%)	$b_0+b_1*[SA]+b_2*[P]+b_3*[CC]+b_4*[AC]+b_5*[AS]+b_6*CRT$ *(Equation 4.9)*	0.63	1.60	112.42
Hydrated Matrix Resilience: pH 6.8 (%)	$b_0+b_1*[SA]+b_2*[P]+b_3*[CC]+b_4*[AC]+b_5*[AS]+b_6*CRT$ *(Equation 4.10)*	0.41	1.94	121.74
Matrix Hardness (N/m)	$b_0+b_1*[SA]+b_2*[P]+b_3*[CC]+b_4*[AC]+b_5*[AS]+b_6*CRT$ *(Equation 4.11)*	0.74	2.20	131.60
Fracture Energy (J)	$b_0+b_1*[SA]+b_2*[P]+b_3*[CC]+b_4*[AC]+b_5*[AS]+b_6*CRT$ *(Equation 4.12)*	0.88	1.75	33.21
Gravimetric Transitions: pH 3	$b_0+b_1*[SA]+b_2*[P]+b_3*[CC]+b_4*[AC]+b_5*[AS]+b_6*CRT$ *(Equation 4.13)*	0.42	1.21	79211.24
Gravimetric Transitions: pH 6.8	$b_0+b_1*[SA]+b_2*[P]+b_3*[CC]+b_4*[AC]+b_5*[AS]+b_6*CRT$ *(Equation 4.14)*	0.37	1.75	78918.52

Table 4.6 Level of Significance of Regression Coefficients in Response Functions at a 95% Confidence Interval ($p<0.05$)

Coefficient	Independent variables	[1]UMR (%)	[2]HMR: pH3 (%)	[3]HMR: pH 6.8 (%)	[4]MH (N/m)	[5]TFE (J)	[6]GT: pH 3	[7]GT: pH 6.8
b0	-	0.376	0.314	0.780	0.616	0.804	0.832	0.804
b1	[SA]	0.01178	0.07611	0.206	0.05355	0.00061	0.431	0.722
b2	[P]	0.03123	0.574	0.751	0.05837	0.01127	0.546	0.373
b3	[CC]	0.937	0.253	0.385	0.173	0.08114	0.435	0.324
b4	[AC]	0.280	0.295	0.434	0.140	0.598	0.423	0.453
b5	[AS]	0.725	0.296	0.698	0.238	0.367	0.654	0.584
b6	CRT	0.690	0.121	0.339	0.139	0.620	0.323	0.357

[1] *Unhydrated matrix resilience*
[2] *Hydrated matrix resilience in pH 3*
[3] *Hydrated matrix resilience in pH 6.8*
[4] *Matrix hardness*
[5] *Total fracture energy*
[6] *Gravimetric transition in pH 3*
[7] *Gravimetric transition in pH 6.8*

Polymer concentrations for sodium alginate and pectin beyond 2%w/v were not feasible as accurate titration was significantly inhibited by their excessively high viscosity. The upper limits for the crosslinking agents were based on their ability to produce optimal crosslinking. The lower limits for both polymers and crosslinking agents were the necessary minima for the production of spherical oilispheres. The crosslinking reaction times were based on minimization of the loss of *Mentha piperita* oil into the crosslinking solution.

Table 4.7 reflects the results based on the above constraint optimization technique for development of the ideal oilisphere formulation. In order to validate the accuracy of the predicted formulation parameters, the model predicted values were compared against the experimental values generated from fracture energy analysis on the oilispheres. Excellent correlation was obtained (Table 4.7).

Table 4.7 Composition of the Optimized Oilisphere Formulation Obtained By the Constrained Technique and Comparison of Experimental and Predicted Total Fracture Energy Values

Formulation Components	**Concentrations (%w/v) and Reaction Time (hours)**
Sodium Alginate	1.5
Pectin	1.5
Calcium Chloride	4
Aluminium Chloride	4
Aluminium Sulphate	4
Crosslinking Reaction Time	3
Formulation Analysis	**Total Fracture Energy (Joules)**
Experimental	0.0115±0.003 (N=10)
Predicted	0.0107

A three-dimensional trajectory residual plot for the total fracture energy corresponding to the 14 formulations (Figure 4.10) showed data homogeneity, without any specific trend and hence no model transformation was required. Frequently simple X-Y plots obstruct internal residual patterns.

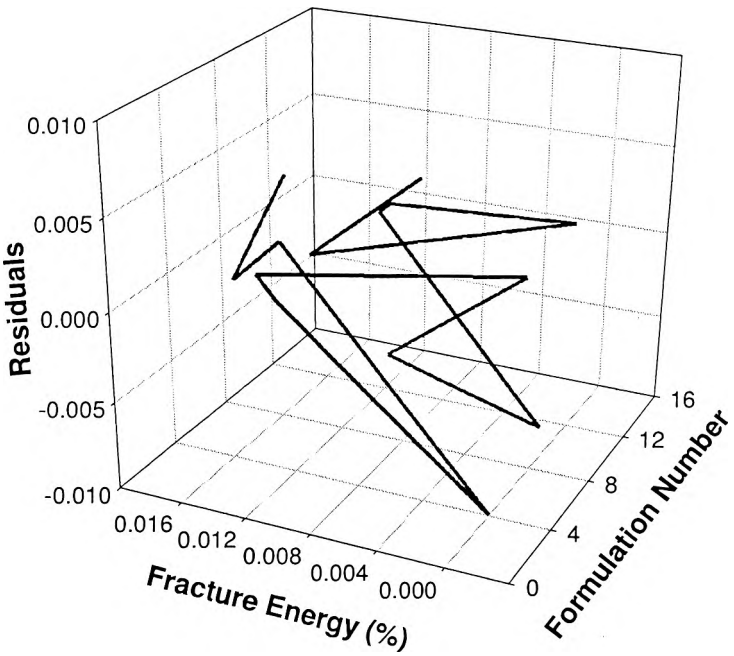

Figure 4.10 Three-dimensional trajectory plot of the residuals for the total matrix fracture energy.

Figure 4.11 illustrates a typical surface response plot for the effects of crosslinking reaction time and crosslinker concentrations on the total fracture energy. All other combinations of the surface plots were analyzed but are not shown due to the statistical emphasis placed on the total fracture energy. It was observed that as the concentration of calcium chloride was increased, the total fracture energy also significantly increased. The same effect was also observed for aluminium chloride and sulphate. However, in the case of the crosslinking reaction time, a maximum of 3 hours was required with no significant effects thereafter. In terms of the polymer concentrations, an increase yielded higher total fracture energy values. It is imperative to account for the fact that the total fracture energy is a function of the elasticity or plasticity of a material.

In this work, a Generalized Feed Forward (GFF) neural model was selected to predict the total matrix fracture energy values using data generated in the Plackett-Burman statistical

matrix format (Tables 4.2). Essentially, a GFF is a generalization of a Multilayer Perceptron (MLP) such that network connections can jump over one or more hidden layers. In theory, a MLP can solve any problem that a GFF network can solve. In practice, however, GFF networks often solve the problem much more efficiently (Nelson and Illingworth, 1992; Principe et al., 1998).

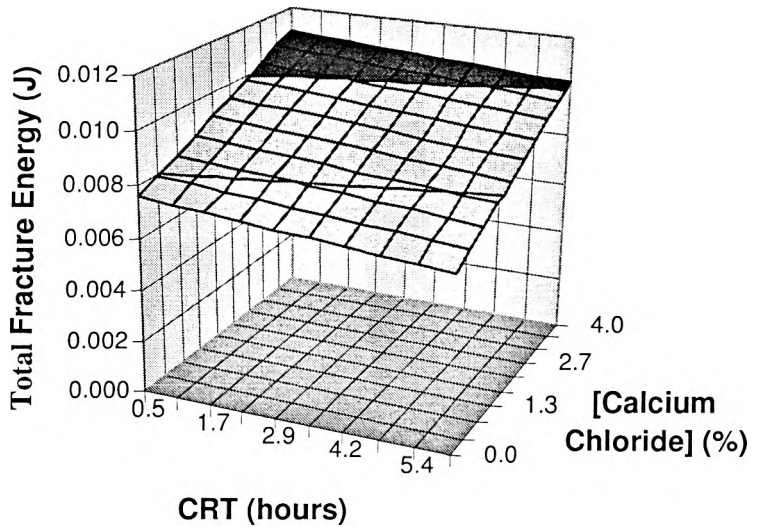

Figure 4.11 Typical surface plot indicating the influence of increasing the crosslinker concentration and crosslinking reaction time (CRT) on the total matrix fracture energy. Note the same effect was observed for the other crosslinkers. An increase in the polymer concentration also increased the total fracture energy in a similar manner.

4.3.7 Comparison of Predicted Response Values for Total Matrix Fracture Energy Using Artificial Neural Networks and the Plackett-Burman Regression Analysis

To analyze the data, the neural model employed one hidden layer. For the hidden and output layers a genetic algorithm with the SigmoidAxon transfer function and the ConjugateGradient learning rule was respectively employed. A maximum of 5000 epochs were run 50 times to ensure optimal training of data. Figure 4.12 illustrates the gradual levelling of the average mean square error (MSE) with standard deviation boundaries for

50 runs. Table 8 reflects the average of the MSE values for all training runs, the best network run out of 5000 epochs run 50 times and also provides and indication of how well the data has been trained. Overall, this data shows that the training model employed was highly efficient. The parameters depicted in Table 4.8 are standard statistical indicators used in neural networks to describe the accuracy of the model prediction. These indicators are used in the selection of the optimal neural model (e.g. MLP versus GFF).

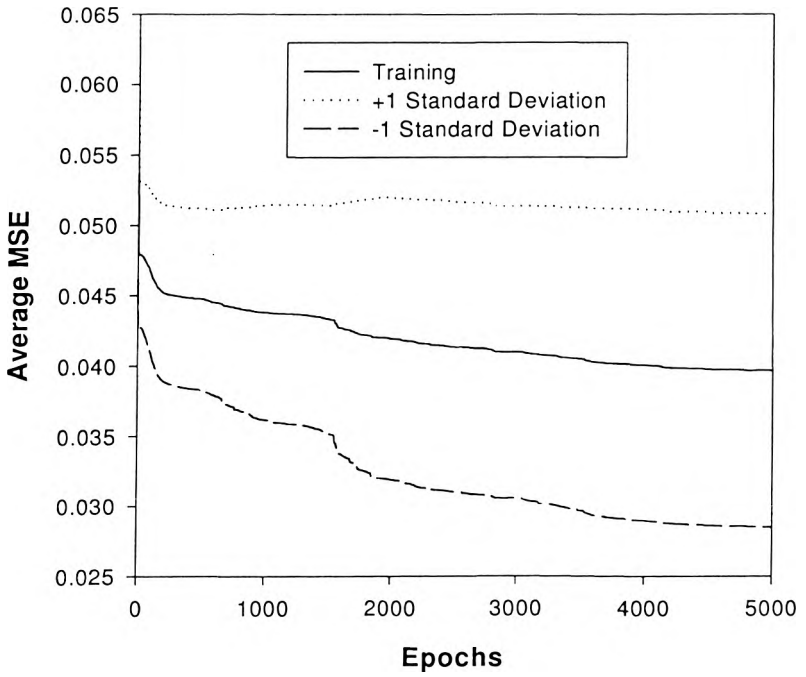

Figure 4.12 Average MSE with standard deviation boundaries for 5000 epochs run 50 times.

Table 4.8 Neural Network Indicators Characterizing the Efficiency of the Training

2 Averages of the Minimum Training Errors	Training Minimum	Training Standard Deviation
Average of Minimum MSEs	0.039647207	0.011162308
Average of Final MSEs	0.039647207	0.011162308
Optimal Network Run Obtained from Data Training	**For Total Matrix Fracture Energy**	
Run #	17	
Epoch #	5000	
Minimum MSE	0.019716412	
Final MSE	0.019716412	
Performance of Neural Network by Testing of Training Data	**For Total Matrix Fracture Energy**	
MSE	1.57731E-05	
Normalized MSE	0.419817367	
Mean Absolute Error	0.002779493	
Minimum Absolute Error	5.16934E-06	
Maximum Absolute Error	0.009048942	
Correlation Coefficient	0.76189204	

Using all 14 formulations (Table 4.9), the total matrix fracture energy was predicted by both Plackett-Burman design and neural networks. The mean differences between the experimental and predicted total fracture energy and neural network values when compared using a two-tailed paired student t-test, showed no significant differences ($p=0.265$). Hence, as a predictive tool, it appears that artificial neural networks may be a better choice in terms ease of operation, time-saving, and no critical need to be able to mathematically factor out solutions. On the other hand, the Plackett-Burman approach like all other traditional Experimental Designs, require the researcher to possess strong mathematical modelling skills and is a time-consuming technique when modelling and optimization has to be conducted.

Table 4.9 Comparisons of Experimental and Predicted Total Matrix Fracture Energy Values Derived for 14 Formulations Using the Plackett-Burman Matrix and Artificial Neural Networks

Oilisphere Formulation	Total Matrix Fracture Energy (Joules)		
	Experimental	Predicted by Plackett-Burman	Predicted by Neural Networks
F1	0.010	0.007	0.011
F2	0.014	0.011	0.013
F3	0.012	0.011	0.012
F4	0.009	0.007	4.274×10^{-5}
F5	0.014	0.017	0.014
F6	0.016	0.017	0.016
F7	0.003	0.001	0.001
F8	0.009	0.011	0.006
F9	0.003	0.001	0.006
F10	0.011	0.009	0.006
F11	0.011	0.009	0.007
F12	0.002	0.001	0.009
F13	0.018	0.017	0.012
F14	0.011	0.007	0.013

Traditional statistical analysis such as the Plackett-Burman design does not provide "ideal values" but rather a list of solutions ranging from the most to least significant. Alternatively, a neural network provides a solution that zooms in only on the target values.

4.3.8 Optimization of the Oil Release as per Constrained Optimization Solution in Conjunction with a Fusion Coating Technique

Based on the fact that *Mentha piperita* oil is unstable in the acidic environment, the delivery system had to possess an ability to protect the oil from the harsh gastric environment, while modulate its delivery in the proximal and distal intestine.

Through application of the Plackett-Burman design and by constrained optimization of the total matrix fracture energy, a pH-dependent zero-order releasing oilisphere system was developed (Figure 4.13). Figure 4.13a,c,e indicate the release of the oil in different buffer media, while Figure 4.13b,d,f reflect a composite profile in sequentially changing buffer

media.

Residual amounts of oil was still detected in buffer medium pH 1.5 (Figure 4.13a,b). In an attempt to resolve this, a coat of alginate and pectin was applied to individual oilispheres using a microwell plate. In the first approach, simple coating of the oilispheres with a solution of native alginate and pectin in a microwell plate followed by drying resulted in a decrease in the drug release over the physiological pH range of 1.5-6.8; however oil was still detected in the acid media (Figure 4.13c,d). In the second approach the applied coat of alginate and pectin was crosslinked by calcium chloride, aluminium chloride and aluminium sulphate. The additional crosslinking resulted in the production of a 2-4 hour lag-time in release of the oil in the acidic environment (Figure 4.13e,f), which from a biopharmaceutical perspective is adequate time for gastric emptying of multiple-units to occur (Wilding et al., 2001). This formulation could be regarded as ideal for the purposes of site-specific delivery of *Mentha piperita* oil.

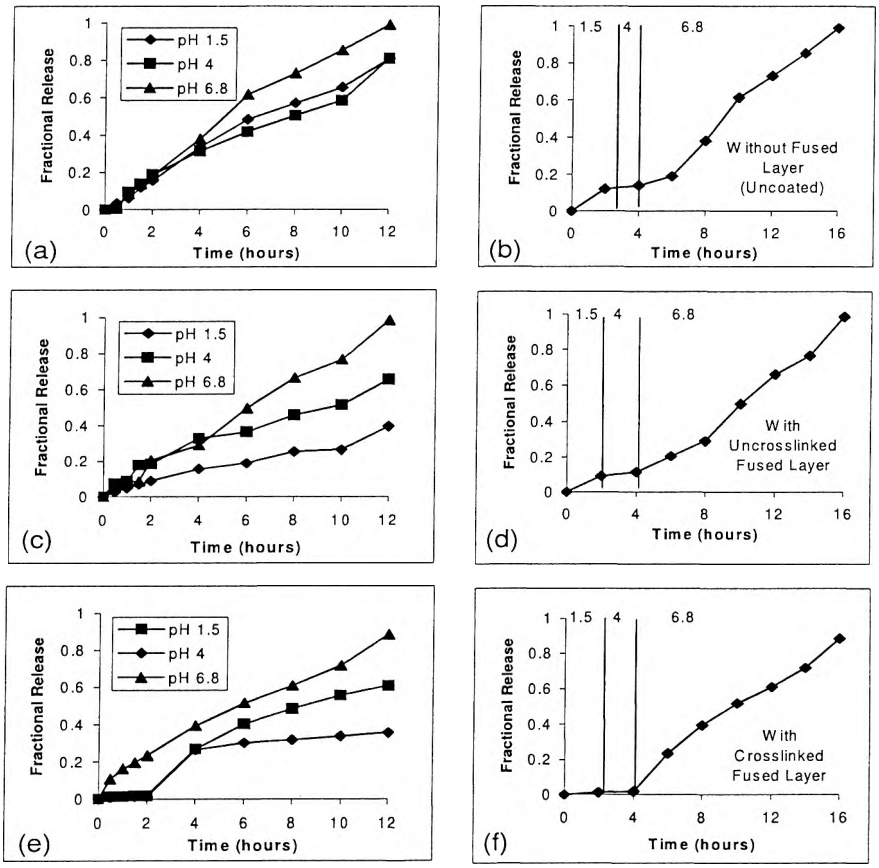

Figure 4.13 Release profiles of *Mentha piperita* oil from oilispheres in simulated gastric and intestinal fluid (pH 1.5, 4, 6.8): (a,b) Without fused coat, (c,d) With uncrosslinked fused coat, and (e,f) With crosslinked fused coat. (In all cases it was observed that SDs<0.09 were obtained, N=3).

4.3.9 Kinetic Modelling of Release Data from the Optimal Formulation Composed of the Crosslinked Fused Coat

Various kinetic models were employed to identify the mechanism involved in the release of the oil from the optimized oilispheres using release data derived from the composite profile (Figure 4.13f), which essentially displayed site-specific biphasic release kinetics, characterized by a 4-hour lag phase followed by zero-order release. We will not describe the equations below in detail as this information can be found elsewhere (Pillay and Fassihi, 1999a). Kinetic modelling was applied using a modified form of the Power Law equation:

$M_t/M_\infty = k_1(t-t_L)^n$ *(Equation 4.15)*

where k_1 is the Fickian kinetic constant, t_L represents the delay or lag time (4 hours) prior to release of the oil and n is a release exponent.

Alternatively, Fickian diffusion and matrix relaxation/dissolution were analyzed through the use of an expanded version of Equation 4.15:

$M_t/M_\infty = k_1(t-t_L)^n + k_2(t-t_L)^{2n}$ *(Equation 4.16)*

where k_2 is the relaxation/dissolution rate constant (i.e. anomalous transport).

Hopfenberg's modified model (Pillay and Fassihi, 1999a) was either applicable to a slab, cylinder or sphere showing heterogeneous erosion. In order to account for the lag time a modification was made:

$M_t/M_\infty = 1-[1- K_1(t- t_L)]^n$ *(Equation 4.17)*

where K_1 is the overall erosion rate constant, and n=1 for a slab, n=2 for a cylinder, and n=3 for a sphere. Table 4.10 indicates the results from kinetic modelling.

Table 4.10 Release Kinetics Obtained from Various Models

Model M_t/M_∞=	k_1 (K_1)	k_2	n	[1]AIC	[2]SC	[3]CN
$k_1(t-t_L)^n$	0.74	-	0.59	-48.49	-50.29	20.44
$k_1t^n+k_2t^{2n}$	0.13	0.02	0.56	-48.02	-50.72	21.26
$1-[1- K_1(t- t_L)]^n$	0.04	-	3	-42.25	-43.16	2377

[1]*Akaike Information Criteria*
[2]*Schwartz Criteria*
[3]*Condition Number*

From Table 4.10 it may appear at first glance that all three models may suitably fit the dissolution data based on the AIC and SC values. However, upon consideration of the CN value, it is evident that the Hopfenberg model is highly unstable (high value). The

Power Law and Power Law variant appear to suitably fit the data and statistically satisfy all parameters. Based on the n-values and the low k_2 value in these equations, it is clear that diffusion is the predominant mechanism. This is also understandable from the fact that the oilisphere consists of a crosslinked membrane encapsulating the oil and acting as a barrier to diffusion.

4.3.10 Antimicrobial Activity of Mentha piperita Oil

Despite evidence of strong antimicrobial activity (Pattnaik et al., 1997; Iscan et al., 2002), *Mentha piperita* oil has not been specifically investigated for an effect on small intestinal bacterial overgrowth. These researchers have shown in a case report that marked improvement in IBS-like symptoms and significant reductions in hydrogen production after treatment with enteric-coated *Mentha piperita* oil may be achieved.

In our antimicrobial studies, it was found that the minimum inhibition concentrations (MIC) ranged between 8-32mg/mL of *Mentha piperita* oil with *E. coli* displaying the greatest resistance (Table 4.11). The microwell plate indicates the red stain (shown as black due to photographic reproduction) which reflects the binding of the oil to microbial DNA (Figure 4.14).

Table 4.11 Minimum Inhibition Concentrations (MIC) of *Mentha piperita* Oil on a Host of Micro-Organisms Commonly Found in the Gastrointestinal Tract

Number Allocated to Organism	Organism	MIC (mg/mL)
1	*Proteus vulgaris*	16
2	*Serratia odorifera*	8
3	*Enterobacter*	8
4	*Salmonella typhi*	8
5	*Salmonella enteriditis*	8
6	*Citrobacter*	8
7	*Enterococcus faecalis*	8
8	*Klebsiella pneumonia*	16
9	*Candida albicans*	8
10	*Staphylococcus aureus*	16
11	*Escherichia coli*	32
12	*Yersinia enterolitica*	8

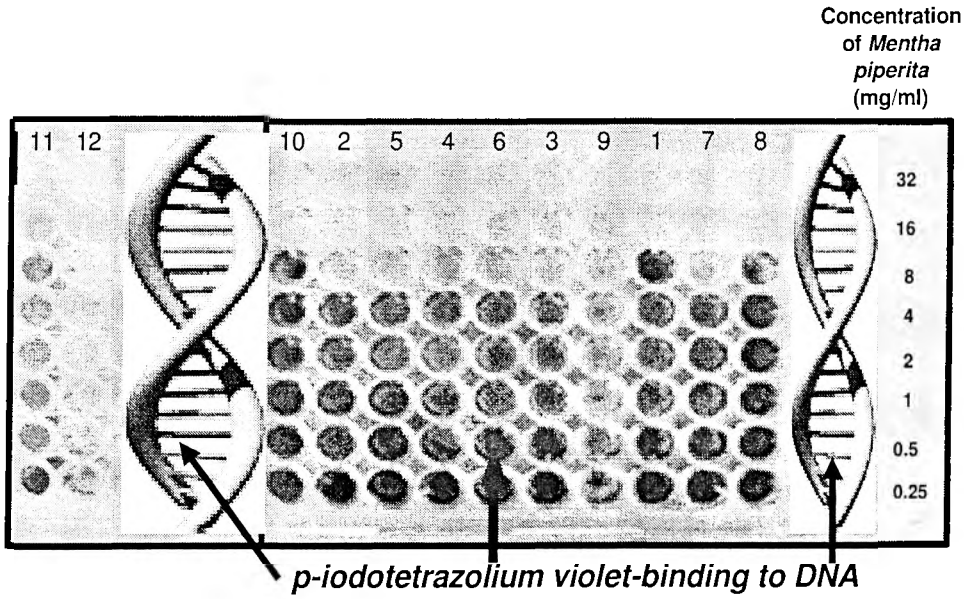

Figure 4.14 Different degrees of binding of p-iodotetrazolium violet dye to DNA of a host of micro-organisms indicated by different stain darkening in each microwell.

4.4 Concluding Remarks

This work has demonstrated a statistically robust approach for the formulation of novel crosslinked oilispheres containing *Mentha piperita* oil for potentially treating IBS. The physicochemical and textural dynamics of the highly complex matrix formed between sodium alginate and pectin crosslinked with calcium chloride, aluminium chloride and aluminium sulphate was significantly influenced by these independent variables. Among the dependent variables (responses) selected for formulation optimization, the total matrix fracture energy provided a statistically feasible optimization objective.

Overall, the Plackett-Burman approach and neural model did not show any significant differences in predicting the physicochemical and physicomechanical properties of the polymeric matrix. However, in terms of modelling efficiency, it appears that Artificial Neural Networks may be a superior alternative. In view of these findings, this study will be of benefit to pharmaceutical scientists particularly involved in the application of experimental designs and computer-aided simulations for the development of natural phytochemical delivery formulations.

Chapter Five

Application of a High Resolution Box-Behnken Design for the Selection of a Crosslinked Zinc-Alginate-Pectinate Framework

5.1 Introduction

In Chapter 4, we have strongly established that Experimental Design is an integral scientific approach for the rational development of novel polymeric complexes via innovative statistical and mathematical manipulation of crosslinking reactions. The present Chapter extends this application by elevating Experimental Design to the higher resolution Box-Behnken matrix to develop a primary crosslinked polymeric backbone that will be employed as a framework in subsequent studies for release-rate modulation of model drug substances. This primary framework comprises a novel crosslinked zinc-alginate-pectinate complex.

Today's ideas on drug administration have far reached the scope of simple tablet manufacturing, and in order to stay ahead, many pharmaceutical companies spend millions of dollars in research and development, in an attempt to outwit their competitors by investing in new technologies. One such challenging field is in the design of novel multiparticulate technology, whereby release rate can be adjusted and controlled in a predictable manner.

In this study, the crosslinking potential of pectin and alginate will be manipulated. Pectins are anionic soluble non-starch polysaccharides extracted from plant cell walls. They are predominantly linear polymers of mainly alpha (1-4) linked D- galactouronic acid monomers interrupted by 1,2-linked L-Rhamnose monomers (Figure 5.1).

Alginic acid, on the other hand is a high molecular weight polysaccharide derived from

kelp. Essentially, it is a linear copolymer composed of 1,4-linked β-D-mannuronic acid and alpha-L-guluronic acid units (Figure 5.2) (Pronova Biopolymers, 1994; Pillay and Fassihi, 1999a,b).

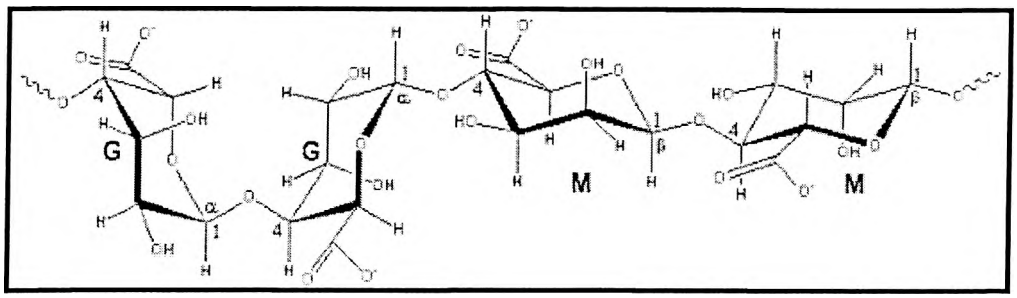

Figure 5.1 Monomeric structure of alginate (M = mannuronic acid units, G = guluronic acid units) (source: http://www.lsbu.ac.uk/water/hyalg.html).

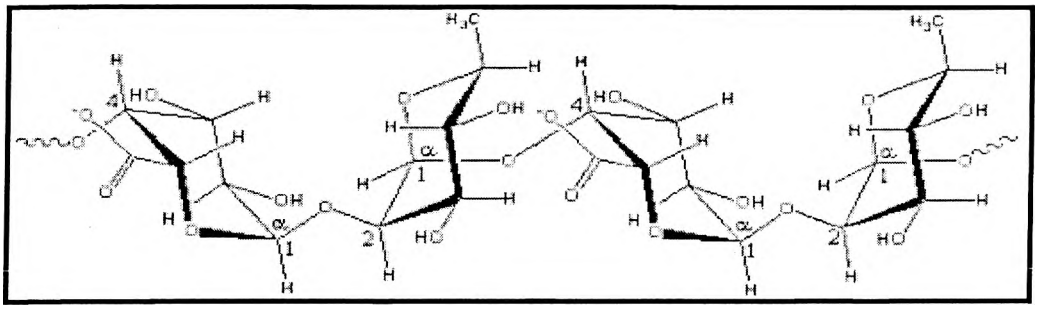

Figure 5.2 Monomeric structure of pectin (source: http://www.cpkelco.com).

Divalent and trivalent ions, in particular, crosslink with these polymers to form a three-dimensional complex structure resembling the putative "egg-box" model (Grant et al., 1973). Our study explored the zinc ion as a potential crosslinker. A microsphere-type system was developed (referred to as a "gelisphere") with drug entrapped within the crosslinked matrix.

The overall aim of this study was to design an ionotropically crosslinked zinc-alginate-pectinate system for rate-adjusted drug delivery. Specifically, we set out to synthesize

statistically-based crosslinked gelispheres using a Box-Behnken design, study their drug release behaviour, establish the degree of crosslinking using textural profiling analysis, and assess the viscoelastic transitions within the native polymers and crosslinked matrix.

5.2 Materials and Methods

The sodium alginate and pectin are of the same grade as those used in Chapter 4. Zinc sulphate heptahydrate, zinc gluconate USP and ibuprofen USP were purchased from Spectrum (USA).

5.2.1 Calibration Curves of Ibuprofen in Buffer Media of pH 3 and pH 6.8

Standard for solutions of ibuprofen were prepared by dissolving appropriate quantities of drug in USP-recommended buffers (0.0052, 0.0136, 0.0252, 0.0504 and 0.0608mg/ml in buffer pH 3; 0.00625, 0.0125 and 0.025mg/mL in buffer pH 6.8).

The absorbance values of the standard solutions were determined by UV at the wavelength maximum of 221nm. Using this information, the calibration curves in buffer media pH 3 and 6.8 were constructed (Figures 5.3 and 5.4). Note that the buffer, polymers and excipients did not show any absorbance readings or interference at 221nm.

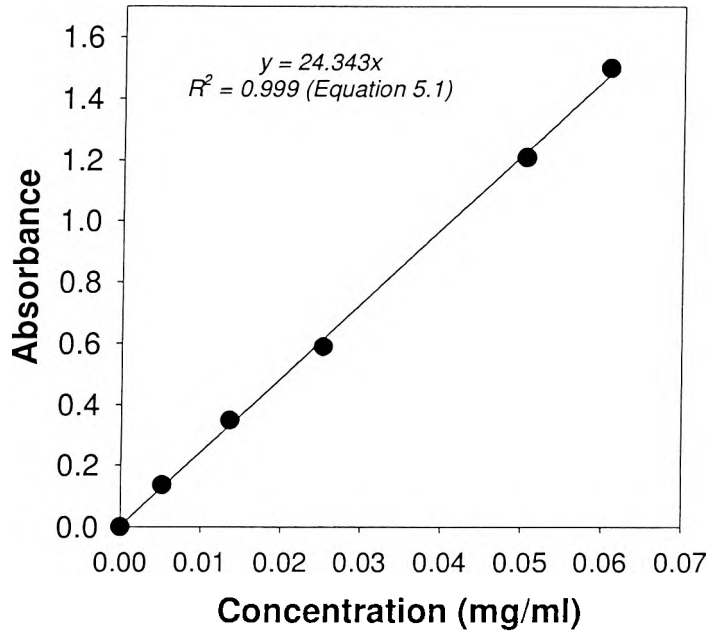

Figure 5.3 Calibration curve of ibuprofen in USP-recommended buffer of pH 3. (In all cases it was observed that SDs<0.03 were obtained, N=3).

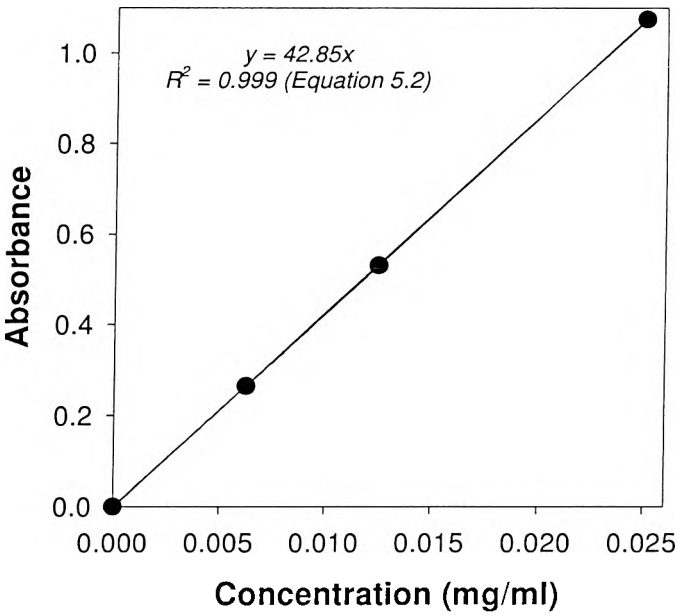

Figure 5.4 Calibration curve of ibuprofen in USP-recommended buffer of pH 6.8. (In all cases it was observed that SDs<0.02 were obtained, N=3).

5.2.2 Formulation of Crosslinked Zinc-Alginate-Pectinate Gelispheres

Gelispheres loaded with ibuprofen were formulated in accordance with a Box-Behnken design having polymer and crosslinking agent concentrations as depicted in Tables 5.1 and 5.2. A similar approach discussed in Chapter 4 was used to develop the Experimental Design.

Table 5.1 Normalized Factor Levels of the Independent Variables for the Box-Behnken Design

Variable	Factor Level		Units
	-1	1	
Sodium Alginate	0	2	% w/v
Pectin	0	2	% w/v
Zinc Sulphate Heptahydrate	0	5	% w/v
Zinc Gluconate USP	0	5	% w/v

A quantity of sodium alginate and/or pectin, and ibuprofen (2:1) was added to deionised water, made up to volume (100mL) and homogenized to form a polymer-drug suspension (Vortex Mixer model 947, England). The crosslinking solution was prepared by dissolving an appropriate quantity of zinc sulphate heptahydrate and/or zinc gluconate (see Tables 5.1 and 5.2) in deionised water and made up to 1000mL. Gelispheres were formed by titrating the above polymer-drug suspension at 2mL/minute into the crosslinking solution by means of a 6-channel peristaltic pump (Desaga, Heidelberg) fitted with Pharmed® tubing (Cole-Parmer, USA) having a flat-tip 19-gauge needle opening. On completion of the titration process, the formed gelispheres were agitated in the crosslinking solution for an additional 30 minutes. Thereafter, the gelispheres were allowed to cure under dark conditions (21^{o}C) for a 24-hour period. Following this curing phase, the crosslinking solution was decanted and the gelispheres were washed with 3x500mL volumes of deionised water. The gelispheres were then air-dried at 21^{o}C for 48 hours under an extractor.

Table 5.2 Box-Behnken Matrix for the Formulation of the Zinc-Alginate-Pectinate Gelispheres

Gelisphere Formulation (F#)	Sodium Alginate (%w/v)	Pectin (%w/v)	Zinc Sulphate Heptahydrate (%w/v)	Zinc Gluconate (%w/v)
1	0	1	2.5	0
2	1	0	2.5	5
3	1	1	5	5
4	1	1	0	0
5	0	0	2.5	2.5
6	2	0	2.5	2.5
7	1	2	2.5	0
8	1	1	2.5	2.5
9	0	2	2.5	2.5
10	0	1	5	2.5
11	1	0	2.5	0
12	1	2	5	2.5
13	1	0	0	2.5
14	1	1	2.5	2.5
15	2	1	5	2.5
16	1	1	0	5
17	1	1	2.5	2.5
18	2	2	2.5	2.5
19	1	2	0	2.5
20	1	0	5	2.5
21	1	1	2.5	2.5
22	1	2	2.5	5
23	0	1	0	2.5
24	2	1	0	2.5
25	2	1	2.5	0
26	0	1	2.5	5
27	2	1	2.5	5
28	1	1	5	0

The quadratic response model with 15 terms generated from the above design included 24 experimental runs and 4 centre points (Equation 5.3):

$$Response = b_0 + b_1*NaAl + b_2*P + b_3*ZnS + b_4*ZnG + b_5*NaAl*NaAl + b_6*P*P + b_7*ZnS*ZnS + b_8*ZnG*ZnG + b_9*NaAl*P + b_{10}*NaAl*ZnS + b_{11}*NaAl*ZnG + b_{12}*P*ZnS + b_{13}*P*ZnG + b_{14}*ZnS*ZnG \quad \textit{(Equation 5.3)}$$

where the concentrations of sodium alginate and pectin are represented by NaAl and P, and the concentrations of the crosslinkers $ZnSO_4.7H_2O$ and $C_{12}H_{22}ZnO_{14}$ are represented by ZnS and ZnG. b_0.....b_{14} are the regression coefficients.

5.2.3 Determination of Drug Encapsulation Efficiency within the Gelispheres

Actual drug loading was determined by dissolving 50mg of gelispheres in 100mL phosphate buffer pH 6.8 and analysed by UV. Based on the theoretical drug loading, the encapsulation efficiency was computed in a manner similar to that described in Chapter 4 (see Equation 4.3).

5.2.4 Textural Profile Analysis on Crosslinked Zinc-Alginate-Pectinate Gelispheres

This study focused on the characterization of the matrix resilience (hydrated), rupture energy and yield value of the gelispheres using TA.XT.*plus* Texture Analyzer (Stable Micro Systems, England) fitted with a 36mm cylindrical steel probe and a 5kg load cell. The techniques used to evaluate the above parameters were performed in a manner similar to that described in Chapter 4. Below are typical profiles used for the calculation of these parameters (Figure 5.5).

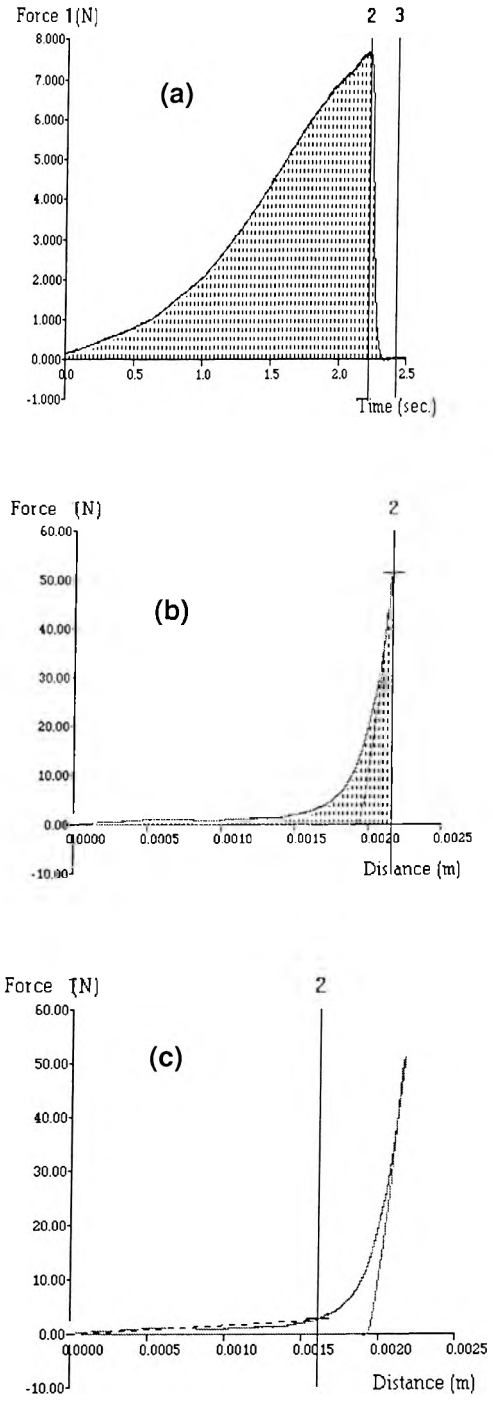

Figure 5.5 Typical textural force-time and force-distance profiles of crosslinked zinc-alginate-pectinate gelispheres for the determination of (a) Matrix resilience (b) Rupture energy, and (c) Yield value. (In all cases it was observed that SDs<0.1 were obtained, N=10).

5.2.5 Viscoelastic Studies

This study was conducted using a Brookfield's Viscometer (Model RV, spindle #2) in order to characterize the viscoelastic transitions of polymers on the incremental addition (µl) of different crosslinkers to polymer/drug combinations, as indicated below (Table 5.3). The homogenized polymer/drug suspensions were gently magnetically stirred. The polymer/drug combinations employed included 1%w/v each of alginate and/or pectin. These combinations, when studied in the presence of drug, contained 0.5%w/v ibuprofen. The crosslinking solutions included 2.5%w/v each of zinc sulphate heptahydrate and/or zinc gluconate.

The polymer/drug suspension was added to a 250mL beaker and magnetically stirred for 5 minutes. Thereafter the beaker was removed from its stirring position and the viscosity of the suspension was tested at 50 rpm. Two minutes were allowed for the viscometer reading to stabilize before any readings were taken. The polymer/drug suspension was replaced on the stirrer and 500µl of the crosslinker solution was added, allowed to stir for a further 5 minutes after which the viscosity was tested.

18 combinations of polymer/drug and crosslinker combinations were studied as indicated below (Table 5.3).

Table 5.3 Polymer-Crosslinker Combinations Used to Assess the Viscoelastic Transitions

Experimental Run	[NaAl] (%w/v)	[P] (%w/v)	[Ibuprofen] (%w/v)	[ZnS] (%w/v)	[ZnG] (%w/v)
1	1	0	0.5	2.5	0
2	1	0	0.5	0	2.5
3	1	0	0.5	2.5	0
4	0	1	0.5	2.5	0
5	0	1	0.5	0	2.5
6	0	1	0.5	2.5	2.5
7	1	1	0.5	2.5	0
8	1	1	0.5	0	2.5
9	1	1	0.5	2.5	2.5
10	1	0	0	2.5	0
11	1	0	0	0	2.5
12	1	0	0	2.5	2.5
13	0	1	0	2.5	0
14	0	1	0	0	2.5
15	0	1	0	2.5	2.5
16	1	1	0	2.5	0
17	1	1	0	0	2.5
18	1	1	0	2.5	2.5

5.2.6 In Vitro Dissolution Studies

In vitro dissolution studies were conducted using the USP 25 rotating paddle method at 50rpm in buffer medium pH 6.8 maintained at 37^{o}C. The method was modified using a ring-mesh assembly, previously described by Pillay and Fassihi (1998). Samples were withdrawn at predetermined time intervals via an autosampler (Hewlett-Packard).

5.3 Results and Discussion

5.3.1 Drug Encapsulation Efficiency

The lowest and highest encapsulation was obtained from formulations F21 and F24 respectively i.e. 37.19% and 82.96%. In the case of F21, this may be attributed to the interference by the pectin monomers and a reduction in the zinc gluconate concentration (see Table 5.4) This could lead to a more open (porous) crosslinked lattice, and thus allowing for the escape of drug into the crosslinking solution during the curing phase. In the case of F24, alginate is highly crosslinked by zinc sulphate heptahydrate (preliminary

studies) and hence provides a three-dimensional network with greater crosslinker density, hence entrapping significantly more drug.

Table 5.4 Drug Encapsulation Efficiency from the Various Statistically-Designed Zinc-Alginate-Pectinate Gelispheres

Formulation Number (F#)	Drug Encapsulation Efficiency (%)		Mean (%)	Standard Deviation (SD)
	Sample 1	Sample 2		
1	64.49	64.01	64.25	0.34
2	76.36	75.82	76.09	0.38
3	55.73	54.65	55.19	0.76
4	-	-	-	-
5	-	-	-	-
6	68.87	65.93	67.40	2.08
7	77.68	74.21	75.94	2.46
8	56.27	56.45	56.36	0.13
9	55.67	54.83	55.25	0.59
10	49.37	48.77	49.77	0.42
11	73.49	72.65	73.07	0.59
12	62.09	65.33	63.71	2.29
13	69.77	66.05	67.91	2.63
14	58.85	58.01	58.42	0.59
15	64.49	65.63	65.21	1.02
16	55.07	56.09	55.58	0.72
17	44.69	48.05	46.37	2.38
18	67.49	66.41	66.95	0.76
19	72.47	76.66	74.57	2.97
20	60.89	63.83	62.36	2.08
21	37.85	36.53	37.19	0.93
22	48.17	48.71	48.44	0.38
23	53.87	55.43	54.65	1.1
24	83.08	82.84	82.96	0.17
25	72.65	72.05	72.35	0.42
26	40.97	36.95	38.96	2.84
27	60.47	60.71	60.59	0.17
28	55.85	55.37	55.61	0.34

5.3.2 Textural Profiling Analysis of Crosslinked Gelispheres

The crosslinked gelispheres were spherical in shape with a uniform diameter of about 1.5mm. Macros created on Texture Exponent Version 3.2 were run on the textural profiles to calculate various parameters: namely, matrix resilience, rupture energy and matrix yield value.

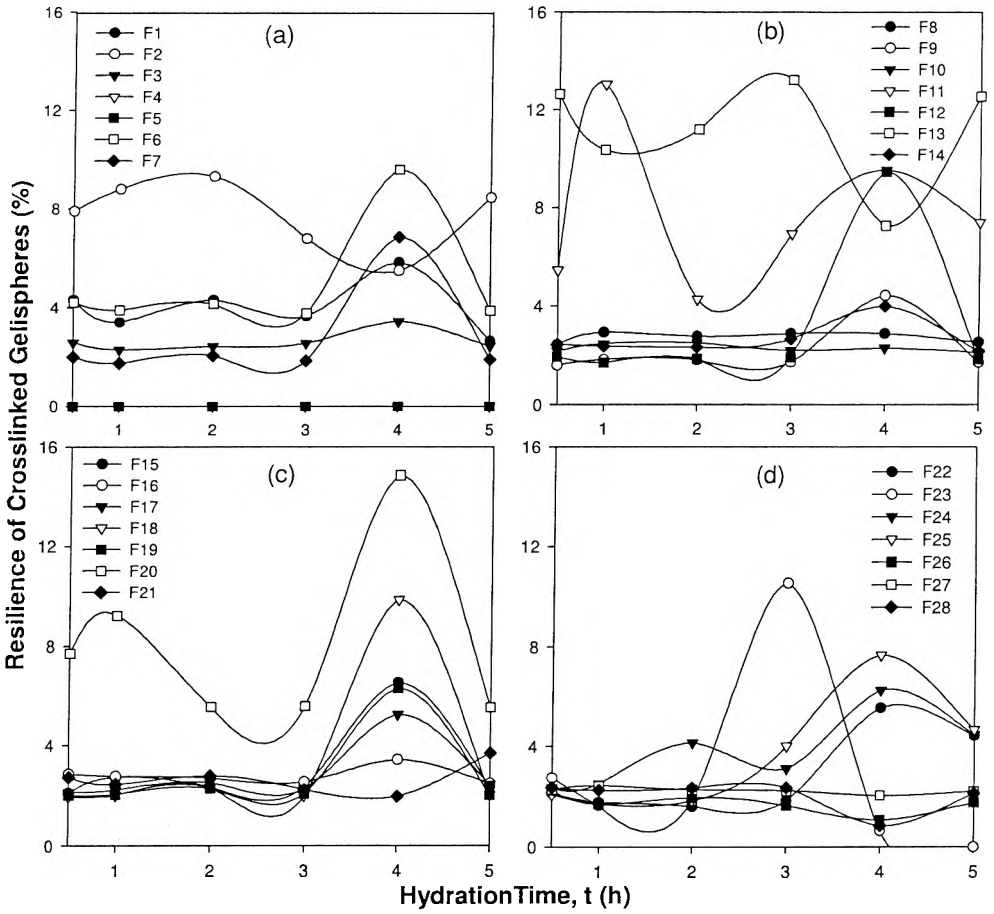

Figure 5.6 Hydrated matrix resilience for the 28 Box-Behnken designed formulations. (In all cases it was observed that SDs<0.25 were obtained, N=10).

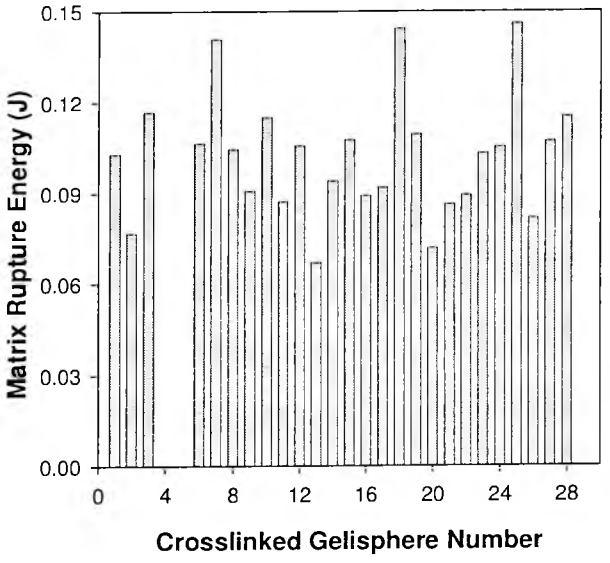

Figure 5.7 Matrix rupture energy for the 28 Box-Behnken designed formulations. (In all cases it was observed that SDs<0.007 were obtained, N=10).

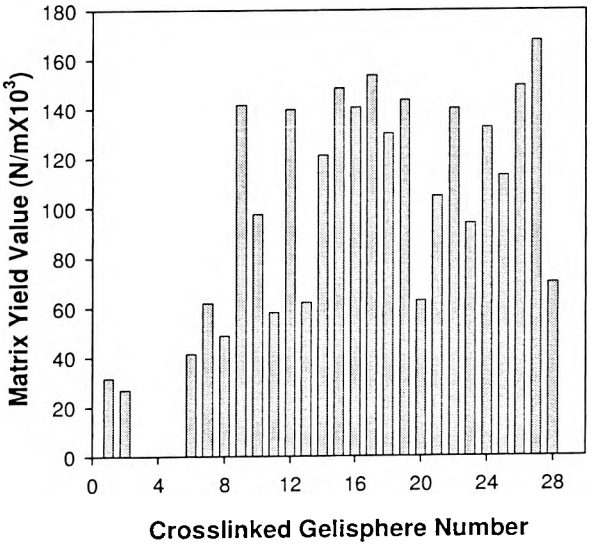

Figure 5.8 Matrix yield value for the 28 Box-Behnken designed formulations. (In all cases it was observed that SDs<0.9 were obtained, N=10).

It is distinctly apparent that the textural properties of the crosslinked gelispheres are significantly influenced by altering the concentration and polymer/drug and crosslinker concentrations. This may be attributed to the different degrees of crosslinking achieved under different conditions.

5.3.3 Viscoelastic Behaviour of Crosslinked Gelispheres

Four different and distinct viscoelastic patterns were observed during *in situ* crosslinking of polymer solutions (Figure 5.9).

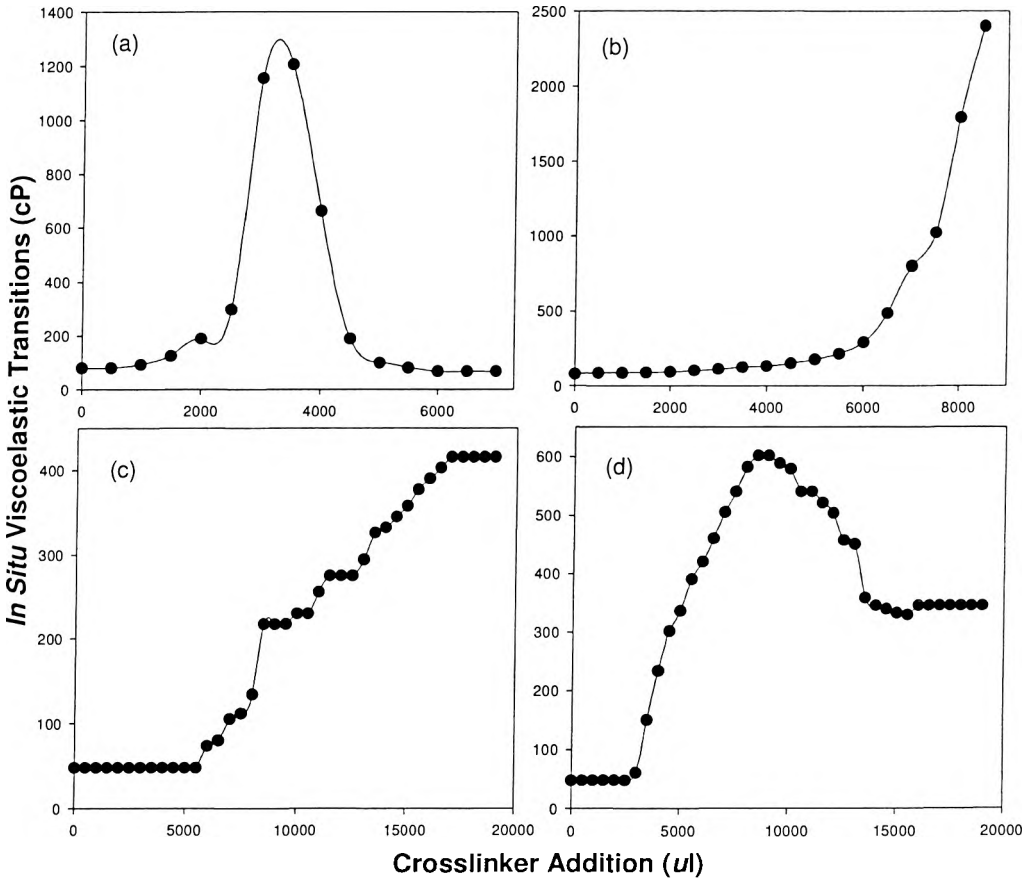

Figure 5.9 Typical viscoelastic behaviour observed among the 28 formulations. The four distinct patterns observed are (a) Bell-shaped, (b) Hyperbolic, (c) Sigmoidal, and (d) Modified bell curve (anomalous distribution).

Figure 5.9a indicates an initial slow rate of change in the viscoelasticity of the polymers involved. Upon reaching a threshold crosslinker value of approximately 2000µl, the rate of polymeric entanglement rapidly progressed and peaked at 1300cP. Subsequent addition of the crosslinker indicated a rapid decline in the viscoelasticity which is attributed to an aqueous dilution effect of the entire polymeric system (Pillay and Fassihi, 1999b; Pillay et al., 2002). This was not a reflection of chain disentanglement.

Figure 5.9b indicates a large lag-phase prior to any change in the viscoelasticity. The threshold value in this case was approximately 6500µl, indicating a significantly higher resistance to chain stiffening, contrary to that observed in Figure 5.9a.

The threshold for chain stiffening shown in Figure 5.9c is very similar to that observed in Figure 5.9b (5500µl). However, viscoelasticity steadily increased over numerous titrations of the crosslinker and peaked at 416cP. At the maximum, the viscoelasticity remained constant despite additional crosslinker. This may be attributed to an influx of the crosslinking ions into the spongy, absorbent matrix and hence accounts for an absence of the aqueous dilution effect seen in Figure 5.9a.

Figure 5.9d exhibits behaviour very similar to that seen in Figure 5.9a, except that after the aqueous dilution phase, beginning from 600cP, the crosslinked matrix tends to become spongy at 350cP and significantly absorbs the crosslinking ions. Hence no change in viscoelasticity was observed.

5.3.4 In Vitro Dissolution Behaviour

This study indicated significantly different dissolution profiles derived for the 28 formulations, which may be attributed to the significantly different degrees of crosslinking achieved in each case.

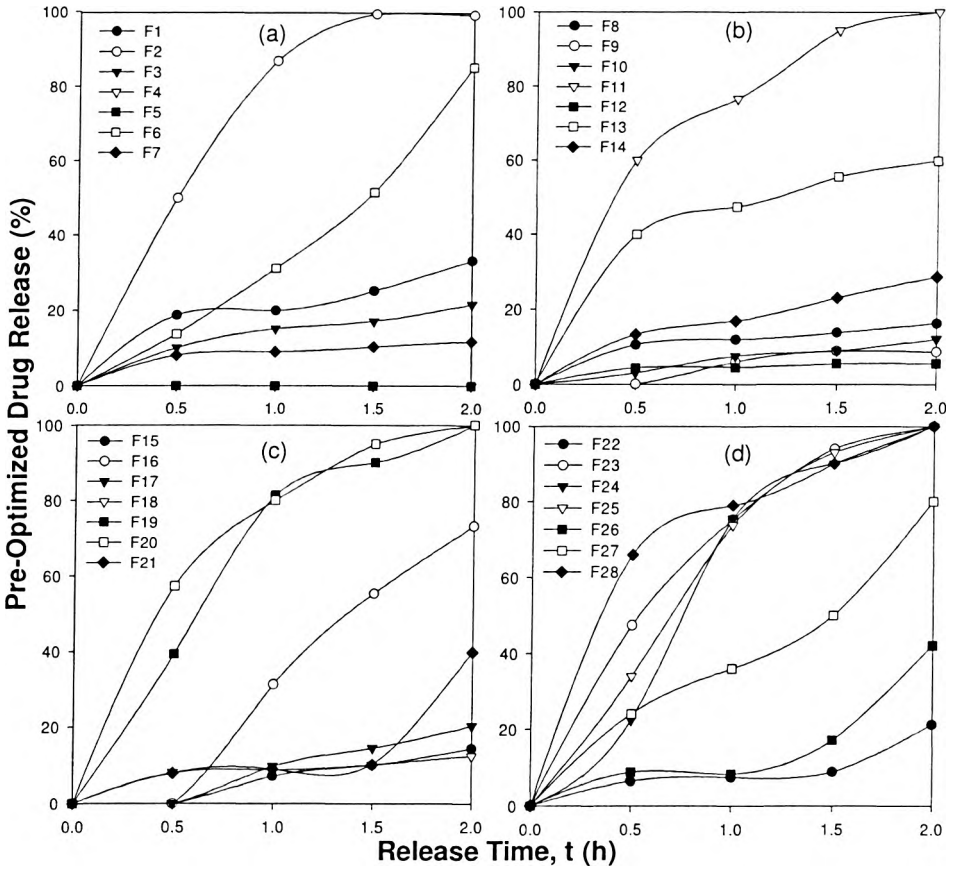

Figure 5.10 Dissolution profiles for the 28 gelisphere formulations in phosphate buffer pH 6.8. (In all cases it was observed that SDs<0.07 were obtained, N=3).

The primary aim of this study was to select a candidate formulation from the 28, in terms of the following criteria:

(i) Absence of burst effect,

(ii) Possible initial lag phase in the release process,

(iii) Slowest release rate, and

(iv) Attainment of a plateau at a very low level of drug release e.g. at 10% drug release.

Based on the above criteria as a selection tool for the candidate formulation, F9 fulfilled the above objectives. Chapter 6 would introduce a newly synthesized crosslinked

polymer that would be used to further investigate the manipulation of the physicochemical properties of F9. The focus of Chapter 6 is to outline the synthesis and sensitivity of this new crosslinked polymer.

5.4 Concluding Remarks

We have indicated that the degree of polymeric crosslinking can considerably change both the physicochemical and physicomechanical properties of the zinc-alginate-pectinate gelispheres. Contrary to Chapter 4, the aim of Chapter 5 was not to undertake formulation optimization by traditional regression analysis. The primary aim of Chapter 5 was to obtain a candidate formulation (namely F9) which could be further manipulated employing the new crosslinked polymer synthesized in our laboratory. The sequential approach towards optimization of this crosslinked polymer will be demonstrated in Chapter 6, while its utility as a release rate-modulating agent of F9 will be elucidated in Chapter 7.

Chapter Six

Synthesis and Sensitivity of a Novel Crosslinked Ethylenic Homopolymer Derived from Native Polyvinyl Alcohol

6.1. Introduction

Chapter 5 generated a primary formulation to be further optimized through the addition of a newly synthesized polymer. This new material, derived from native polyvinyl alcohol (PVA) as the starting compound, has to date never been synthesized by any other research group and applied in drug delivery in the described manner. The new material is referred to as a "crosslinked ethylenic homopolymer" (CEH). CEH will initially be formulated as gelispheres prior to its use as a release rate-modulating agent. The current Chapter details its synthesis, physicochemical and physicomechanical sensitivity, and numerical optimization.

A thorough literature survey on the application of PVA in drug delivery was conducted, and the relevant information is henceforth presented. PVA and its copolymers have found various applications in controlled drug release (Diluccio et al., 1994; Orienti et al., 2000; Soppimath et al., 2000; Doria-Serrano et al., 2001; Orient et al., 2001). Despite their higher water content, PVA hydrogels have been reported to be useful for the release of both hydrophobic and hydrophilic drugs. Since PVA is hydrophilic and easily swells upon hydration, some grades of PVA (based on molecular weight), have shown volume expansion up to 500% at 37^{O}C. However, this expansion can be inhibited by swelling controlling agents, namely electrolytes. Based on this unique property of PVA, different types of controlled release systems can be developed, whereby the release rate is controlled by the content of PVA, swelling controlling agent in the matrix core, and the application of coating films (Morita et al., 2000). At the initial stage of drug release, the rate is determined by water permeation through the membrane. However, when the

membrane bursts as a result of swelling, the release rate is controlled by the PVA matrix, which typically produces traditional first order and square root kinetics. The attainment of such release behaviour is no longer a challenge to pharmaceutical scientists.

To prolong drug release from the inherently hydrophilic polymer network, PVA may be modified by crosslinking to reduce the macromolecular pore size available for drug diffusion. The crosslinking process can be carried out either before or after drug loading, the former process being preferred since further possible side reactions between the drug and crosslinking agent may additionally reduce its diffusion (Korsmeyer and Peppas, 1981; Ahlin et al., 2002).

PVA can also be crosslinked by ultra-violet irradiation on its surface to produce prolonged drug delivery (Colombo et al., 1987). This irradiation in conjunction with chemical reactions can also be used to prepare hydrogel membranes. In addition, PVA has been classically crosslinked by glutaraldehde and ethylene glycol dimethacrylate to prepare microspheres and interpenetrating networks (Peppas and Wright, 1998; Gohel and Amin, 1999).

Crosslink density affects the size of the macromolecular pores of the hydrogel network and thus the water content, which is responsible for the transport (efflux) of solute molecules (Pillay et al., 2002). The diffusion coefficient can be linearly increased for solute molecules by increasing water content in the hydrogel, indicating that diffusion occurs primarily through hydration of the network (Burczak et al., 1994).

Most commonly, PVA has been used as a surfactant in the formulation of polylactic co-glycolic acid (PLGA) microparticles. In this case PVA influences different pharmaceutical properties of the microparticles, such as size, zeta potential, polydispersity index, surface hydrophobicity, drug loading and *in vitro* release of encapsulated molecules (Shameem et

al., 1999; Soppimath et al., 2000; Sahoo et al., 2002).

It is well known that the reaction between PVA and boric acid results in an incompatibility which produces a "slime". However, to date, this reaction in this context has not been further explored to synthesize a "useful slime". This became the objective of this part of the study. Based on the Hofmeister series, various inorganic ions were tested to modify the physicochemical properties of the PVA slime, namely thiocyanates, nitrates, chlorides, citrates, acetates, phosphates, sulphates, calciums, magnesiums, sodiums, potassiums and ammoniums. In addition a series of organic crosslinkers were evaluated. The overriding motive was to optimize this slime such that a crosslinked ethylenic homopolymer (CEH) could be formed and used to modify the candidate zinc-pectinate system (F9) in order to achieve zero-order drug release over an extended period of time. Theophylline was employed as the model drug.

6.2 The Specificity of Our Discovery

We discovered that instead of a slime, an aqueous solution of specific ratios of inorganic agents boric acid and sodium sulphate heptahydrate when reacted with PVA results in a rapid salting-out/crosslinking phenomenon. This process could be facilitated by the addition of prescribed organic crosslinkers such that a desirable plastically-deforming, rubbery material was the end product.

6.3 Materials and Methods

Theophylline was purchased from Fluka Chemicals (Switzerland), PVA from Aldrich Chemical Company (USA) and boric acid, sodium sulphate heptahydrate, ammonia and n-propanol were obtained from Rochelle Chemicals (South Africa).

6.3.1 Preformulation Study

6.3.1.1 Calibration Curve of Theophylline in Water and Buffer Media of pH 6.8

Theophylline was dissolved in deionised water and phosphate buffer pH 6.8 to produce a series of standard solutions: 0.0004, 0.0008, 0.001, 0.0012, 0.0014 and 0.0018mg/mL. Their absorbance values were determined at the wavelength maximum of 271nm. Using this information the calibration curves were constructed (Figure 6.1). No significant difference was found between the regression lines ($p>0.05$). This may be due to the fact that theophylline demonstrates pH-independent solubility. Hence one calibration curve was statistically feasible for use under both conditions.

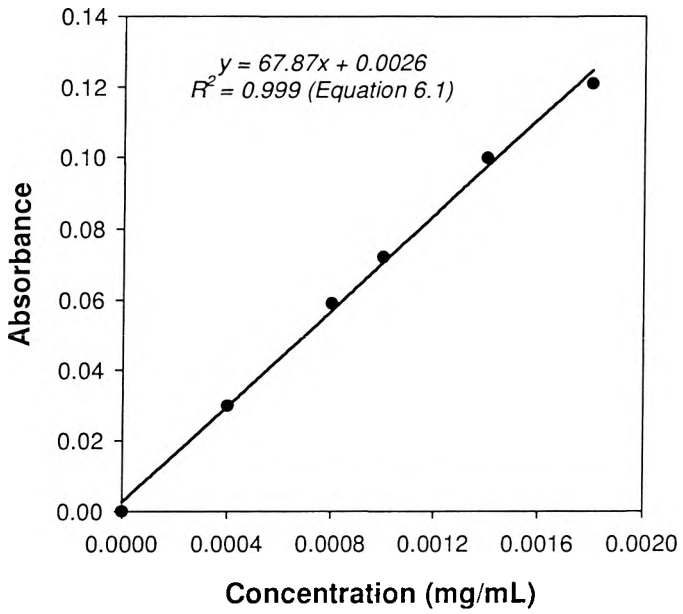

Figure 6.1 Calibration curve of theophylline in deionised water and phosphate buffer pH 6.8 ($p>0.05$). (In all cases it was observed that SDs<0.001 were obtained, N=3).

6.3.1.2 Preparation of CEH Gelispheres

A 2:1 PVA-theophylline aqueous suspension was made up to 100mL. This suspension was thereafter titrated into a crosslinking solution comprised of different concentrations of

boric acid, sodium sulphate heptahydrate, ammonia and n-propanol.

The resulting gelispheres were allowed to stir in the crosslinking solution for a further 30 minutes, after which they were placed in a dark area to cure for a period of 24 hours. At the end of this period the CEH gelispheres were washed with 3x500mL deionised water and air-dried under an extractor for 48 hours.

6.3.1.3 Size Analysis of Gelispheres

The size of the gelispheres were determined using a vernier calliper (N=10).

6.3.1.4 Drug Loading and Encapsulation Efficiency

Drug loading was conducted by dissolving 50mg of CEH gelispheres in 100mL deionised water. Based on the theoretical drug loading, the encapsulation efficiency was computed in a manner similar to that described in Chapter 4.

6.3.1.5 In Vitro Dissolution Studies

Drug release studies were conducted using a modified method of the USP 25 employing a ring mesh assembly (Pillay and Fassihi, 1998) in deionised water at 50rpm (N=3). At 10 minute intervals, samples were removed by an automated system described in Chapter 5 and analysed by ultraviolet spectroscopy at 271nm. Deionised water was selected as the dissolution medium so as to account for the sole behaviour of the CEH system in the absence of any interfering ions (e.g. phosphate buffer ions). In cases where dilution of samples was required, an appropriate correction factor was employed.

6.3.1.6 Textural Profiling Studies

The textural properties, namely matrix fracture energy, fracture force and hardness were measured in a manner similar to that illustrated in Chapter 4 (Texture Analyzer, Stable Micro Systems, England).

6.4 Results and Discussion

6.4.1 Crosslinking of PVA to Produce the CEH Gelispheres

6.4.1.1 Influence of Preformulation Levels of Inorganic Crosslinkers Boric Acid and Sodium Sulphate Heptahydrate

In order to firstly explore the crosslinking phenomenon of PVA in the presence of boric acid and sodium sulphate heptahydrate, gelisphere formation was attempted by titration of an aqueous PVA solution into a solution, as illustrated in Table 6.1. Based on Preformulation studies, various concentrations of each component were selected to provide significantly different results.

Table 6.1 Preliminary Selection of Concentrations of PVA and Initial Crosslinker Combination of Boric Acid and Sodium Sulphate Heptahydrate for the Formation of CEH gelispheres

Components	Concentrations (%w/v)			
Polymer: PVA	0.25	1	4	6
Inorganic Crosslinkers				
Boric Acid	0.25	1	5	15
Sodium Sulphate Heptahydrate	0.25	1	5	15
	Physical Observation			
	No gelispheres formed	No gelispheres formed	Aggregated weak gelispheres formed. Dissolved in crosslinkers within 2 hours	No aggregation, irregularly shaped, weak, gelispheres formed. Dissolved in crosslinkers within 2 hours

Based on the above study, the following concentrations of PVA and crosslinkers were selected: 6%w/v PVA and 15%w/v each of boric acid and sodium sulphate heptahydrate. The range of organic solvents selected (Table 6.2) significantly affected the ability of the gelispheres to form. In general, aggregated and irregularly shaped gelispheres were formed and then dissolved in the crosslinkers within 2 hours, irrespective of the volume (10-70mL), except for those formulated in n-propanol and ammonia.

6.4.1.2 Influence of Preformulation Levels of Organic Solvent Crosslinkers

Table 6.2 Preliminary Selection of Organic Solvents for CEH Gelisphere Production in Combination with 15%w/v each of Boric Acid and Sodium Sulphate Heptahydrate

Crosslinkers	Volume (mL)												
	1	2	3	4	5	6	7	8	9	10	11	12	13
Chloroformate	10-70	0	0	0	0	0	0	0	0	0	0	0	0
Butaraldehyde	0	10-70	0	0	0	0	0	0	0	0	0	0	0
Glyoxal	0	0	10-70	0	0	0	0	0	0	0	0	0	0
Hydroxyadipaldehyde	0	0	0	10-70	0	0	0	0	0	0	0	0	0
Urea-Formaldehyde	0	0	0	0	10-70	0	0	0	0	0	0	0	0
Melamine-Formaldehyde	0	0	0	10	0	10-70	0	0	0	0	0	0	0
Zinc Zirconium Carbonate	0	0	0	0	10	0	10-70	0	0	0	0	0	0
Acetone	0	0	0	0	0	10	0	10-70	0	0	0	0	0
Chloroform	0	0	0	0	0	0	10	0	10-70	0	0	0	0
Methylene Chloride	0	0	0	0	0	0	0	10	0	10-70	0	0	0
n-Propanol	0	0	0	0	0	0	0	0	10	0	10-70	0	0
Ammonia (25% Strength)	0	0	0	0	0	0	0	0	0	10	0	10-70	0

6.4.1.3 Selection of Final Polymer and Crosslinker Combination for the Production of Spherical Discrete CEH Gelispheres

Based on the observations in Table 6.2, it was apparent that separate 10mL volumes each of n-propanol and ammonia produced superior results when compared to the other organic solvents. A minimum volume of 10mL was selected in each case in order to minimize remaining residual quantities within the gelispheres. Hence the following combination of components was further tested for gelisphere production (Table 6.3).

Table 6.3 Polymer and Crosslinker Combination for the Production of CEH Gelispheres

Components	Quantity (mL)	Concentration (%w/v)
PVA	100	6
Boric Acid	100	15
Sodium Sulphate Heptahydrate	100	15
n-Propanol	10	-
Ammonia (25% Strength)	10	-
Observation	Spherical Discrete Robust Gelispheres Formed	

6.4.2 Evaluation of the Physicochemical and Physicomechanical Properties of the Gelispheres Using a Box-Behnken Design with Pre-Determined Low and High Statistical Levels of the Crosslinkers

In order to quantitatively understand the dynamics of the crosslinking process of native PVA in the proposed inorganic and organic combination, we opted to build a Box-Behnken Experimental Design (Table 6.4).

Based on the preliminary experiments the lower and upper factor levels for the concentrations of crosslinkers were as follows: boric acid and sodium sulphate heptahydrate (5-15% w/v) and, ammonia and n-propanol (10-70mL).

Table 6.4 Box-Behnken Design to Establish the Physicochemical and Physicomechanical Properties of the CEH Gelispheres

Experimental Number	Boric Acid (% w/v)	Sodium Sulphate Heptahydrate (%w/v)	Ammonia (mL)	n-Propanol (mL)
1	10	10	5	10
2	5	5	10	70
3	10	10	10	40
4	10	10	5	40
5	10	10	10	40
6	5	5	15	40
7	10	10	10	10
8	10	10	5	70
9	15	15	10	70
10	15	15	10	40
11	15	15	15	40
12	10	10	10	40
13	10	10	5	40
14	15	15	5	40
15	10	10	10	10
16	5	5	10	40
17	5	5	10	10
18	15	15	10	40
19	15	15	10	10
20	10	10	15	40
21	10	10	15	70
22	10	10	15	10
23	10	10	10	40
24	10	10	15	40
25	5	5	10	40
26	10	10	10	40
27	5	5	5	40
28	10	10	10	70
29	10	10	10	70

The general quadratic response function (Equation 6.2) for the design encompassed 15 terms with 4 factors and 5 centre points:

$$Response = b_0 + b_1*A + b_2*B + b_3*C + b_4*D + b_5*A*A + b_6*B*B + b_7*C*C + b_8*D*D + b_9*A*B + b_{10}*A*C + b_{11}*A*C + b_{12}*B*C + b_{13}*B*D + b_{14}*C*D \quad \textit{(Equation 6.2)}$$

where A, B, C and D represent the concentrations (%w/v) and volumes (mL) of boric acid, sodium sulphate heptahydrate, ammonia and n-propanol, respectively.

The responses that were measured included size (mm), drug encapsulation efficiency

(%), dissolution after 30 minutes (t_{30min}) (%), fracturability (N) and fracture energy (J) required for matrix rupture. The following quadratic equations were generated to predict each of these responses:

$$Size = 2.44 + 0.21*A + 0.030*B + 0.33*C+0.13*D+0.21*A_2+0.057*B_2+0.14*C_2 + 0.19*D_2 + 0.23*A*B + 0.35*A*C + 0.20*A*D + 0.080B*C + 0.27*C*D$$

Root MSE = 0.26, DF = 10 *(Equation 6.3)*

$$Drug\ Encapsulation\ Efficiency = 25.05 + 8.72*7.68*B + 15.57*C + 4.24*D +1.23*A*A + 4.21*B*B + 2.63*C*C + 8.46*D*D + 11.10*A*B + 10.55*A*C + 3.32*A*D + 8.73*B*C + 0.86*B*D + 13.08*C*D$$

Root MSE = 17.24, DF = 10 *(Equation 6.4)*

$$Dissolution\ (t_{30min}) = 50.12+ 5.66*A + 6.73*B + 11.76*C7.12*D + 2.54*A*A + 10.50*B*B + 1.10*C*C + 14.94*D*D + 9.04*A*B + 7.72*A*C + 2.83*A*D + 4.52*B*C + 24.25*B*D + 2.50*C*D$$

Root MSE=19.55, DF=10 *(Equation 6.5)*

$$Fracturability = 48.09 + 2.96*A* + 2.70*B + 12.65*C + 0.80*D + 1.06*A*A + 5.30*B + 1.09*C*C + 7.73*D*D + 8.85*A*B* + 8.6*A*C + 0.90*A*D* + 3.33*B*C + 7.95*B*D + 3.25*C*D$$

Root MSE=22.22, DF=10 *(Equation 6.6)*

$$Fracture\ Energy = 0.012 + 9.109\times10^{-4}*A + 1.977\times10^{-3}*B + 3.083\times10^{-3}*C + 1.477\times10^{-3}*D + 2.208\times10^{-3}*A*A + 3.124\times10^{-3}*B_2 + 3.464\times10^{-3}*C2 + 5.105\times10^{-}4*D*D + 2.003\times10^{-3}*A*B + 5.020\times10^{-4}*A*C + 4.800\times10^{3}*A*D + 4.515\times10^{-3}*B*C* + 1.943\times10^{-3}*B*D + 5.35910^{-3}*C*D$$

Root MSE=9.234x10^{-3}, DF=10 *(Equation 6.7)*

In the above equations MSE = Mean Square Error, DF = Degrees of Freedom and t_{30min} = percentage drug dissolution after 30 minutes.

6.4.3 Variability in the Physicochemical and Physicomechanical Properties of the CEH Gelispheres

Table 6.5 and Figure 6.2 indicate the different experimental values derived for the selected responses.

Table 6.5 Experimental Responses for the 29 Statistical CEH Gelispheres

Formulation Number (F#)	Experimental Response Values				
	Size (mm)	Drug Loading (%)	Fracturability (N)	Fracture Energy (Joules)	Fractional Dissolution (t_{30min})
1	1.99	9.83	49.91	0.014	0.647
2	2.00	11.72	45.57	0.017	0.784
3	2.02	13.57	75.57	0.021	0.769
4	2.40	35.43	38.54	0.018	0.248
5	1.66	73.60	45.13	0.013	0.322
6	2.28	9.77	12.64	0.001	0.747
7	1.77	8.28	16.00	0.006	0.726
8	1.39	8.11	41.19	0.006	0.658
9	1.97	18.09	24.33	0.005	0.206
10	1.94	10.65	53.65	0.011	0.533
11	1.13	9.77	34.72	0.004	0.868
12	1.17	7.30	48.16	0.006	0.662
13	0.99	9.93	36.09	0.016	0.936
14	1.36	11.84	35.10	0.010	0.903
15	2.31	61.34	25.06	0.013	0.423
16	2.50	22.47	31.02	0.008	0.565
17	1.00	14.51	66.48	0.020	1.057
18	1.10	7.76	46.07	0.006	0.760
19	2.50	48.97	32.86	0.016	0.199
20	2.50	11.69	17.52	0.001	0.527
21	3.00	64.37	36.40	0.012	0.373
22	2.50	15.02	23.12	0.002	0.604
23	2.50	8.65	26.98	0.003	0.638
24	2.00	5.81	95.54	0.023	0.471
25	2.10	4.60	86.11	0.029	0.491
26	3.00	46.25	37.71	0.020	0.448
27	2.00	53.38	29.17	0.010	0.306
28	Irregular	2.50	-	45.13	0.031
29	Irregular	2.00	-	37.34	0.014

t_{30min} indicates fractional dissolution after 30 minutes

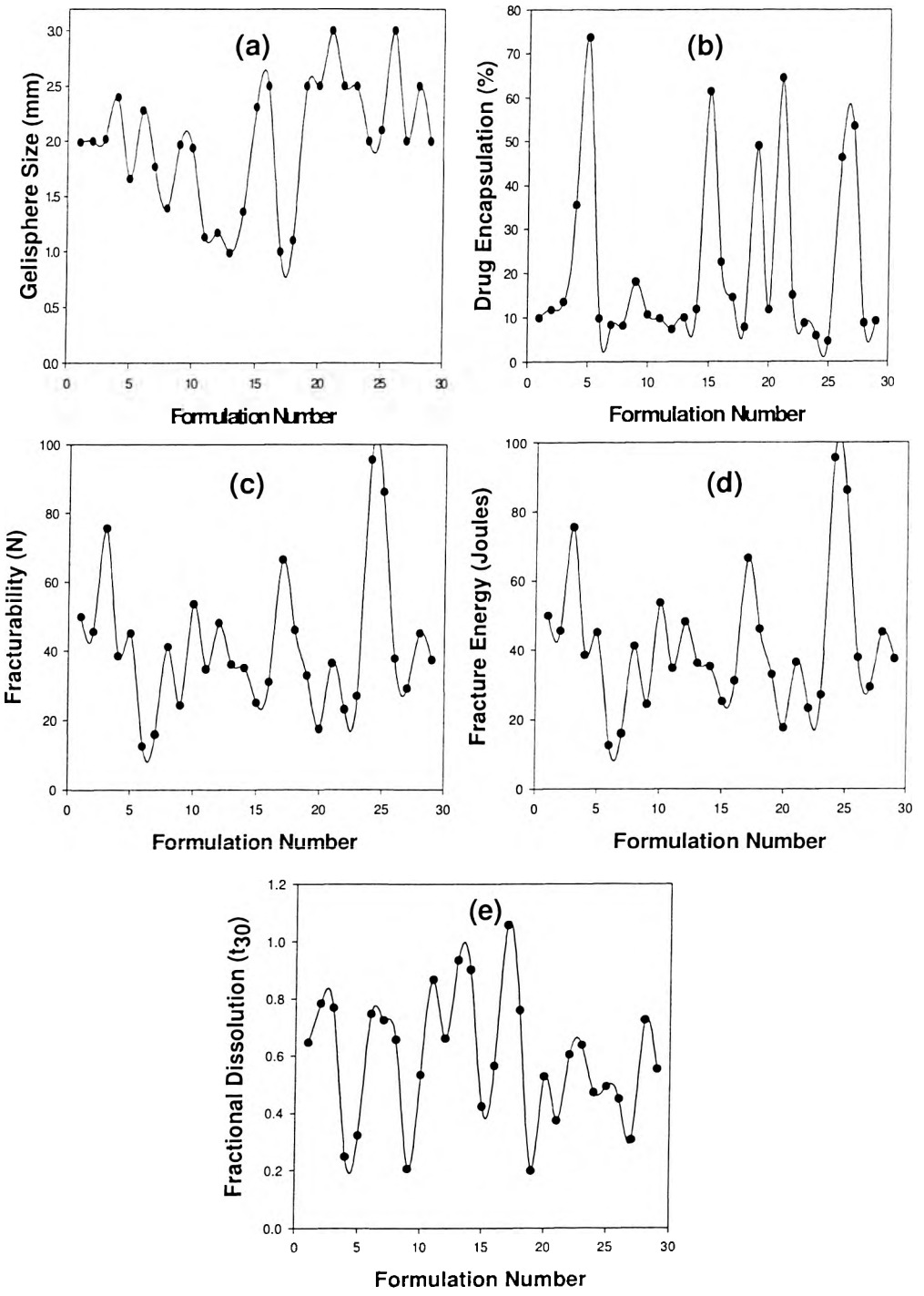

Figure 6.2 Inter-formulation variations in responses for the CEH gelispheres: (a) Size, (b) Drug encapsulation, (c) Fracturability, (d) Fracture energy, and (d) (e) Fractional dissolution after 30 minutes (t_{30min}). (In all cases it was observed that SDs<0.07 were obtained, N=10 except for dissolution where N=3).

6.4.4 Statistical Fit of Parameters for Optimization of the CEH Gelispheres Derived from Native PVA

Using a modification of the constrained settings in conjunction with solving simultaneous equations on Design Expert Version 6 (Stat-Ease, USA), the CEH gelispheres were optimized. Tables 6.6 and 6.7 provide the indicators of the model stability.

Table 6.6 Statistical Power of the Quadratic Model

Parameters	Degrees of Freedom
Model	14
Residuals	14
Lack of Fit	10
Pure Error	4
Correlation Total	28

Table 6.7 Efficiency of the Quadratic Model

Parameters	Goodness-of-Fit
Average Leverage	0.517
Maximum Prediction Variance	0.583
Average Prediction Variance	0.517
G-Efficiency	88.70%
Scaled D-Optimality Criterion	5.153
Condition Number	1.933

6.4.5 Numerical Optimization

The matrix design was optimized to produce a model capable of generating set goal values for the responses as indicated in Table 6.8. Table 6.9 depicts the 10 significant solutions generated after 5000 iterations.

Table 6.8 Theoretical Goals Set for Optimization of the Combined Response Surface Model

Parameter	Goal
Boric Acid (%w/v)	5-15
Sodium Sulphate Heptahydrate(%w/v)	5-15
Ammonia (mL)	10-70
n-Propanol (mL)	10-70
Size (mm)	1.8-3.8
Drug Encapsulation (%)	90
Dissolution (t_{30min})	10
Fracturability (N)	$\geq$96
Fracture Energy (Joules)	>0.031

Table 6.9 Predicted Solutions Derived from the Combined Response Surface Model

Solution	Formulation Parameters									
	A	B	C	D	Size	DE	Diss	F	FE	Des
1	15	12	10	11	3.6	79.4	28	30	0.021	0.562
2	15	12	10	11	3.6	80	28	30	0.021	0.562
3	15	15	10	10	3.6	89	12	93	0.051	0.891
4	15	12	11	10	3.5	78	28	31	0.021	0.561
5	15	12	12	12	3.5	77	28	31	0.021	0.561
6	15	12	14	10	3.4	74.4	28	32	0.020	0.558
7	15	12	10	18	3.6	78.1	28	31	0.020	0.556
8	15	12	15	17	3.5	73.4	26	33	0.019	0.555
9	5	14	10	31	2.6	33.6	32	42	0.019	0.486
10	5	7	70	55	2.8	21.1	72	44	0.026	0.381

A = Boric acid (%w/v), B = Sodium sulphate heptahydrate (%w/v), C = Ammonia (mL), D = n-propanol (mL), DE = Drug Encapsulation (%), Diss = Drug dissolution after 30 minutes (t_{30min}), F = Fracturability (N), FE = Fracture Energy, and Des = Desirability function indicating the predictive power of achieving the best experimental response.

Based on the desirability function of 0.891, it is apparent that Solution 3 may provide the best experimental outcome.

A CEH gelisphere formulation was prepared according to Solution 3 and the necessary experimental responses were measured (Table 6.10).

Table 6.10 Comparison of Experimentally-Derived Responses with those Statistically Predicted from Solution 3

Formulation	Responses from Predicted Solution and Experimental Study				
	Size (mm)	Drug Encapsulation (%)	Dissolution (t_{30min})	Fracturability (N)	Fracture Energy (J)
Predicted Statistical Solution 3	3.60	89	12	93	0.051
Experimental Solution	3.72	92.95	8.60	82.39	0.032

Note: Optimized experimental formulation is subsequently referred to as FD

6.5 Concluding Remarks

The Box-Behnken Design served as a useful tool to augment the various responses (size, drug encapsulation, dissolution, fracturability and fracture energy) related to the CEH gelisphere system. Depending on the required behaviour of the system, as in the case of

in vitro dissolution, the statistically-derived model for drug release was numerically solved to provide tailor-made release-rate modulation from the crosslinked system. The ensuing Chapter 7 of this study will focus on using the optimized CEH gelisphere formulation (FD) derived from numerical Solution 3 to control the release rate properties of the candidate zinc-pectinate formulation (F9) developed in Chapter 5.

Chapter Seven

Application of the Crosslinked Ethylenic Homopolymer as a Drug Release Modifying Agent: It's Effect on the Candidate Zinc-Pectinate Gelispheres

7.1 Introduction

In summary, we first tested the utility of Experimental Design using the Plackett-Burman matrix as an optimization tool. In order to develop a primary formulation for further manipulation, a high resolution Box-Behnken design was employed to develop zinc-alginate-pectinate gelispheres which would serve as a pool for the selection of a single formulation that be used as a candidate platform to test the influence of the novel crosslinked ethylenic homopolymer (CEH) synthesized from native PVA in Chapter 6.

The present Chapter explores the final stage of this research using a Face-Centred Central Composite Design (CCD) to optimize the candidate zinc-pectinate system with drug-free CEH gelispheres as a novel formulation excipient. This was performed by triturating the CEH gelispheres into a fine powder (5-12μm) and then incorporating it during the preparation of the zinc-pectinate matrix. The purpose of this task was to evaluate CEH as a potential release rate-modifying material.

The responses assessed in this optimization study included two significant formulation objectives, namely maximization of the drug encapsulation efficiency and modulation of *in vitro* drug release.

In addition, Differential Scanning Calorimetry (DSC), Fourier Transform Infra-Red (FTIR) and X-Ray Diffraction (XRD) studies were used to trace any characteristic physicochemical transitions within the polymeric matrices such as glass transition, drug melting endotherm, vibrations of molecular pendants and crystal disposition of the

complex.

7.2 Methods and Materials

The materials and their source used in this part of the study can be found in previous chapters.

7.2.1 Formulation of CEH-Zinc-Pectinate Gelispheres

CEH was incorporated together with pectin and ibuprofen, and thereafter crosslinked. The crosslinking technique was similar to that described in Chapters 4, 5 and 6, except that a Face-Centred Central Composite Design was used with factors depicted in Tables 7.1 and 7.2. Note that the quantities of pectin, zinc sulphate and zinc gluconate were the same as that employed in Formulation F9 developed in Chapter 5 (see Figure 7.1 for original dissolution profile of F9).

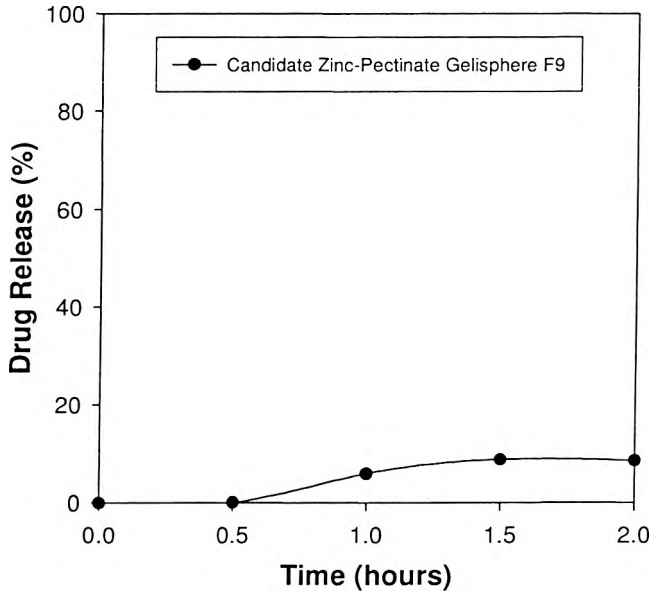

Figure 7.1 Dissolution profile of the candidate zinc-pectinate gelisphere formulation F9.

In this study ibuprofen (100mg) was substituted with theophylline (100mg), based on the fact that both drugs have a low solubility. However, theophylline behaves in a pH-independent manner (0.8% at 25°C). Ibuprofen on the other hand demonstrates pH-dependent solubility, increasing from acid to basic conditions with a minimum solubility of 0.0078% to maximum solubility of 2.9% at 25°C. This transition was merely done to observe any changes in the dissolution profiles with drugs that have low solubility but exhibit different behaviour based on pH of the medium. In general, it is well-known that control of the release of pH-dependent drugs is a challenge.

The factor levels and experimental runs of the Face-Centred Design are depicted in Tables 7.1 and 7.2.

Table 7.1 Normalized Factor Levels of the Independent Variables for the Face-Centred Central Composite Design

Variable	Factor Level		Units
	-1	1	
CEH	0	0.1	%w/v
Crosslinking-Reaction Time (CRT)	2	24	hours
Drying Temperature (dT)	20	60	°C

Note: CEH (drug-free) was prepared using the numerically optimized quantities of 6%w/v PVA, 10%w/v each of boric acid and sodium sulphate heptahydrate, and 15mL each of ammonia and n-propanol, as depicted for Solution 3 in Table 6.9.

The quadratic model comprised 3 factors and 5 centre points with 10 terms as shown below:

$$Response = b_0 + b_1*CEH + b_2*CRT + b_3*dT + b_4*CEH*CEH + b_5*CRT*CRT + b_6*dT*dT + b_7*CEH*CRT + b_8*CEH*dT + b_9*CRT*dT \quad \textit{(Equation 7.1)}$$

The abbreviations for terms CEH, CRT and dT are explained in Table 7.2. b_0 to b_9 are the regression coefficients.

Table 7.2 Face-Centred Central Composite Design (CCD)

CEH Gelisphere Number	Crosslinked Ethylenic Homopolymer (CEH) Concentration (%w/v)	Crosslinking Reaction Time (CRT) (hours)	Drying Temperature (dT) (^{o}C)
1	0.05	24	40
2	0.10	24	60
3	0.00	13	40
4	0.05	13	20
5	0.00	2	20
6	0.10	2	60
7	0.10	13	40
8	0.05	13	40
9	0.05	13	40
10	0.00	2	60
11	0.05	13	60
12	0.10	2	20
13	0.00	24	60
14	0.00	24	20
15	0.05	13	40
16	0.05	2	40
17	0.05	13	40
18	0.05	13	40
19	0.10	24	20

7.2.2 Determination of the Drug Encapsulation Efficiency of the CEH-Zinc-Pectinate Gelispheres

Drug loading was conducted by dissolving 50mg of CEH-zinc-pectinate gelispheres in 100mL of USP-recommended phosphate buffer pH 6.8. Based on the theoretical drug loading, the encapsulation efficiency was computed in a manner similar to that described in Chapter 4.

7.2.3 In Vitro Dissolution Studies

In vitro dissolution studies were performed on the 19 formulations using the modified USP 25 rotating paddle method at 37°C in phosphate buffer pH 6.8 at 50rpm, as described in Chapter 5.

7.2.4 Differential Scanning Calorimetry (DSC) Studies

DSC studies were conducted on the drug, native polymers and 19 CEH-zinc-pectinate gelispheres. A linear temperature gradient at a rate of 5°C per minute was performed from 25°C to 400°C (Perkin Elmer Pyris-1). Samples of 5-10mg were placed within crimped aluminium pans and subjected to the test.

7.2.5 Fourier Transform Infra-Red (FTIR) Studies

FTIR studies were conducted on the drug, native polymers and 19 CEH-zinc-pectinate gelispheres at 21°C (Nicolet Impact 400D). Samples of 7.5mg were mixed with 1.5g potassium bromide and triturated. From this mixture 150mg was compressed on a Beckman Hydraulic Press to produce a transparent disc. This disc was inserted into the spectrophotometer cell and its transmittance was read.

7.2.6 X-Ray Diffraction (XRD) Studies

XRD studies were conducted on the drug, native polymers and 19 CEH-zinc-pectinate gelispheres at 21°C (Bruker D8 Advance Diffractometer). The measurement conditions were as follows: voltage 40kV, current 30mA, divergence slit 2mm, anti-scatter slit 0.6mm, detector slit 0.2mm, scanning speed: 2° per minute (step size 0.025°) and step time 1.0 second. Approximately 200mg of a CEH gelisphere sample was loaded into an aluminium holder and subjected to the test, taking care not to introduce any preferential orientation of the crystals.

7.3 Results and Discussion

7.3.1. Responses for the 19 CEH-Zinc-Pectinate Gelisphere Formulations

Table 7.3 illustrates the drug encapsulation efficiency, and dissolution values obtained after 6 hours (t_{6h}). We postulated that on the basis of the plastically-deforming character of CEH, considerable reduction in drug release may be achieved. Our intention was to

use the t_{6h} value as a marker to indicate the degree of drug release suppression (Figure 7.2).

Table 7.3 Response Outcomes for the 19 Formulations

CEH Gelisphere Number	Drug Encapsulation Efficiency (%)	Dissolution (%) at t_{6h}
1	4.56	89.69
2	23.59	28.42
3	34.3	36.77
4	28.71	90.72
5	24.43	8.35
6	21.46	23.48
7	16.24	21.39
8	35.2	57.7
9	19.42	43.52
10	32.08	58.66
11	22.27	48.94
12	33.21	34.37
13	24.09	12.68
14	21.33	53.69
15	14.59	31.64
16	22.02	4.96
17	32.85	22.59
18	10.56	24.29
19	5.98	56.04

From Figure 7.2, it is apparent that the CEH polymer, crosslinking reaction time and drying temperature produced significantly different drug release profiles. In order to isolate the factor that was more significant among the three, 4 optimization objectives were developed and predicted using Solver technology (Frontline Systems, USA) (Table 7.4).

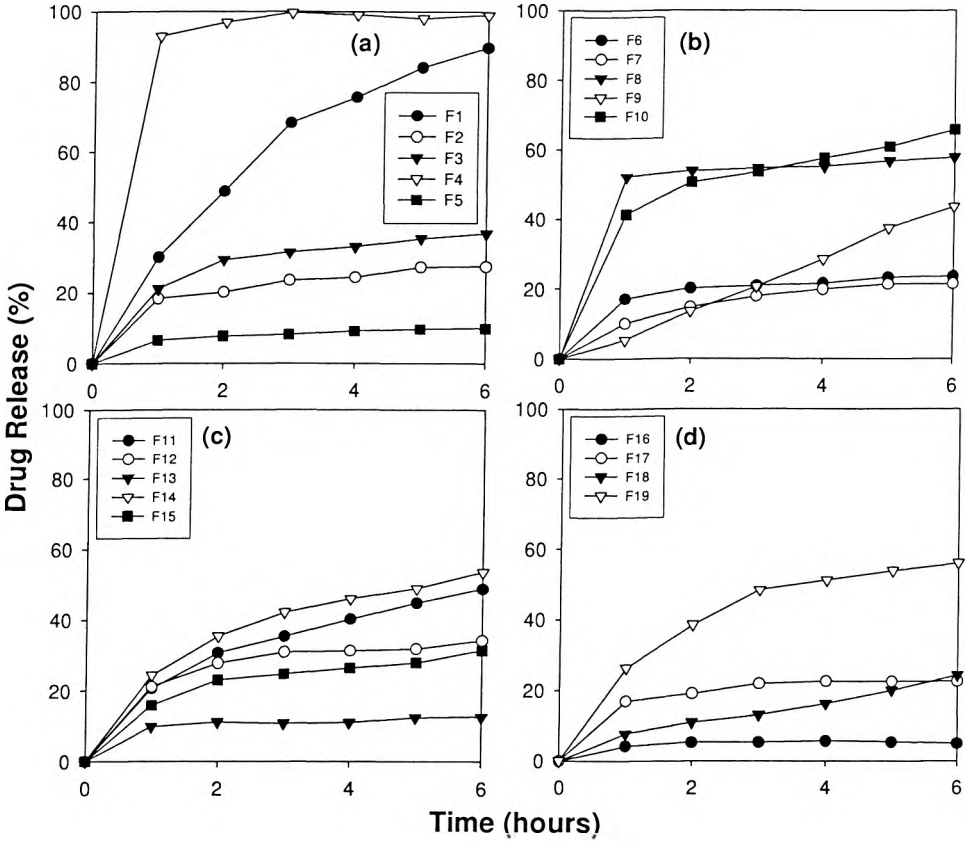

Figure 7.2 Dissolution Profiles for (a) Formulations 1-5, (b) Formulations 6-10, (c) Formulations 11-15, and (d) Formulations 16-19. (In all cases it was observed that SDs<0.02 were obtained, N=3).

7.3.2 Statistical Optimization of the CEH-Zinc-Pectinate Gelisphere Matrices

Based on numerical optimization studies using forward and backward stepwise regression the following equations were derived for the drug encapsulation efficiency and dissolution (at 6 hours):

$$\textit{Drug Encapsulation Efficiency} = b_0 + b_1{*}CEH + b_2{*}CRT + b_3{*}dT + b_4{*}CEH{*}CEH + b_5{*}CRT{*}CRT + b_6{*}dT{*}dT + b_7{*}CEH{*}CRT + b_8{*}CEH{*}dT + b_9{*}CRT{*}dT \qquad \textit{(Equations 7.2)}$$

$$\textit{Dissolution at } t_{6h} = b_0 + b_1{*}CEH + b_2{*}CRT + b_3{*}dT + b_4{*}CEH{*}CEH + b_5{*}CRT{*}CRT + b_6{*}dT{*}dT + b_7{*}CEH{*}CRT + b_8{*}CEH{*}dT + b_9{*}CRT{*}dT \qquad \textit{(Equation 7.3)}$$

The optimization objectives were processed using the following rationale:

(i) Maximization of the drug encapsulation efficiency - Economic perspective,

(ii) Minimization of drug encapsulation efficiency - Reduce the diffusion gradient in the direction from the polymeric matrix towards the dissolution medium, hence reducing drug release,

(iii) Minimization of dissolution up to 6 hours (t_{6h}) - Obtain an early phase of release rate-modulation, and

(iv) Maximization of dissolution up to 6 hours (t_{6h}) - Used as a marker to evaluate the influence of CEH.

Objectives (ii) and (iii) above are intended to enhance the lag-phase seen in Figure 7.1. This may be beneficial for targeted drug delivery to the proximal and distal intestine, particularly if drugs are sensitive to the acidic gastric juice, demonstrate enhanced absorption in the intestine or are intended for the treatment of colonic disorders.

Table 7.4 indicates the necessary parameters to obtain solutions to Objectives (i)-(iv) after application of the Solver technology (Frontline Systems, USA). Note that no statistical significance ($p>0.05$) was observed between the predicted and experimental responses.

Table 7.4 Formulation Parameters to Obtain Selected Drug Encapsulation and Dissolution Properties

Optimization Objective	Solver-Predicted Formulation Parameters			Solution (%)	
	CEH (%w/v)	CRT (hours)	dT (°C)	Predicted Response	Experimental Response
(i)	0	13	60	35.84 (drug encapsulation efficiency)	28.63
(ii)	0.08	24	40	6.42 (drug encapsulation efficiency)	9.66
(iii)	0.10	24	40	2.31 (dissolution after t_{6h})	5.1
(iv)	0.02	24	20	90.74 (dissolution after t_{6h})	74.12

Based on the above optimization objectives, the corresponding experimental dissolution profiles were obtained (Figure 7.3).

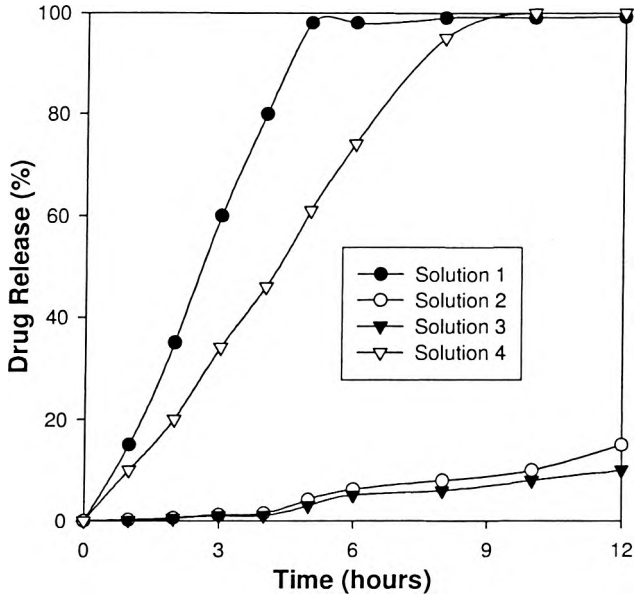

Figure 7.3 Dissolution profiles derived from Optimization Objectives (Table 7.4). (In all cases it was observed that SDs<0.14 were obtained, N=3).

From the above profiles it was apparent that the concentration of CEH together with the appropriate crosslinking reaction time and drying temperature, a range of drug release profiles may be tailor-made. In all cases zero-order drug delivery at different rates were produced. More interestingly, it was observed that as the concentration of CEH was increased, a large lag time was introduced (4 hours), hence enabling prolonged delivery over several hours to days. This was a major improvement from the original zinc-pectinate profile seen in Figure 7.1 (0.5 hour lag-phase). In this regard, we propose that the CEH-zinc-pectinate gelisphere system may be suitable for colonic drug delivery, or alternatively as a subcutaneous implant.

7.3.3 Thermal and Molecular Disposition Properties

Figure 7.4a-c depicts typical DSC, FTIR and XRD profiles for a typical CEH-zinc-pectinate formulation. The following essential characteristics were observed:

(i) DSC: The glass transition temperature (T_g) of native PVA and pectin was found to be 15°C and 20°C respectively. In addition, the melting endotherm of pure theophylline peaked at 272.77°C. The T_g value for the CEH-zinc-pectinate complex appeared between 30°C to 35°C, indicating greater molecular mobility due to a transition into a more rubbery phase. This also explains the plastically-deforming nature of CEH. The melting endotherm of theophylline was significantly reduced to ≈180°C in all 19 formulations. This may be attributed to a significant interaction between the polymers, crosslinkers and drug (Figure 7.4a), hence weakening the inter-atomic bonds of the drug.

(ii) FTIR: These studies indicated that crosslinking markedly produced significant vibrations for aromatic C=C, C-H, N-H and C=O groups. This is expected based on the individual molecular structures of native PVA and pectin. However, the extent of the vibrations was significantly suppressed based on the creation of a three-dimensional network (Figure 7.4b).

(iii) XRD: These studies indicated that the crosslinked polymeric system was highly amorphous based on the typical bell-shaped curve (Figure 7.4c).

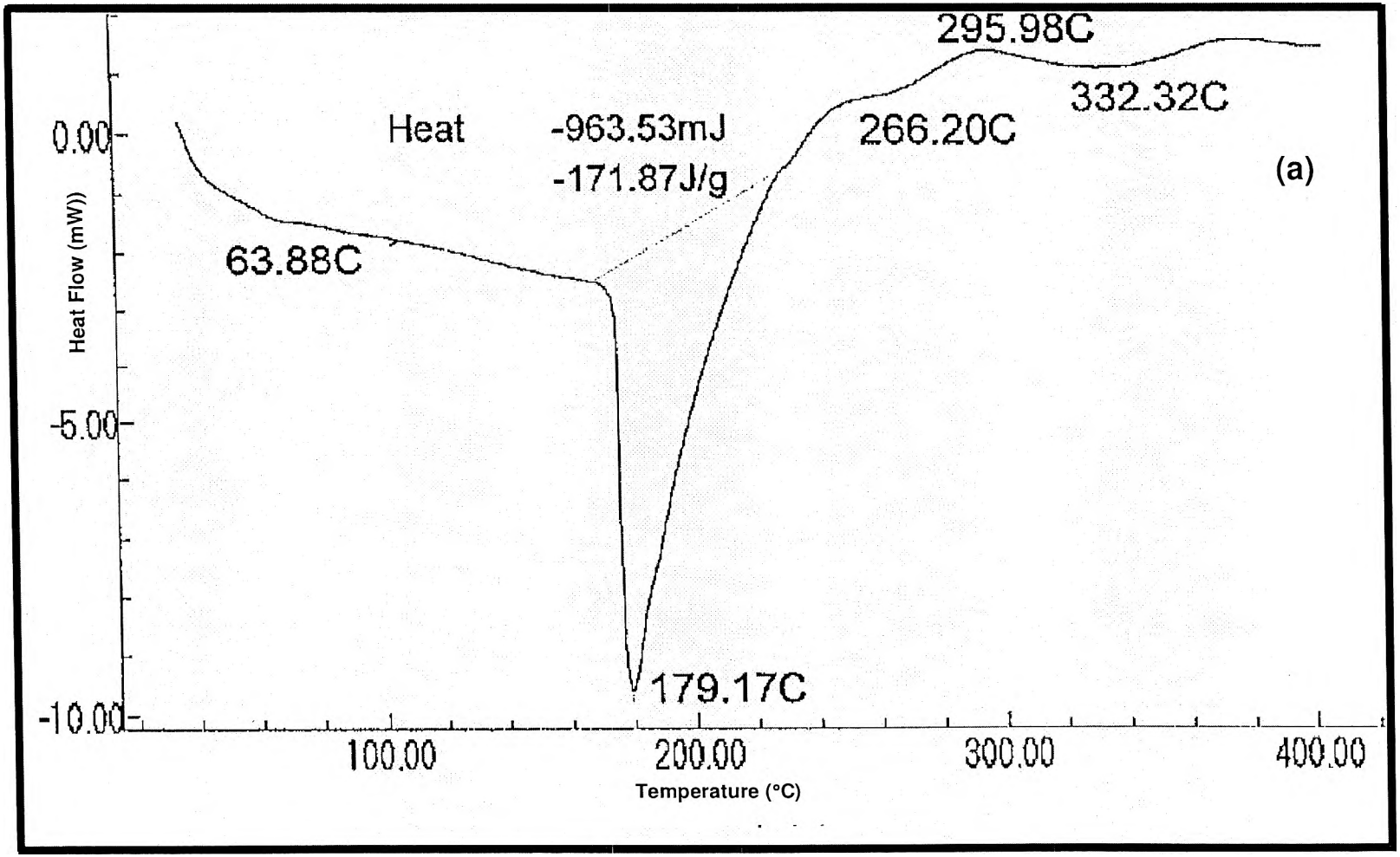
295.98C
332.32C
Heat
-963.53mJ
-171.87J/g
266.20C
(a)
0.00
63.88C
Heat Flow (mW))
-5.00
179.17C
-10.00
100.00
200.00
300.00
400.00
Temperature (°C)

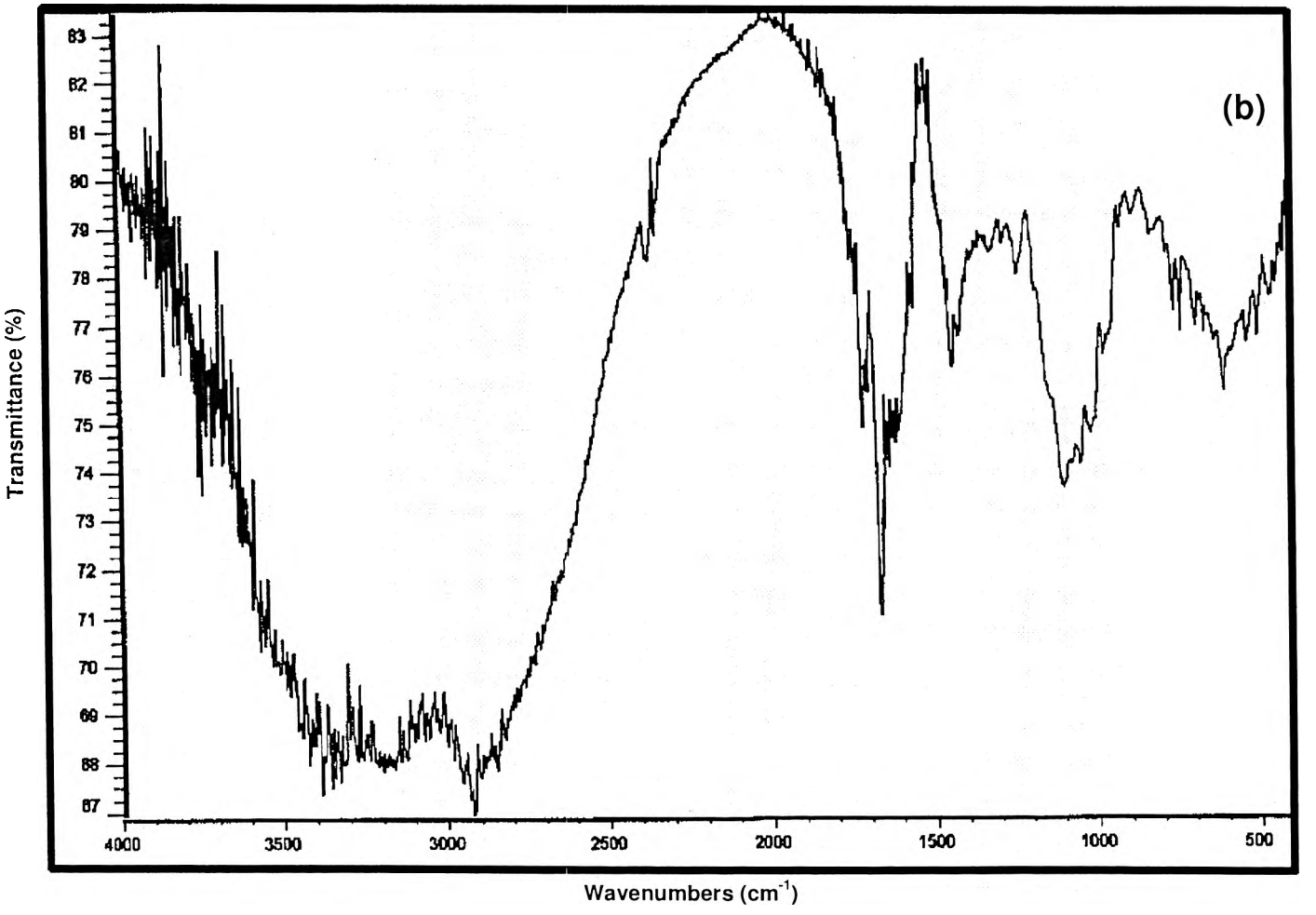
(b)
Transmittance (%)
83
82
81
80
79
78
77
76
75
74
73
72
71
70
69
68
67
4000
3500
3000
2500
2000
1500
1000
500
Wavenumbers (cm-1)

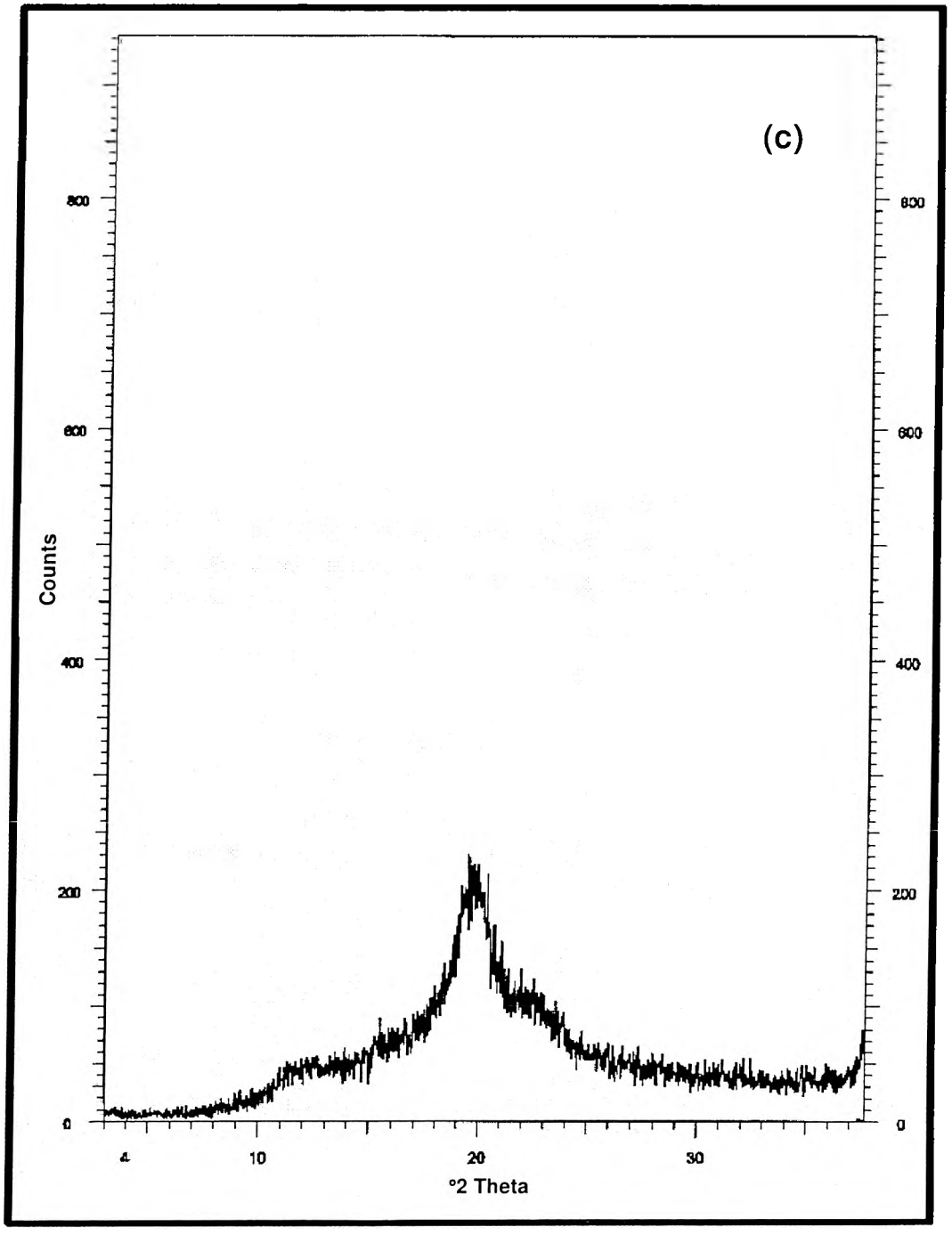

Figure 7.4 Typical (a) DSC, (b) FTIR, and (c) XRD profiles for a CEH-zinc-pectinate formulation.

7.4 Concluding Remarks

The new crosslinked ethylenic homopolymer (CEH) can be used as a time release rate-modulating excipient, rather than a traditional polymer. This crosslinking procedure is the first to be reported in this study based on the manipulation of previous incompatibilities of PVA with boric acid and sodium sulphate. The introduction of organic crosslinkers helped to facilitate this reaction.

Conclusions and Recommendations

(i) Design of Experiments, employing a statistical and mathematical basis, is a useful approach to develop predictable and "intelligent" formulations for drug delivery.

(ii) Depending on the required resolution and sensitivity of the statistical output, sequential designs can be selected which use either linear or polynomial quadratic functions.

(iii) Polymeric materials in their existing form are capable of limited function. Expansion of their behaviour can be manipulated by rationally designed chemical interactions.

(iv) Crosslinking ionotropic reactions applied to polymeric materials enable strict control over matrix hydration, erosion, polymeric relaxation and disentanglement, and ultimately drug release rate.

(v) Based on the achievement of extended zero-order drug delivery using multiple-unit technology, this work is unique, since such reports in the literature are rare. Even with prolonged drug delivery from multiple-units described over the years, the duration is characteristically no longer than 8 hours. This work has provided a deliberate approach of extending drug release from hours to days.

(vi) The novel crosslinked ethylenic homopolymer (CEH) synthesized in this study is a potent material, based on the fact that very limited quantities are required for significant release rate-modulation.

In terms of future studies, it is recommended that the statistically-designed drug delivery systems developed in this work should be evaluated *in vivo* to ascertain the influence of physiological variables and subsequent pharmacokinetics. That study should first begin with an animal model to establish safety and efficacy, followed by investigations in healthy human volunteers. This will elucidate the true efficacy of these devices, which we anticipate would be superior drug carriers for common, yet currently incurable disorders, namely irritable bowel syndrome, musculo-skeletal deformations (e.g. arthritis) and

pulmonary airway constriction (e.g. asthma).

Overall, we believe that this thesis has presented a significant contribution to the magnanimous database of pharmaceutical knowledge, and would be invaluable to scientists involved in drug design and delivery systems development.

In closing, while many scientists will embrace this work, others will challenge it. After all, it's the only way to unveil the many mysteries in pharmaceutical sciences.

References

Ahlin P, Kristl J, Kristl A, Vrecer F. Investigation of polymeric nanoparticles as carriers of enalaprilat for oral administration. *Int J Pharm.* 2002; 239:113-120.

Allescher HD. Further extension of the brain-gut axis. *Neurogastroentrol Motil.* 2003; 15:243.

Beesley A, Hardcastle J, Hardcastle PT, Taylor CJ. Influence of peppermint oil on absorptive and secretory processes in rat small intestine. *Gut.* 1996; 39:214-219.

Bolassa LL, Fanger T. Microencapsulation in the food industry. *CRC reviews in food technology.* 1971; 245:10.

Burczak K, Fujisato T, Hatada M, Ikada Y. Protein permeation through poly (vinyl alcohol) hydrogel membranes. *Biomaterials.* 1994; 15:231-238.

Cascone MG, Sim B, Downes S. Blends of synthetic and natural polymers as drug delivery systems for growth hormone. *Biomaterials.* 1995; 16:567-574.

Chawla V, Tiwary AK, Gupta S. Characterization of polyvinyl alcohol microspheres of diclofenac sodium: Application of statistical design. *Drug Dev Ind Pharm.* 2000; 26:675-680.

Colombo P, Gazzaniga A, Caramella C, Conte U, La Manna A. In vitro programmable zero-order release drug delivery system. *Acta Pharm Technol.* 1987; 33:15-20.

Danckwerts MP. Development of zero-order release tablets. *Ph.D. Thesis.* 1996; University of the Witwatersrand, Johannesburg, South Africa.

Davis SS, Hardy JG, Fara JW. Transit of Pharmaceutical dosage forms through the small intestine. *Gut.* 1986; 27:886-892.

Diluccio RC, Hussain MA, Coffin-Beach D, Torosian G, Shefter E, Hurwitz AR. Sustained-release oral delivery of theophylline by use of poly vinylalcohol and poly vinylalcohol-methyl acrylate polymers. *J Pharm Sci.* 1994; 83:104-6.

Doria-Serrano MC, Ruiz-Trevino FA, Rios-Arciga C, Hernandez-Esparza M, Santiago P. Physical characteristics of poly (vinyl alcohol) and calcium alginate hydrogels for the immobilization of activated sludge. *Biomacromolecules.* 2001; 2:568-74.

Dunn AJ, Ando T, Brown RF, Berg RD. HPA Axis activation and neurochemical responses to bacterial translocation from the gastrointestinal tract. *Ann NY Acad Sci.* 2003; 992:21-29.

FDA. FDA approves first treatment for women with constipation-predominant irritable bowel syndrome. TO2-33. 2002.

Fonner DE, Buck JR, Banker GS. Mathematical optimization techniques in drug product design and process analysis. *J Pharm Sci.* 1970; 59:1587-1597.

Gohel MC, Amin AF. Formulation design and optimization of modified-release microspheres of diclofenac sodium. *Drug Dev Ind Pharm.* 1999; 25:247-251.

Grant GT, Morris ER, Rees DA, Smith PJC, Thom D. Biological interactions between polysaccharides and divalent cations: The Egg-box model. *FEBS Letters.* 1973; 32:195-198.

Harris D, Robinson JR. Controlled drug delivery: New approaches to controlled drug delivery. *5th International Pharmaceutical Technology Symposium.* 1990; Hacettepe University, Ankara.

Hendrix CD. What every technologist should know about experimental design. *Chem Tech.* 1979; 1:167-174.

Hills JM, Aaronson PI. The mechanism of action of peppermint oil on gastrointestinal smooth muscle: An analysis using patch clamp electrophysiology and isolated tissue pharmacology in rabbit and guinea pig. *Gastroenterology.* 1991; 101:55-65.

Hopfenberg H.B. Controlled release polymeric formulations. Paul DR, Harris FW (Eds.). American Chemical Society, Washington DC. 1976; pp. 26-32.

Iscan G, Kirimer N, Kurkcuoglu M, Husnu Can Baserk K, Demirci F. Antimicrobial screening of Mentha piperita essential oils. *J Agric Food Chem.* 2002; 50:3943-3946.

Juliano R. Nanoparticles in drug delivery systems. Oxford, Oxford University Press, 1980; 1:177-188.

Katzhendler I, Hoffman A, Goldberger A, Friedman M. Modeling of drug release from erodible tablets. J Pharm Sci. 1997; 86:110-115

King TS, Elia M, Hunter JO. Abnormal fermentation in irritable bowel syndrome. *Lancet.* 1998; 352:1187-1189.

Kline RM, Kline JJ, Di Palma J, Barbero GJ. Enteric-coated pH-dependent peppermint oil capsules for the treatment of irritable bowel syndrome in children. *J Pediatr.* 2001;

138:125-128.

Korsmeyer RW, Peppas NA. Effect of the morphology of hydrophilic polymer matrices on the diffusion and release of water-soluble drugs. *J Membr Sci.* 1981; 9:211-227.

Lai MC, Schowen RL, Borchardt RT, Topp EM. Deamidation of a model hexapeptide in poly (vinylalcohol) hydrogels and xerogels. *J Pept Res.* 2000; 55:93-101.

Lin S, Chien YW, Daggy BP, Mirchandani HL. Statistical optimization of gastric floating system for oral controlled delivery of calcium. *AAPS PharmSciTech.* 2001; 2:1-12.

Liu JH, Chen GH, Yeh HZ, Huang CK, Poon SK. Enteric-coated peppermint oil capsules in the treatment of irritable bowel syndrome: Prospective randomized trial. *J Gastroenterol.* 1997; 32:765-768.

Madden JA, Hunter JO. A review of the role of the gut microflora in irritable bowel syndrome and the effects of probiotics. *Br J Nutr.* 2002; 88:67-72.

Meese TM, Hu Y, Nowak RW, Marra KG. Surface studies of coated polymer microspheres and protein release from tissue-engineered scaffolds. *J Biomater Sci Polym.* 2002; 13:141-151.

Micklefield G, Jung O, Greving I, May B. Effects of intraduodenal application of peppermint oil (WS(R)1340) and caraway oil (WS(R)1520) on gastroduodenal motility in healthy volunteers. *Phytother Res.* 2003; 17:135-140.

Mojaverian P. Mechanisms of gastric emptying of non-disintegrating radiotelemetry in man. *Pharm Res.* 1991; 8:97-100.

Morita R, Honda R, Takahashi Y. Development of oral controlled release preparations, a PVA swelling controlled release system (SCRS). I. Design of SCRS and its release controlling factor. *J Control Rel.* 2000; 63:297-304.

Muller L, Blum AL. Duodenogastric reflux in the fasting dog; role of pylorus and duodenal motility. *Am J Physiol Gastrointest Liver Physiol.* 1981; 241:159-162.

Nakai A, Kumakura Y. Sex differences of brain serotonin synthesis in patients with irritable bowel syndrome using alpha-[11C]-methyl-L-tryptophan positron emission tomography and statistical parametric mapping. *Can J Gastroenterol.* 2003; 17:191-196.

Nelson MM, Illingworth WT. A practical guide to neural nets, 4th Ed. Addison-Wesley Publishing Company, Massachusetts. 1992; pp. 15.

Orienti I, Di Pietra I, Luppi B, Zecchi V. Crosslinked polyvinylalcohol hydrogels as vehicles for hydrophilic drugs. *Arch Pharm (Weinhem).* 2000; 333:421-424.

Orienti I, Trere R, Zecchi V. Hydrogels formed by crosslinked polyvinylalcohol as colon-specific drug delivery systems. *Drug Dev Ind Pharm.* 2001; 8:877-884.

Paradossi G, Cavalieri F, Chiessi E, Ponassi V, Martorana V. Tailoring of physical and chemical properties of macro-and microhydrogels based on telechelic PVA. *Biomacromolecules.* 2002; 3:1255-1262.

Pattnaik VR, Subramanyam M, Bapaji CR. Antibacterial and antifungal activity of aromatic constituents of essential oils. *Microbios.* 1997; 89:39-46.

Peppas NA, Sahlin JJ. A simple equation for the description of solute release. III.

Coupling of diffusion and relaxation. *Int J Pharm.* 1989; 57:169-172.

Peppas NA, Wright SL. Drug diffusion and binding in ionizable interpenetrating networks from PVA and polyacrylic acid. *Eur J Pharm Biopharm.* 1998; 46:15-29.

Perez C, Sanchez A, Putnam D, Ting D, Langer R, Alonso MJ. Poly(lactic)-poly(ethylene glycol) nanoparticles as new carriers for the delivery of plasmid DNA. *J Control Rel.* 2003; 75:211-224.

Pillay V, Fassihi R. Evaluation and comparison of dissolution data derived from different modified release dosage forms: An alternative method. *J Control Rel.* 1998; 55:45-55.

Pillay V, Fassihi R. In vitro release modulation from cross-linked pellets for site-specific delivery to gastrointestinal tract. I. Comparison of pH-responsive drug release and associated kinetics. *J Control Rel.* 1999a; 59:229-242.

Pillay V, Fassihi R. In vitro release modulation from cross-linked pellets for site-specific delivery to gastrointestinal tract. II. Physicochemical characterization of calcium-alginate, calcium-pectinate and calcium-alginate-pectinate pellets. *J Control Rel.* 1999b; 59:243-256.

Pillay V, Fassihi R. In situ electrolyte interactions in a disc-compressed System for up-curving and constant drug delivery. *J Control Rel.* 2000a; 67:55-65.

Pillay V, Fassihi R. A novel approach for rate delivery of highly soluble bioactives from a simple monolithic system. *J Control Rel.* 2000b; 67:67-78.

Pillay V. Rate-modulating polymeric complexes. *National Research Foundation Proposal.*

2002, University of the Witwatersrand, Johannesburg, South Africa.

Pillay V, Danckwerts MP. Textural profiling and statistical optimization of crosslinked calcium-alginate-pectinate-cellulose acetophthalate gelisphere matrices. *J Pharm Sci.* 2002; 91:2559-2570.

Pillay V, Danckwerts MP, Fassihi R. A crosslinked calcium-alginate-pectinate-cellulose acetophthalate gelisphere system for linear drug release. *Drug Del.* 2002; 9:77-86.

Praveen T. Specialized drug delivery systems. *Manufac Product Tech.* 1990; 41:32.

Principe JC, Euliano NR, Lefebvre WC. Neural and adaptive systems: Fundamentals through simulations. John Wiley and Sons, New York, 1998.

Pronova Biopolymers. Alginate as immobilization material for cells. Technical Sheets. 1994; pp.1-4.

Ravve A. Principles of polymer chemistry, 2nd Ed. Kluwer Publishers, New York. 2000; pp. 1-50.

Reiner M. Deformation, strain and flow, 3rd Ed. HK Lewis and Company Ltd., London. 1969; pp. 98-100.

Ritger PL, Peppas NA. Simple equation for the description of solute release. II. Fickian and anomalous release from swellable devices. *J Control Rel.* 1987; 5:37-42.

Rosemore JG, Lacy BE. Irritable bowel syndrome: Basis of clinical management strategies. *J Clin Gastroenterol.* 2002; 35:37-44.

Sahoo SK, Panyam J, Prabha S, Labhasetwar V. Residual polyvinyl alcohol associated with poly (DL-lactide-co-glycolide) nanoparticles affects their physical properties and cellular uptake. *J Control Rel.* 2002; 82:105-114.

Schwartz JB, O'Connor RE, Schnaare RL. Optimization techniques in pharmaceutical formulation and processing. Modern Pharmaceutics 4th Ed. Marcel Dekker, New York, 2002.

Semval PB. Procedure and usefulness of statistical design of experiments in chemical processes and evaluations with two case studies. *Chem Eng World.* 1997; 32:9.

Shameem M, Lee H, DeLuca PP. A short term (accelerated release) approach to evaluate peptide release from PLGA depot-formulations. *AAPS PharmSci.* 1999; 1:1-6.

Sibanda W, Pillay V, Danckwerts MP, Viljoen AM, Van Vuuren S, Khan RA. Experimental design for the formulation and optimization of crosslinked oilispheres developed for *in vitro* site-specific release of *Mentha piperita* oil. *AAPS PharmSciTech.* 2004; 5:1-14.

Siepmann J, Podugal K, Sriwongjanya M, Peppas NA, Bodmeier R. A new model describing the swelling and drug release kinetics from hydroxypropyl methylcellulose tablets. *J Pharm Sci.* 1999; 88:65-72.

Siepmann J, Peppas NA. Modeling of drug release from delivery systems based on hydroxypropyl methylcellulose (HPMC). *Adv Drug Deliv Rev.* 2001; 11:139-57.

Soppimath KS, Kulkarni AR, Aminabhari TM. Controlled release of antihypertensive drug from the interpenetrating network PVA-guar gum hydrogel microspheres. *J Biomater Sci Poly Ed.* 2000; 11:27-43.

Soppimath KS, Kulkarni AR, Aminabhavi TM, Bhaskar C. Cellulose acetate microspheres prepared by o/w emulsification and solvent evaporation method. *J Microencapsul.* 2001; 18:811-817.

Thanoo BC, Sunny MC, Jayakrishnan A. Crosslinked chitosan microspheres, preparation and evaluation as a matrix for controlled release of pharmaceuticals. *J Pharm Pharmacol.* 1992; 44:283-286.

Turner DE. Clinical aspects of new drug delivery systems: New approaches to controlled drug delivery. *5th International Pharmaceutical Technology Symposium.* 1990; Hacettepe University, Ankara.

Weydert JA, Ball TM, Davis MF. Systemic review of treatments for recurrent abdominal pain. *Pediatrics.* 2003; 111:1-11.

Widder KJ, Senyei AE, Sears B. Experimental methods in cancer therapeutics. *J Pharm Sci.* 1982; 71:377-387.

Wilding R, Coupe AJ, Davis SS. The role of gamma-scintigraphy in oral drug delivery. *Adv Drug Deliv Rev.* 2001; 46:103-124.

Wood JD. Neuropathophysiology of irritable bowel syndrome. *J Clin Gastroenterol.* 2002; 35:11-22.

Yang L, Fassihi R. Modulation of diclofenac release from a totally soluble controlled release drug delivery system. *J Control Rel.* 1997; 44:135-140.

Yasuda H, Rosengren KJ. Isobaric measurement of gas permeability of polymers. *J Appl*

Polymer Sci. 1971; 14:2839-2877.

Zar S, Benson MJ, Kumar D. Review Article: Bloating in functional bowel disorders. *Aliment Pharmacol Ther.* 2002; 16: 1867-1876.